JOURNAL OF MANAGEMENT AND ENGINEERING INTEGRATION

Scope: The Journal of Management and Engineering Integration (JMEI) is a double-blind refereed journal dedicated to exploring the nexus of management and engineering issues of the day. JMEI publishes two issues per year, one in Summer and another in Winter. The Journal's scope is to provide a forum where engineering and management professionals can share and exchange their ideas for the collaboration and integration of Management and Engineering research and publications. The journal will aim on targeting publications and research that emphasizes the integrative nature of business, management, computers and engineering within a global context.

EDITORIAL REVIEW BOARD

REVIEWERS

The Journal Editorial Team would like to thank the reviewers for their time and effort. The comments that we received were very constructive and detailed, and helped us to continue to produce a consistently top-quality journal. Your participation is very important in the success of providing a distinguished outlet for original valuable articles. Again I would like to thank you all for your assistance in the review process.

Nabeel Yousef
Editor-in-Chief

Ahmed Abukmail
Ali Ahmad
Tareq Ahram
Kamal Ali
Stephen Allen
Mohamad Almaoui
Osama Almenazel
Yousef Al-Turki
Gordon Arbogast
Khalid Bachkar
Judith Barlow
Ann Becker
Noureddine Bekhouche
Edwin R. Bellman
Nourredine Boubekri
Deborah S. Carstens
Andrew Cudmore
Stephen Frempong
Sandy L. Furterer
Andrzej Gapinski
Sampson Gholston
Jean Gourd
Indra Gunawan
Mohammad M. Hamasha
Randall Harris
Xiaochun Jiang
Jeng-Nan Juang
Nipoli Kamdar
Mohammad T. Khasawneh
Ekaterina Koromyslova
Mohamed Labidi
Hesham Mahgoub
Tamer Mohamed
Karla Moore
Faissal A. Moslehy
James Ngeru
Pierre Ngnepieba
Kevin O'Neill
Al Petrosky
R. Radharamanan
Ahmad Rahal
Dennis Ridley
Ewa Rudnicka
Moe Saouli
Nabin Sapkota
Alexandra Schönning
Sunshil Shetty
J.S. Sutterfield
Edem Tetteh
Ha Van Vo
Paulus Wahjudi
John Wang
Gamal Weheba
Chen Xiang
James Yao
Wei Zha

TABLE OF CONTENTS

Development of the Audit-Calc Software System: A Case Study

Mohammad Kanan
Gamal Weheba
Bassam Jaradat

Department of Industrial and Manufacturing Engineering
Wichita State University
Wichita, KS 67260
gamal.weheba@wichita.edu

Abstract

This paper represents a case study involving the development of the Audit-Calc© web based software. The development was aimed at achieving a consistent implementation of the 9104/1 Aerospace Standard. The software walks customers through certification requirements and helps determine the appropriate organization structure and minimum audit durations. Design efforts followed closely an integrated software development model where customer requirements were solicited and used to specify performance measures and their targets. The software was successfully developed within the planned time and budget with high levels of customer satisfaction.

1. Introduction

Seventy eight percent of the United States population used the internet in 2012 (Internet Web Stats 2012). Gartner (2014) predicted that worldwide IT will spend $3.8 Trillion in 2014. This requires developers to produce high quality software to achieve customer satisfaction and gain their loyalty. Maintaining a higher level of product or service quality provides a competitive advantage. A business that can delight customers by improving and controlling quality can dominate its competitors (Montgomery, 2013). In order to achieve these goals, developers have to use an appropriate software development approach. This approach should allow for customer involvement during the design phase to minimize ambiguity and eliminate any misunderstanding between the customers and the developers. In this paper, we utilize an integrated model for software development. The model builds on the strength of well-known quality and software engineering approaches to achieving high levels of customer satisfaction. The following section represents a review of the literature pertaining to the most commonly used development models in both fields. This is followed by a discussion of the anticipated advantages of the integrated model presented in section 4. Section 5 represents a case study involving the development of the Audit-Calc software using the integrated model. Final conclusions and recommendations are represented in Section 6.

2. Literature Review

The waterfall model, developed by Royce (1970), represents a sequential design process incorporating an ordered set of phases organized in a linear fashion. This model is depicted in Figure 1. In this model, the software requirement specifications (SRSs) are documented during the first phase of project development. In the next, or design phase, modules of the software are designed using information provided by the SRSs and other diagrams produced in the first phase. Then, during the implementation (construction)

Figure 1. Waterfall Model

phase, modules are coded and tested to uncover defects/bugs as early as possible during the testing phase. After testing, the software is ready for release. The final phase of maintenance includes correcting uncovered defects and system evolution.

Sage and Palmer (1990) indicated that the waterfall model is linear and very easy to implement, requiring a minimum amount of resources with documentation at every phase of development. However, Munassar and Govardhan (2010) pointed out that this model cannot be applied to all situations. For example, requirements must be stated before beginning the design phase, the complete design must be confirmed before coding, and there is no overlap between the proposed phases. The tester role is only allowed during the testing phase.

In addition, the model progresses under the assumption that all requirements are fixed. In real-world development, one can discover issues during the design or coding stages that point to errors or gaps in the requirements.
When this is the case, the development should begin again from scratch.

The prototyping model, proposed by Curtis, Krasner et al. (1988), allows for a high level of interaction with customers during the design phase.

This approach starts with gathering the requirements and defining the overall objectives from the perspectives of customers and developers. The prototype tends to work as a tool to identify customers' requirements and enables developers to better understand their needs and expectations. The development phase begins after customer satisfaction is achieved, with testing and maintenance following, as shown in Figure 2.

Doke and Swanson (1995) stated that the popularity of the prototyping model is due to its efficiency, which is achieved by considering the inputs from customers during the early stages of the project. By listening to the customers, the software can be improved to include new requirements before the project moves into the development phase. Usually, this leads to fewer changes and modifications after release. In addition, the prototyping model is suitable for estimating the feasibility of a certain approach when building large projects (Davis, Bersoff et al. 1988). During the prototyping phase, customers can assess the functionality as well as recommend modifications to the software.

During the 1980s, the emphasis on customer satisfaction gave rise to applications of quality management concepts to software development. These included the quality function deployment (QFD) proposed by Akao (Akao, 1990). The main tool associated with QFD is the house of quality (HoQ) matrix as was named by Hauser and Clausing (1988). The matrix is used to convert customers' needs into design characteristics. It is aimed at reducing development time and increasing market share by focusing on customer satisfaction (Terninko 1997). Lowe and Ridgway (2000) stated that "the HoQ matrix is used to convert a structured set of customer statements, market research and benchmarking data into an appropriate number of engineering targets to be met by a new product design".

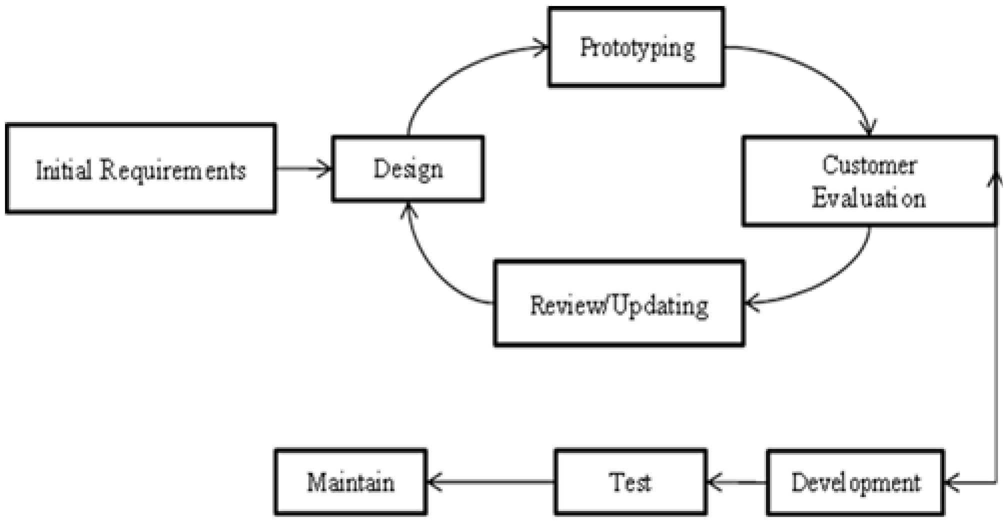

Figure 2. Prototype Model

3. Discussion

One of the ultimate measures of quality is customer satisfaction. The ability of any organization to meet and exceed the expectations of its customers determines its future. ISO 9126 defines software quality as "the totality of features and characteristics of a software product that bear on its ability to satisfy stated or implied needs." This supports the need for customer involvement during the development projects to minimize the risk of failure. Based on the review in the previous section, the waterfall model is linear and very easy to implement (Sage and Palmer, 1990). However, as was noted by Amlani (2012), it is not flexible for changes in customer requirements. Whereas, the prototyping model allows for interactions before development to assure clear understanding of customer requirements. It involves customers helping to elect and verify requirements. Critics argue that it can be costly and time consuming since customers do not initially know their requirements (Davis, Bersoff et al. 1988).

The HoQ, on the other hand, is customer oriented and generates technical requirements traceable to customer needs. However, it is highly dependent on the clarity of customer stated needs and can be time consuming when projects are very large and complex. It appears that achieving high levels of customer satisfaction calls for an integrated approach that builds on the strengths of the above models while overcoming their limitations.

4. The Integrated Model

The model shown in Figure 3, allows for an effective integration of the cited models with the objective of achieving high levels of customer satisfaction. The model is recommended for applications where the system can be divided into modules or subsystems. It incorporates six stages starting with solicitation of initial requirements and ending with maintenance after system release. The model is a modification of the waterfall model with the addition of two critical stages. The first involves the selection of a pilot application to help focus the initial scope of development. This is typically a fraction of the software system representing a major function or application of high priority. Whereas the second, involves an application of the prototyping model guided by the discipline and structure of the HoQ. During this stage an initial set of features and characteristics are generated based on customer requirements following the HoQ matrix. Target levels of software performance are used to develop the prototype. In essence, the resulting prototype is used to test the clarity and completeness of customer requirements. This is accomplished through a formal evaluation of the prototype by a sample of users. The feedback provided and comments made by users while testing the prototype should be incorporated into the HoQ and translated into new performance targets. A number of iterations may be required to achieve an acceptable level of customer satisfaction. Each iteration represents discovery of unstated needs or clarification of stated requirements. The knowledge gained should be documented as lessons learned to support the deployment stage. This latter stage is aimed at the design of the complete system based on clear, accurate and verified requirements. This is typically followed by a verity of tests to detect and eliminate errors and assure software quality. These efforts can result in significant reduction of the cost of maintenance after release.

This integrated model has some phases that are similar to other models, such as, gathering requirements, implementation, testing, and maintenance. The first unique feature of this model is the selection of the highest priority application to minimize both development cost and time. Whereas the second is using and documenting the lessons learned- in auxiliary storage such as a Database- to minimize the risk of not meeting customer requirements. In other words, the model allows for a better comprehension of customer requirements to help reduce the total software development cost and time.

5. Case Study

This case study represents the development of the Audit-Calc© software system for the International Aerospace Quality Group (IAQG). This group was established in 1998 with the goal of achieving significant improvements in quality and reducing the cost throughout the value stream. The IAQG developed specific requirements for Aviation, Space and Defense (AS&D) quality management systems that are implemented and maintained throughout the supply chain for the design, manufacture, and maintenance of products. These requirements are published as the AS9104/1 Standard. The standard outlines requirements of a global scheme for the acceptance and recognition of certification audits for the ISO 9100, ISO 9110 and ISO 9120 Quality Management Standards. The standard was published during the end of 2011, and includes multiple options for an organization to be certified with the corresponding audit

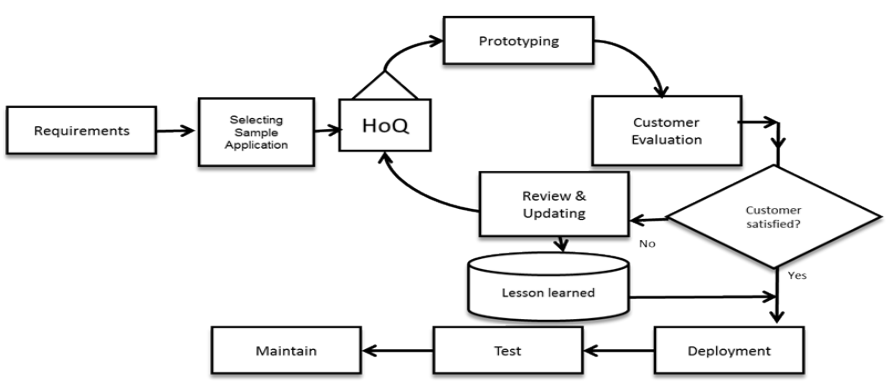

Figure 3. The Integrated Model

1	Documents justifications for modified audit durations
2	Allows sharing information with clients
3	Assures consistent interpretation of certification structures
4	Fast to access
5	Provides accurate calculation of audit duration
6	Alerts customers to issues requiring resolution
7	Easy to use

Figure 4 List of Initial Requirements

durations. Depending on the configuration of its value stream, an organization may seek certification as single-site, multiple-site, campus, several sites or complex structure. The Other Party Management Team (OPMT) recognized the need for a user-friendly computer program that would step AS&D stakeholders through the criteria for certification and audit durations. A team of researchers from Wichita State University (WSU) was selected to develop the system. The following is a brief description of the project and steps taken following the model in Figure 3.

During the first step, an initial list of seven general requirements was developed by members of the OPMT and recorded in the project charter. This list is shown in Figure 4. An initial survey was designed to solicit additional needs and the relative importance of each form the users' prospective.

The survey was administered electronically by the OPMT and included 150 certified auditors. Out of the 52 responses received, 47 (31.3%) were considered valid responses. These included 21 from the US (44.7%), 24 from the European Union (51%), and 2 from the Asian pacific (4.3%). The results indicated three additional requirements (records of planning activities, retrieval and modification of audit plans, and communication with other audit management systems).

Feature	Score	Weight
Assures consistent interpretation of certification structures	212	1.0
Provides accurate calculation of audit duration	210	0.99
Easy to use	199	0.94
Fast to access	195	0.94
Documents justifications for modified audit durations	192	0.91
Alerts customers to issues requiring resolution	168	0.79
Provides record of planning activities	160	0.75
Facilitates retrieval and modification of audit plans	153	0.72
Allows sharing information with clients	152	0.72
Communicates with other audit management systems	138	0.65

Figure 5 Prioritized Requirements Based on Total Score

The final list of needs with their relative importance as perceived by participants is shown in Figure 5. In addition, participating auditors indicated that 79% of their clients are seeking certifications under the single-site structure. This was used to establish the scope of the prototyping step.

The HoQ shown in Figure 6 was constructed to translate these ten requirements into a set of features and attributes. As can be seen, the foundation of the HoQ includes target levels and measurements selected for the development of the prototype to support single-site applications. Target levels and measurements were set based on ISO 9126 software quality standard (ISO/IEC 9126-1, 2001). The resulting prototype was represented at a meeting of the Registration Management Committee (RMC) on July 2012 at Minneapolis, Minnesota.

The feedback indicated the need to consider an additional feature to allow auditors to specify their future plans for performing recertification audits and justify modified durations in days as opposed to percentages of the audit durations. These were used to update the HoQ and modify the prototype accordingly.
Based on a review by members of the OPMT, the decision was made to move ahead with full deployment of the remaining organizational structures. The Audit-Calc (Beta1) was developed and tested using artificial cases designed by the OPMT. These included all potential combinations of organizational structures, scope of certification, number of employees and combined audits. The system was released to all users together with a tracking system to obtain real time feedback from users. All issues identified by users were addressed in developing Audit-Calc (Beta 2). Audit-Calc© V 1.0 was copyrighted to WSU and released on March 2013 as scheduled. The system can be accessed through http://www.auditcalc.wichita.edu/auditcalc/

6. Conclusions

Achieving high levels of customer satisfaction and reducing the risk of failure requires the use of an appropriate software development approach. This approach should consider the voice of customer and assure customer involvement throughout the design phase. In this paper, an integrated model has been utilized for the development of the Audit-Calc software. The model builds on the popularity of the waterfall model and the flexibility of the prototyping model. It offered protection against project overruns by limiting the scope of prototyping to a selected module or pilot function. In so doing, the integrated model has shown an advantage over traditional models by eliminating the risk of developing systems based on vague or inaccurate requirements. The iterative use of the prototype, representing only a fraction of the system size, allowed for the accumulation of valuable knowledge regarding customer needs and expectations. The HoQ was utilized to secure documentation of knowledge, track changes in customer requirements and the prototype design targets. Such additional knowledge assured successful deployment and led to high levels of users' satisfaction. These authors are in the process of developing a cost function that can capture the economic benefits of applying the integrated model and its impact on the software maintenance costs.

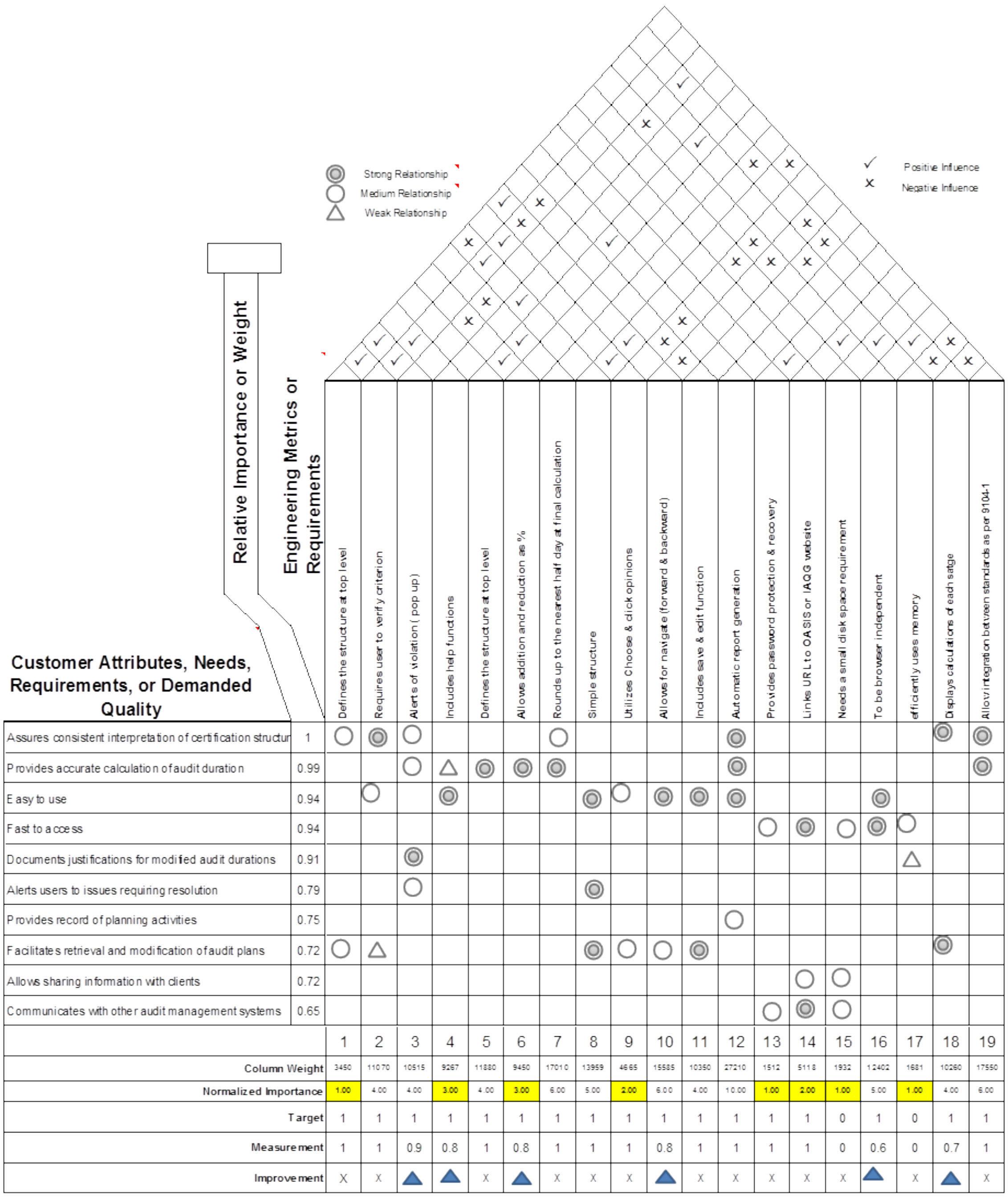

Figure 6. HoQ Matrix for Prototype Design

References

Akao, Y. (Ed.). 1990. Quality Function Deployment: Integrating Customer Requirements into Product Design. Productivity Press, Cambridge, MA.

Amlani, R. D. (2012). Advantages and Limitations of Different SDLC Models.IJCAIT, 1(3), 6-11.

Curtis, B., et al. (1988). "A field study of the software design process for large systems." Communications of the ACM 31(11): 1268-1287.

Davis, A. M., et al. (1988). "A strategy for comparing alternative software development life cycle models." IEEE Transactions on Software Engineering 14(10): 1453-1461.

Doke, E. R., & Swanson, N. E. (1995). Decision variables for selecting prototyping in information systems development: a Delphi study of MIS managers. Information & Management, 29(4), 173-182.

Gartner. (2014). Gartner says worldwide it spending on pace to reach $3.8 trillion in 2014. Retrieved March 30, 2014, from http://www.gartner.com/newsroom/id/2643919

Hauser, J. R. and D. Clausing (1988). "The house of quality."

International Standard. ISO/IEC 9126-1 (2001), Institute of Electrical and Electronics Engineering, Part 1,2,3: Quality Model, 2001.

Internet Web Stats (2012). "Internet use in the world." Retrieved March 4, 2014, from http://www.internetworldstats.com/stats.htm.

Lowe, A. and K. Ridgway (2000). "UK user's guide to quality function deployment." Engineering Management Journal 10(3): 147-155.

Montgomery, D. C. (2013). Introduction to statistical quality control. John Wiley & Sons.

Munassar, N. M. A., & Govardhan, A. (2010). A Comparison Between Five Models Of Software Engineering. International Journal of Computer Science Issues (IJCSI), 7(5).

Royce, W. W. (1970, August). Managing the development of large software systems. In proceedings of IEEE WESCON (Vol. 26, No. 8).

Sage, A. P., & Palmer, J. D. (1990). Software systems engineering. Wiley-Interscience.

Terninko, J. (1997). Step-by-step QFD: customer-driven product design, CRC Press.

The Impact of Variance on Combining Antithetic Time Series

Dennis Ridley[1]
Pierre Ngnepieba[2]
[1]*SBI, Florida A&M University and Scientific Computing, Florida State Univ., dridley@fsu.edu*
[2]*Department of Mathematics, Florida A&M University, Pierre.ngnepieba@famu.edu*

Abstract

Combining lognormal antithetic time series is a method for reducing bias and mean square error (MSE) in the fitted values obtained from a time series model. The method works because the variance of the logarithm of the time series is naturally small. Since some time series may have large variance, the implication of the amount of variance is investigated. The percentage reduction in MSE increases with variance up to a limit then falls. An antithetic combined MSE analytical function of variance is presented.

1. Introduction

The problem of bias in time series models is well known (see Copas (1966), Griliches (1961), Kendall (1954), Klein (1958), Koyck (1954), Marriott and Pope (1954), and Nerlov (1958)). When the parameters of the model are biased, fitted and forecast values are also biased. Traditional combining involves independent estimates obtained from two or more different models (see Armstrong (1989), Bates and Granger (1969), Bunn (1979), Clemen (1989), Clemen and Winkler (1986), Hibon and Evgeniou (2005), Lahiri, K. & Martin, G. (2010), Makridakis and Hibon (1979), Makridakis, et. al., (1982), Zou and Yang (2004)). The independent models may collectively contain more information than any one model, thereby improving the model. However they do not necessarily correct systematic bias that might occur in any one or more of the models.

The method of combining antithetic time series is used to reduce systematic bias in fitted values from a time series model. Mathematical proof of the method exists for lognormally distributed data. This method of reducing bias also reduces model fitted MSE. The theory of combining antithetic time series relies on the reversal of correlation in the component of fitted values that is biased. Perfect correlation reversal relies on infinitesimally small variance in the logarithm of a time series. In practice the time series data have finite variance. The variance of the logarithm is also finite, albeit small. The method works because the variance of the logarithm is naturally small. However, we are interested to know the practical implication of increasing variance. We observe that the percentage reduction in MSE increases with variance up to a limit then falls. An analytical function that shows the relationship between the antithetic combined MSE and variance is presented.

The paper is organized as follows. The theoretical basis for combining antithetic time series is reviewed in sections 2 and 3. The effect of variance on percentage reduction in MSE is illustrated in section 4. The analytical MSE function of variance is given in section 5. The conclusions in section 6 contain recommendations for future research. An empirical example is given the Appendix.

2. Background

The method of combining antithetic time series for reducing bias was proved by Ridley (1999) and demonstrated by Ridley and Ngnepieba (2014) for the well-known CompanyX data. The CompanyX data was first published by Chatfield and Prothero (1973) who demonstrated the nature of the bias while attempting to fit various autoregressive integrated moving average (ARIMA) models. Ridley and Ngnepieba (2014) also showed that combining antithetic time series satisfied the Diebold and Mariano (1995) test for significance in forecast improvement. See also Ngnepieba and Ridley (2011), Ridley, et. al. (2012), and the empirical example in the Appendix.

The Ridley (1999) antithetic time series theorem states that 'if $X_t > 0, t = 1,2,3,...$ is a discrete realization of a lognormal stochastic process, such that ln $X_t \sim N(\mu,\sigma)$, then if the correlation between X_t and X_t^p is ρ_{XX^p}, then $\lim_{p\to 0^-,\sigma\to 0} \rho_{XX^p} = -1$.' The standard deviation σ_x and variance σ^2 are for the logarithm of the time series. Therefore, in practice, they are naturally small. However, in practical time series, the variance will not actually approach zero. Therefore, there will be some loss of efficacy in reversing the correlation and in combining antithetic time series. We will explore the impact on percentage reduction in MSE.

3. The antithetic combining model

The antithetic combining model (Ridley, 1999) is summarized as follows:

$$\hat{x}_{c,t} = \omega\hat{x}_t + (1-\omega)\hat{x}_t^{'}, t \in n \quad (1)$$

where x_t are obtained from *n* data observations indexed by time *t*, and $\hat{x}_t$ are fitted values obtained from a time series model $x_t = \Phi x_{t-1} + \epsilon_t, t \in n$. The parameter $-\infty<\omega<\infty$ is a combining weight. The fitted values $\hat{x}_t$ and $\hat{x}_t^{'}$ are antithetic in the sense that they contain components of error $\hat{\epsilon}_t$ and $\hat{\epsilon}_t^{'}$, respectively, that are biased. When weighted, $\omega\hat{\epsilon}_t$ and $(1-\omega)\hat{\epsilon}_t^{'}$ are perfectly negatively correlated and therefore cancel. The antithetic component $\hat{x}_t^{'}$ is estimated from

$$\hat{x}_t^{'} = \bar{x} + r_{\hat{x}\hat{x}^p}\left(\frac{s_{\hat{x}}}{s_{\hat{x}^p}}\right)\left(\hat{x}_t^p - \bar{\hat{x}}^p\right), t \in n \quad , \quad (2)$$

where *s* denotes sample standard deviation, *r* denotes sample correlation coefficient, and the exponent of the power transformation is set to the small negative value *p*=-0.001. The value of ω is selected to minimize the combined fitted MSE in $\hat{x}_{c,t}$. If $\hat{x}_t$ are biased, then as *p* approaches zero from the left (not including zero), the correlation $r_{\hat{x}\hat{x}^p}$ approaches -1 and the bias in $\hat{x}_{c,t}$ diminishes. If $\hat{x}_t$ are unbiased then ω =1 and the combined fitted values are just the original fitted values. The combining calculations are performed by FOURCAST (2012).

4. The effect of variance on combined MSE

There is no way to control the variance of the actual time series data. The only way to investigate different variances is by computer simulation. To illustrate the effect of variance, let us consider the results of a hypothetical simulation for the lognormal time series $x_t = \exp(y_t)$, where $y_t = \beta y_{t-1} + e_t, t = 2,3,...,1000$, and $y_t \sim N(0,\sigma^2)$. Let the model to be fitted to x_t be $x_t = \Phi x_{t-1} + \epsilon_t, t = 2,3,...,1000$.

The least squares estimate $\hat{\Phi}$ of Φ and the fitted values $\hat{x}_t$ obtained from $\hat{\Phi}x_{t-1}$ will be biased if there is any model deficiency such as model misspecification, missing variables, data truncation or serial correlation in the errors, resulting in the covariance $Cov(\epsilon_t, x_{t-1}) \neq 0$. When σ^2=0, there is no variance. That is, no variations in the time series. Therefore, there is no MSE to be explained by the time series model. No improvement in MSE is possible by antithetic combining. Of course, the antithetic time series theorem does not include σ^2=0.

To simulate the theorem we consider small values of $\sigma^2>0$. For example, when $\sigma^2 = 0.01$, and *p*=-0.001, the correlation $r_{\hat{x}\hat{x}^p}$ starts out close to -1 (see Figure 1a). This is consistent with the Ridley (1999) theory of combining antithetic time series. The contribution to MSE reduction by antithetic combining is near maximum. As the variance increases, the potential to reduce unexplained variance by the fitted model increases. This contributes to the percentage MSE improvement that is possible. At the same time, the correlation moves away from the optimal value of -1 (see Figure 1b), reducing the ability for antithetic combining to improve MSE.

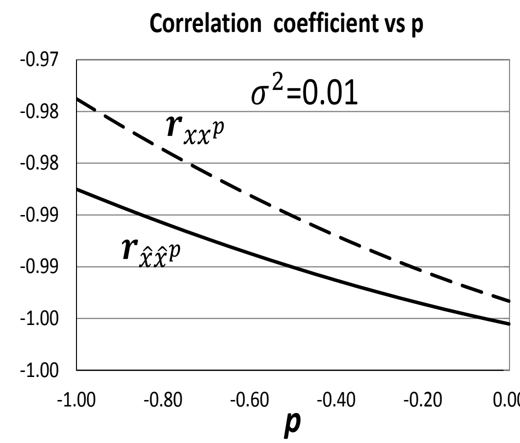

a. Correlation coefficient vs *p*

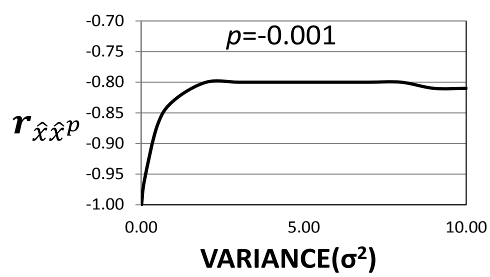

b. Correlation coefficient vs σ^2

Figure 1. Correlation coefficient (β=0.8)

Figure 2 shows the net of these two effects for different values of autoregressive coefficient (β).

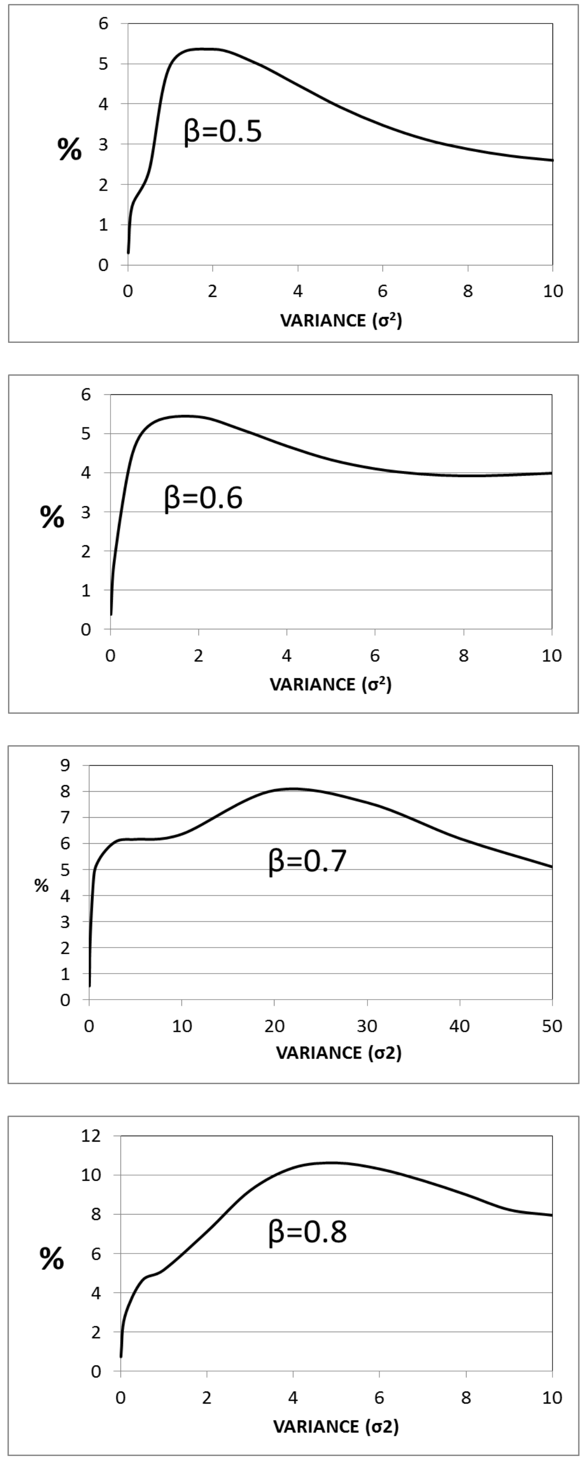

Figure 2. Percentage reduction in MSE vs σ^2

In general, the percentage reduction in MSE increases to a peak then it falls. For example, when $\beta = 0.8$, the maximum improvement (10.6%) in MSE reduction occurs at a variance of about 5. Also, the peak values are higher for larger values of β. Therefore, we can expect that antithetic combining will perform more or less well depending on the variance of an actual time series.

5. An MSE analytical function of variance

From equations (1) and (2),

$$\hat{x}_{c,t} = \omega\hat{x}'_t + (1-\omega) \times \{\bar{x} + r_{\hat{x}\hat{x}^p}\left(s_{\hat{x}}/s_{\hat{x}^p}\right)\left(\hat{x}^p_t - \bar{\hat{x}}^p\right)\}, p\to 0^-.$$

It has been shown (Ridley, et. al, 2013) that

$$\hat{x}_{c,t} = \omega\hat{x}_t + (1-\omega) \times [\bar{x} + r_{\hat{x}\hat{x}^p}\frac{\exp\{\bar{\ln \hat{x}} + s^2/2\}\sqrt{\exp(s^2)-1}}{\exp\{p\cdot \bar{\ln\hat{x}} + p^2s^2/2\}\sqrt{\exp(p^2s^2)-1}} \times \{\hat{x}^p_t - \exp(p\cdot \bar{\ln \hat{x}} + p^2s^2/2)\}], p\to 0^-.$$

Taking the limit as $p\to 0^-$, it can be shown that

$$\lim_{p\to 0^-}\hat{x}_{c,t} = \omega\hat{x}_t + (1-\omega) \times \{\bar{x} + \exp(\bar{\ln}\hat{x} + s^2/2) \times (-\bar{\ln}\hat{x} + \ln\hat{x}_t)\} \quad (3)$$

The error in $\hat{x}_{c,t}$ is given by

$$\lim_{p\to 0^-}\hat{x}_{c,t} - x_t.$$

Denoting the combined mean square error of $\hat{x}_{c,t}$ by MSEc,

$$\text{MSEc} = \lim_{p\to 0^-}\sum_{t=2}^{n}(\hat{x}_{c,t} - x_t)^2/(n-1).$$

Applying the power rule for limits,

$$\text{MSEc} = \sum_{t=2}^{n}\lim_{p\to 0^-}(\hat{x}_{c,t} - x_t)^2/(n-1)$$

Substituting for $\hat{x}_{c,t}$ from equation (3),

$$MSEc = \sum_{t=2}^{n}[\omega\hat{x}_t + (1-\omega)\{\bar{x} + \exp(\bar{\ln}\hat{x} + s^2/2) \times (-\bar{\ln}\hat{x} + \ln\hat{x}_t)\} - x_t]^2/(n-1)$$

We are interested in understanding the impact of variance (s^2) on MSEc. To that end, it may also be helpful to analyze the limit of the derivative $\lim_{p\to 0^-}\frac{d}{ds}MSEc$, or more simply by permutation of the limit and the derivative (see Buck,1978)) and analyzing $\frac{d}{ds}\lim_{p\to 0^-}\sum_{t=2}^{n}MSEc = \frac{d}{ds}\lim_{p\to 0^-}\sum_{t=2}^{n}MSEc.$

$$\frac{dMSEc}{ds} = 2\sum_{t=2}^{n}[\omega\hat{x}_t + (1-\omega)\{\bar{x} + \exp(\bar{\ln}\hat{x} + s^2/2)(-\bar{\ln}\hat{x} + \ln\hat{x}_t)\} - x_t] \times s(1-\omega) \times \exp(\bar{\ln}\hat{x} + s^2/2)(-\bar{\ln}\hat{x} + \ln\hat{x}_t)/(n-1).$$

$MSEc$ and $\frac{dMSEc}{ds}$ are functions of s and can be used to study its sensitivity with respect to the variance s^2 of the actual time series data.

6. Conclusion

Antithetic time series has applications in the analysis of engineering, scientific, medical and economic time series. Combining antithetic time series reduces bias and MSE in the fitted values obtained from a first order autoregressive time series model. As the variance of the time series increases, the reduction in MSE increases to its maximum value then it falls. Therefore, combining antithetic time series works more or less well depending on the variance of the time series. This research was based on the lognormal time series. Suggestions for future research are to apply antithetic time series theory to empirical time series of varying distributional characteristics.

7. Appendix

The below empirical example is for the CompanyX electric heater sales data. The 77 months of data are plotted in Figure 3. The model fitting period is January 1965 to April 1968. The forecast period is from May 1968 to May 1971. The Chatfield and Prothero (1973) method is based on the autoregressive integrated moving average model given by ARIMA: $(1+.37\mathcal{B})\nabla\nabla_{12}x_t^{.34} = (1-.79\mathcal{B}^{12})a_t$, where x_t are data, ∇ is the differencing operator, $\mathcal{B}$ is the backward shift operator, and a_t are random errors. The combined antithetic method is based on the twelfth order autoregressive model given by AR12: $x_t = \sum_{l=1}^{12} \Phi_l x_{t-l} + e_t$, where Φ_l are model parameters and e_t are random errors.

The AR12 model original MSE=2226 and the combined MSE=1906. The percentage reduction in MSE=14%. The forecasting results are plotted in Figure 3. Whereas the biased ARIMA foreasts diverge, the unbiased combined forecasts converge.

The results for the ARIMA model show that the forecasts diverge. This is due to the bias in the parameters of the ARIMA forecasting model. In order to extrapolate from the forecasting model, forecast values must be used in place of actual values that are not yet known. Therefore, the bias in the forecasts accumulates. The results of the combining model show that the forecasts converge. This is due to the correction of the bias. The forecast will continue to contain errors. But, the average error and the MSE will remain constant over the forecast horizon. Theoretically, this will continue indefinitely.

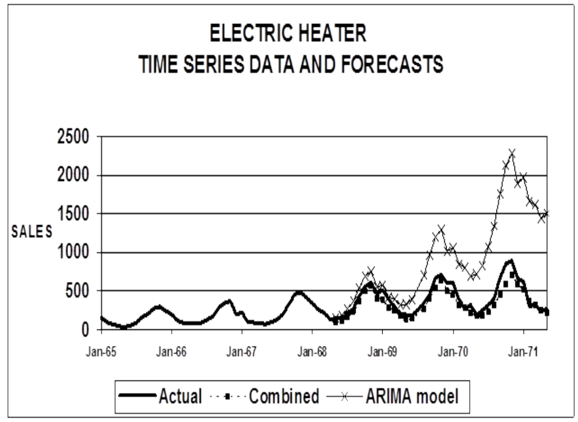

Figure 3. CompanyX data: Electric Heater sales forecasts for May 1968 to May 1971.

8. References

Armstrong, J. S. (1989). Combining forecasts: The end of the beginning or the beginning of the end, *International Journal of Forecasting,* 5, 585-588.

Bates, J. M., & Granger, C. W. J. (1969). The Combination of Forecasts, *Operational Research Quarterly,* 20, 451-468.

Buck, C. R., (1978). *Advanced Calculus, 3rd Edition*, New York: McGraw-Hill, p.270.

Bunn, D. W. (1979). The synthesis of predictive models in marketing research, *Journal of Marketing Research,* 16, 280-283.

Chatfield, C., & Prothero, D. L. (1973). Box-Jenkins seasonal forecasting: problems in a case study, *Journal of the Royal Statistical Society: Series A*, 136, 295-336.

Clemen, R. T. (1989). Combining forecasts: a review and annotated bibliography, *International Journal of Forecastng,* 5, 559-583.

Clemen, R. T., & Winkler, R. L. (1986). Combining economic forecasts, *Journal of Business and Economic Statistics,* 4, 39-46.

Copas, J.B. (1996). Monte Carlo results for estimation in a stable Markov time series, *Journal of the Royal Statistical Society, Series A,* 129 (1), 110-116.

Diebold, F. X. & Mariano, R. S. (1995). Comparing Predictive Accuracy, *Journal of Business and Economic Statistics*, 13, 253–263.

FOURCAST (2012). *Application program, EMC, Inc., Version 2012.1*, http://www.fourcast.net/fourcast. File: CompanyX.zip.

Griliches, Z. (1961). A note on serial correlation bias in estimates of distributed lags, *Econometrica,* 29, 65-73.

Hibon, M. & Evgeniou, T. (2005). To Combine or not to combine: selecting among forecasts and their combinations, *International Journal of Forecasting*, 21, 15-24.

Kendall, M. G. (1954). Note on bias in the estimation of autocorrelation, *Biometrika,* 41, 403-404.

Klein, L.R. (1958). The Estimation of Distributed Lags, *Econometrica,* 26, 553-618.

Koyck, L. M. (1954). *Distributed Lags and Investment Analysis.* Amsterdam: North-Holland Publishing Co.

Lahiri, K. & Martin, G. (2010). Bayesian forecasting in economics. *International Journal of Forecasting*, *26*, 211-215.

Makridakis, S., & Hibon, M. (1979). Accuracy of forecasting: An empirical investigation (with discussion), *Journal of the Royal Statistical Society, Series A,* 142, 97-145.

Makridakis, S., Anderson, A., Carbone, R., Fildes, R., Hibon, M., Lewandowski, R., Newton, J., Parzen, E., & Winkler, R. (1982). The accuracy of extrapolation (times series) methods: Results of a forecasting competition, *Journal of Forecasting,* 1, 111- 153.

Marriott, F. H C., & Pope, J. A. (1954). Bias in the estimation of autocorrelations, *Biometrika*, 41, 390-402.

Nerlov, M. (1958). *Distributed Lags and Demand Analysis for Agricultural and Other Commodities*. Washington: U.S.D.A Agricultural Handbook No. 141(June)

Ngnepieba, P., & Ridley, A. D. (2011). Inverse correlated gamma variables, *Journal of Management and Engineering Integration*, 4(2), 77-82.

Ridley, A. D. (1999). Optimal antithetic weights for lognormal time series forecasting, *Computers & Operations Research*, 26, 189-209.

Ridley, A. D., & Ngnepieba, P. (2014). Antithetic time series analysis and the CompanyX data, *Journal of the Royal Statistical Society,* A, 177(1), 83-94.

Ridley, A.D., Ngnepieba, P., & Duke, D. (2012). Optimal Parameters for Combining Antithetic Time Series, *Proceedings of the 18th Annual International Conference on Industry, Engineering, and Management Systems*, Cocoa Beach, FL., USA, March 25-28, pp.123-124.

Ridley, A. D., Ngnepieba, P., & Duke, D. (2013). Parameter Optimization for Combining Lognormal Antithetic Time Series, *European Journal of Mathematical Sciences,* 2(2), 235-245.

Zou, H. & Yang, Y. (2004). Combining time series models for forecasting, *International Journal of Forecasting*, 20, 69-84.

Biofuel Production: Stakeholders' Identification

Mostafa F. Fawzy

Iowa State University
mostafafady@gmail.com

Paul J. Componation

The University of Texas at Arlington
componation@uta.edu

Abstract

This article reports on the identification of Biofuel Production Stakeholders (BPS). Some researchers view BPS as a set of independent biofuel supply chains. Others focused on production without showing the BPS identification. Up to the researchers' knowledge, no research in the literature provide a detailed classification and selection of BPS. Thus, this paper uses a scientific and systematic method to determine the biofuel production stakeholders. Moreover, this methodology could be used as a guideline to build the scientific decision-making team for biofuel production. By application of the modified theory of stakeholder identification and salience, stakeholders are evaluated and classified into eight different groups according to their typologies. Identified stakeholders in this article are often the primary team of BPS, who should be included in any decision-making process related to the biofuel production process.

1. Introduction

Biofuel production as an energy resource has become a strategic issue for many countries. In 2011, 8% of the U.S. energy was from renewable resources. The remaining 92% came from non-renewable resources, including oil, natural gas, nuclear, and coal. Of the 8% renewable, slightly over half, 51% was produced from biomass. Within approximately a century, scientists predict that the world would run out of all the non-renewable resources of energy and renewable energy will be required to cover 100% of the world's energy needs (Wang, 2013).

The U.S. government realized the importance of renewable energy production and has established policies production. In 2005, the government adopted a federal level regulation known as the Renewable Fuel Standard (RFS) calling for the produce of 7.5 billion gallons of renewable fuel by 2012. This policy was revised in 2007 (RFS2) and production of renewable fuel target was increased to 36 billion gallons by 2022. Additionally, the U.S. government established tax credits for renewable fuel production to motivate investment in this industry (Wang, 2013). To promote further development, all stakeholder perspectives will need to be considered.

Biofuel production and its impact have been studied from many different perspectives. Most of the previous research focused on the economic or the environmental perspectives, or both (An, Wilhelm, & Searcy 2011; Ayoub et al.

2007; Dwivedi & Alyavalapati, 2009; EBTP Stakeholders, 2012; Larasati, Liu, & Epplin, 2012). Other researchers have looked at the legal perspective (Talamini et al., 2012; Youngs 2012), as well as the technical perspective and social impacts of biofuel (Meiera & Schrödera, 2013; Perimenis et al., 2011).

2. Study objective

The objective of this study is to identify biofuel production stakeholders (BPS) perspectives to provide decision makers with a comprehensive view of all biofuel production requirements and explore how these different perspectives may influence production approaches. The work will also serve as a basis for further exploratory research into renewable energy production strategies.

This is a methodology to identify, evaluate, and classify different BPS according to five different perspectives of biofuel production. This work is done through a management theory implementation on BPS, whereby different stakeholders' opinions have been explicitly taken into account for the decision-making process for biofuel production. This confirms all decision-makers' contributions in the decision-making, each with the right position.

3. Literature review

Industry, government and researchers have not yet reached a consensus on how to balance the multiple and often conflicting perspectives that influence biofuel production. To move toward this consensus we will need a better understanding of stakeholder groups, what their individual requirements are, and find ways to combine these perspectives so that alternative strategies for biofuel production can be explored.

Some work has been done to define and identify stakeholders. Turcksin and his colleagues (2010) defined stakeholders in general as "people who have an interest, financial or otherwise, in the consequences of any decision taken." Youngs (2012) pointed out that every person in the world, from their perspective, is considered as a biofuel stakeholder. Some have a direct relationship or impact on biofuel production and consumption where others have an indirect relationship. The European Biofuels Technology Platform (EBTP) defined stakeholders (2012) as "any organization who's commercial or business activities affects, or can be affected directly by the actions taken by the actions or recommendations of the EBTP."

Stakeholders' identification is a very early and important step in any decision-making process (Bomb, McCormick, Deurwaarder, & Kåberger, 2007; United States Department of Agriculture, 2012). Some studies in this area begin with a listing of stakeholders. Huertas and his colleagues (2010) began the study by mentioning BPS. Youngs (2012) also presented BPS and values related to biomass feedstock choices. Another example is the study done by Talamini's and his colleagues (2012) in which they studied the structure and effect of stakeholders' agendas on U.S. ethanol production. Each study focused on understanding BPS rather than how each BPS was identified. For example, Turcksin and his colleagues relied on the stakeholders' groups represented by Turcksin and Macharis stockholders workshop (Turcksin & Macharis, 2009; Turcksin et al., 2010). This study identified the BPS as seven stakeholders groups for biofuel supply chain, which contained five people in their study.

A review of current and previously completed work shows multiple perspectives used, including financial, businesses (An, Wilhelm, & Searcy 2011; Ayoub et al. 2007; Dwivedi & Alyavalapati, 2009; EBTP Stakeholders, 2012; Larasati, Liu, & Epplin, 2012), research (Perimenis et al., 2011), legal and decision-making, and public and society (Talamini et al., 2012; Mteiera & Schrödera, 2013; Youngs 2012). The Roundtable on Sustainable Biofuels noted stakeholders include farmers, companies, non-governmental organizations, experts, governments (national & local), and inter-governmental agencies (Fortin, 2011; Lee, Rist, Obidzinski, Ghazoul, & Koh, 2011). Scientists, journalists, and policy-makers also are groups of stakeholders identified by Talamini and other (2012). One common theme found in the literature was to identify the BPS based on the needs of the specific study undertaken. This is a logical approach, however it does limit generalization of prior work to address a more system based assessment of biofuel production strategies.

As Dwivedi and Alavalapati stated (2009) in their study, the literature review shows that no study exists that quantifies stakeholders' perceptions regarding biomass-based bioenergy development.

Theory of stakeholder identification was initiated be Freeman (1984) in this book "Strategic Management: A Stakeholder Approach". At that time, he presented the concept of stakeholders and their importance in the management area (Mitchell, Agle, & Wood, 1997). Mitchell and his colleagues (1997) modified Freedman's original work by dividing stakeholders' attributes into legitimacy, power, and urgency. Stakeholders with legitimacy are those who influence value identification. This group of people or organizations set the requirements (customers' needs). Stakeholders with power are the group of people or organizations who have influence on value positions, which means the impact on requirements' ranking and priorities. The last attribute is urgency and this group influences value execution. This means this group affects how the solution is done to meet the set requirements. Figure 1 shows the three stakeholders' attributes with their overlapping (Mitchell, Agle, & Wood, 1997).

Mitchell and his colleagues (1997) identified the three classes and overlapping areas. The derivative four classes generated from the intersection areas are also shown in Figure 1. Mitchell also identified an eighth class as those who do not have any power, legitimacy, or urgency; this is called Non-stakeholders class. From Youngs (2012) definition of biofuel stakeholders, it seems that this class of stakeholders is not applicable for biofuel stakeholders in general and therefore does part of BPS research.

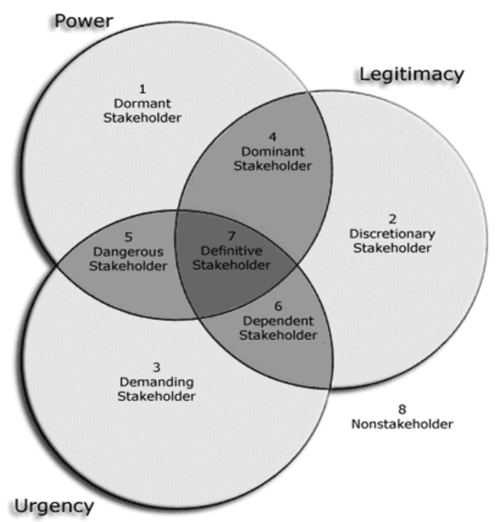

Figure 1. Stakeholders' typologies:
Source (Change Management Toolbook, 2013)

After that, Mitchell and his colleagues worked on what they call it latent stakeholders. They discussed the eight stakeholders' classes and suggested the stakeholder typology for each class. These typologies are shown in Figure 2. Change Management Toolbook represents the eight stakeholders' typologies through the three attributes zones and their intersections as in Figure 2 (Change Management Toolbook, 2013). In this figure the eights stakeholders' typology (Non-stakeholder) appears outside all the three attributes.

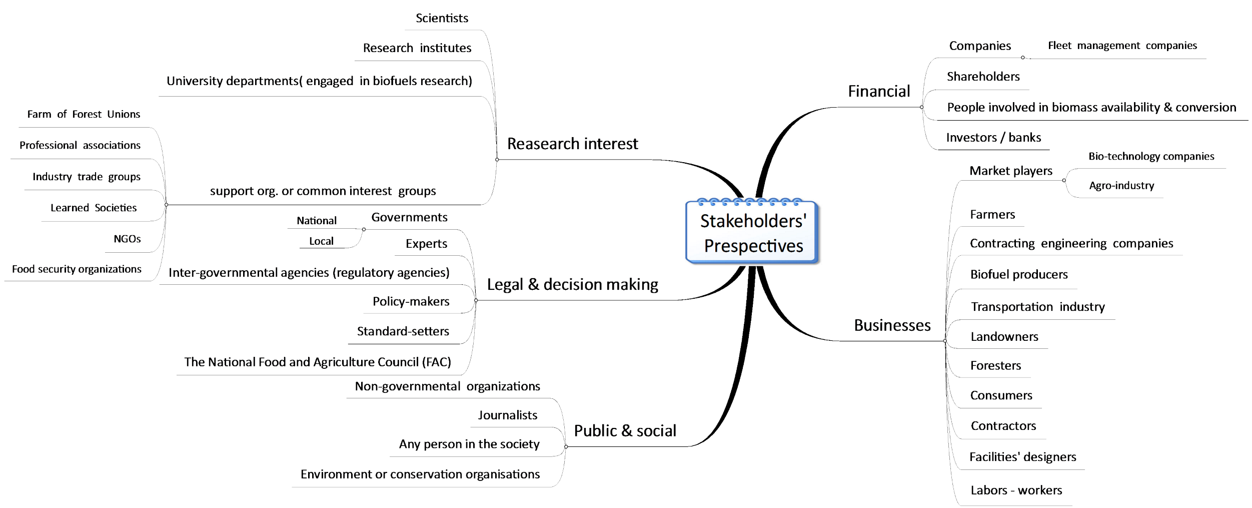

Figure 2. Mind map diagram for BPS perspectives and teams

According to Change Management Toolbook, stakeholders' groups are classified as shown in table 1 (Change Management Toolbook, 2013). This table presents the eight groups and the related attribute(s) for each one of them. Consequently, any stakeholder could be sorted by one of these attributes or by any of the intersected areas between them.

Table 1. Stakeholders classes based on attributes

#	Stakeholders group	Legitimacy	Power	Urgency
1	Dormant stakeholders		✓	
2	Discretionary stakeholders	✓		
3	Demanding stakeholders			✓
4	Dominant stakeholders	✓	✓	
5	Dangerous stakeholders		✓	✓
6	Dependent stakeholders	✓		✓
7	Definite stakeholders	✓	✓	✓
8	Non-stakeholders			

4. Methodology

To reach the research objective, six steps have been followed. First, the literature has been reviewed and the different perspectives for biofuel production have been identified. Then, different BPS teams were identified and linked to their related perspectives. After that, the researchers added some stakeholders' teams with explanations of their importance in such decision-making process of biofuel production that has not been mentioned in the literature. Next, the mind map diagram of BPS with different biofuel production perspectives has been created. Finally, BPS teams have been classified into different classes according to their typologies, which was identified by the theory of stakeholder identification.

5. BPS Identification and Analysis

In addition to BPS teams identified from the literature, the researchers believe in that contractors, facilities' designer(s), and labors / workers should also be considered as groups of the BPS. Although, Youngs (2012) limited contractors into those who "owns the commodity and pays the farm operator to raise it" while EBTP (2012) limited them into the contracted engineering companies, the researchers suggest that contractors' group should be expanded to include any contractor that involved in the biofuel production process. This definition exceeds Youngs and the EBTP definitions and it is the one used in this article.

In addition, the researchers believe that facilities' designer(s) should also be a team of the BPS especially at decisions that related to design, layout, and building phase of biofuel production facilities. The facilities' designer(s) participation(s) in decision-making during this phase will be derived from their core work.

Front line employees in biofuel production should contribute in decisions related to their work because they provide important details and ideas related to their daily work that helps the decision-making process. Furthermore, first line employees will be affected by these decisions. Their contributions could enhance decisions related to biofuel production and reduce their resistance to implementing the decisions (Al-Amre & Al-Fowzan, 1998; Jordanian government, Jordanian e-government program, 2007).

The researchers believe that each team has to be classified separately to get its value and attention in the decision-making process for biofuel production. With the researchers' proposed stakeholders' teams plus what have been mentioned previously in the literature as BPS, table 2 represents the complete BPS diagram. This diagram shows the five perspectives of biofuel production with the related teams of each perspective. As a total, thirty-six BPS teams in this figure are distributed on five perspectives for biofuel production.

6. Result and discussion

To recognize BPS teams' priorities, the theory of stakeholder identification has been used with its conducted modification, which is done by Mitchell and his colleagues (1997). To identify BPS teams according to typologies, stakeholders are listed and identified in a matrix as shown in table 2. In this matrix, BPS teams are sorted based on their related perspectives in rows. Then, typologies are listed in the top row. After that, the researchers filled the matrix based on the attributes definitions and their knowledge about each team's nature of the work in biofuel production.

In this matrix, thirty-six BPS teams are classified into seven different typologies and from five different perspectives for biofuel production process.

Table 2. Stakeholders' typologies matrix

Perspective	BPS Teams		Stakeholders' Typologies							
			Legitimacy/ Discretionary	Power / Dormant	Urgency / Demanding	Dominant	Dangerous	Dependent	Definite	Non-stakeholder
Financial	Companies (Fleet management com.)								■	▨
	Shareholders								■	▨
	People involved in biomass availability & conversion					■				▨
	Investors / banks			■						▨
Businesses	Bio-technology companies				■					▨
	Agro-industry				■					▨
	Farmers				■					▨
	Contracting engineering companies				■					▨
	Biofuel producers				■					▨
	Transportation industry				■					▨
	Landowners		■							▨
	Foresters		■							▨
	Consumers		■							▨
	Contractors					■				▨
	Facilities' designers				■					▨
	Labors – workers				■					▨
Research interest	Scientists				■					▨
	Research institutes				■					▨
	University departments(engaged in biofuels research)				■					▨
	Support org. or common interest groups	Farm of Forest Unions							■	▨
		Professional associations			■					▨
		Industry trade groups							■	▨
		Learned Societies			■					▨
		NGOs						■		▨
		Food security organizations		■						▨
Legal & decision-making	Governments (Local)			■						▨
	Governments (National)			■						▨
	Experts							■		▨
	Inter-governmental agencies (regulatory agencies)			■						▨
	Policy-makers			■						▨
	Standard-setters			■						▨
	The National Food and Agriculture Council (FAC)			■						▨
Public & social	Non-governmental organizations		■							▨
	Journalists		■							▨
	Any person in the society		■							▨
	Environment or conservation organizations			■						▨

As a result, out of these thirty-six teams, six are classified as the ones who have the legitimacy, nine as having the power, and thirteen as having the urgency. Moreover, by looking to the teams who combine two attributes together it was found that two groups are classified as having both legitimacy and power. These groups called Dominant groups. Likewise, two groups are classified as having both legitimacy and urgency, which are called Dependent groups. On the other hand, none of the groups is classified as having both power and urgency, which is called the Dangerous group. Similarly, none of the groups is classified as a non-stakeholder group. For this group, the result is expected due to the Youngs (2012) standpoint when he indicated that every person in the world is considered as a biofuel stakeholder. As he mentioned, some of them have a direct relation or impact on biofuel production and consumption where others have an indirect relationship. Thus, the researchers blocked out this column of stakeholders' typology in the analysis matrix. The result of BPS teams' distribution among the eight typologies is summarized in table 3.

Table 3. Summarized BPS teams' typologies

Legitimacy/ Discretionary	Power / Dormant	Urgency / Demanding	Dominant	Dangerous	Dependent	Definite	Non-stakeholder
6	9	13	2	0	2	4	0

The pie chart in figure 3 represents the percentage of BPS distribution among the eight typologies. From this pie chart as well as from the previous results table, it is noticed that the biggest group that will be affected by biofuel production is those teams who have the urgency (36.11%). After that, comes the group of people and / or organizations who have the power. This class represents exactly 25% of all BPS. The percentages of each stakeholders' typology is illustrated in Figure 3.

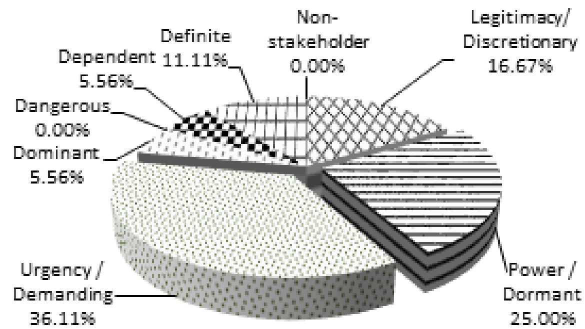

Figure 3. BPS distribution among typologies

Although, BPS identification is just an early step in the decision-making, however, upon the serious consideration of this step affects the validity of the decision taken. The amount of work in this step should rely on the size and importance of the decision. BPS could assess the decision according to their typologies. Their participation could be done through a questionnaire, workshop, meeting, or any other method, each according to the role and effectiveness in decision-making.

7. Assumptions and limitations

This study was conducted under three assumptions. First, the five perspectives educed from the literature are the only ones for the biofuel production. Second, the thirty-three BPS teams from the literature plus the three suggested teams by the researchers are considered the BPS teams. Last, the assessment and classification of BPS teams was done based on the researchers' understanding and belief of the nature and the role of BPS in the biofuel production process. Thus, this is the appropriate distribution for them in to the typologies' matrix.

8. Conclusion

In conclusion, this work proposed a supposed BPS teams' evaluation and classification in the eight typologies teams. In addition, these teams have been classified according to their perspectives of biofuel production. This was done through the application of theory of stakeholder identification and its modification that was done by Mitchell and his colleagues (1997). This work highlights the importance of stakeholders' identification, classifications, and the impact of this on the decision-making in general and especially for the biofuel production process. Instead of relying on any researchers' point of view or making workshops for a group of the BPS teams as what has been previously done, this paper used a scientific theory in management science as a method to present and classify BPS. This article provides a scientific method to assess BPS and classify them into several categories according to the extent of their influence and their perspectives about the subject. The results of this study could be used to get biofuel production decisions. Finally, this study might help to identify those who are responsible for decision-making and their influence into the decision.

9. Recommendations and Future work

For future work, this analysis could be re-conducted with a group of Subject Matter Experts to study the result's robustness or to have more validated analysis for the BPS classifications and typologies. Moreover, some other BPS teams if found could be added to the mind-map chart as well as to the analysis matrix. The additional teams could be evaluated and analyzed by using the same methodology applied in this study. Future work should be conducted to classify efficient methods of all BPS(s) involvement in decision-making process, where different tools and techniques could be used to get each BPS voice. Finally, the same study could be applied to identify other biomass products stakeholders.

10. References

Amre, Ahmad S. and Al-Fowzan, Naser M. (19/4/1421 A.H. - 8/6/1998) Employees Resistance to Change in governmental sectors, its reasons and ways of administration (Fieldwork presented in a scientific conference), Jeddah: King Saud University, Science Faculty, General Administration Department, Saudi Arabia.

An, H., Wilhelm, W. E., & Searcy, S. W. (2011). Biofuel and petroleum-based fuel supply chain research: a literature review. Biomass & Bioenergy, 35(9), 3763-3774.

Anonymous, Change Management Toolbook, (2013). Retrieved from: http://dev.change-management-toolbook.com/mod/book/print.php?id=74&chapterid=68.

Ayoub, N., Martins, R., Wang, K., Seki, H., & Naka, Y. (2007). Two levels decision system for efficient planning and implementation of bioenergy production. Energy conversion and management, 48(3), 709-723.

Bomb, C., McCormick, K., Deurwaarder, E., & Kåberger, T. (2007). Biofuels for transport in Europe: Lessons from Germany and the UK. Energy Policy, 35(4), 2256-2267.

Componation, P., "The Case for a Structured Analytic Decision Process," [PowerPoint slides] (2013). Retrieved from https://bb.its.iastate.edu/webapps/portal/frameset.jsp

Dwivedi, P., & Alavalapati, J. R. (2009). Stakeholders' perceptions on forest biomass-based bioenergy development in the southern US. Energy Policy,37(5), 1999-2007.

EBTP Stakeholders. (18 December, 2012). EBTP Stakeholders. In The European Biofuels Technology Platform . Retrieved March 16, 2013, from http://www.biofuelstp.eu/stakeholders.html.

Fortin, E. (2011). Multi-stakeholder initiatives to regulate biofuels: the Roundtable for Sustainable Biofuels.

Freeman, R. E. (1984). Strategic management: A stakeholder approach. Cambridge University Press.

Huertas, D. A., Berndes, G., Holmén, M., & Sparovek, G. (2010). Sustainability certification of bioethanol: how is it perceived by Brazilian stakeholders?. Biofuels, Bioproducts and Biorefining, 4(4), 369-384.

Jordanian government, Jordanian e-government program (2007) Change Management Manual, Edition 1, Pp. 2-14, Jordan: Jordanian government.

Larasati, A., Liu, T., & Epplin, F. M. (2012). An Analysis of Logistic Costs to Determine Optimal Size of a Biofuel Refinery. Engineering Management Journal , 24 (4), 63-72.

Lee, J. S. H., Rist, L., Obidzinski, K., Ghazoul, J., & Koh, L. P. (2011). No farmer left behind in sustainable biofuel production. Biological Conservation, 144(10), 2512-2516.

Meiera, H., and Schrödera, S., "Improving changeability by designing modularly structured production systems – considering production systems as sociotechnical systems," Procedia Computer Science, (March 19-22, 2013).

Mitchell, R. K., Agle, B. R., & Wood, D. J. (1997). Toward a theory of stakeholder identification and salience: Defining the principle of who and what really counts. Academy of management review, 22(4), 853-886.

Perimenis, A., et. al, "Development of A Decision Support tool for the Assessment of Biofuels," Energy Policy Journal, Vol. 39, No. 1 (January2011), pp. 1782–1793.

Talamini E, et al., (2012). "The Composition and Impact of Stakeholders' Agendas on U.S. Ethanol Production," Energy Policy Journal, Vol. 50, No. 1, pp. 647–658.

Turcksin, L., Macharis, C., 2009, Dedicated workshop for biofuel representatives in Belgium on 4th of June 2009, Vrije Universiteit Brussel.

Turcksin L., et al., (2010). "A multi-actor multi-criteria framework to assess the stakeholder support for different biofuel options: The case of Belgium," Energy Policy Journal, Vol. 39, No. 1, pp. 200–214.

United States Department of Agriculture, Summary Report of Stakeholder Responses to USDA's Regional Biofuel Roadmap, (2012). Retrieved from: http://dev.change-management-toolbook.com/mod/book/print.php?id=74&chapterid=68.

Wang, L., "Potential Competition for Biomass between Biopower and Biofuel under RPS and RFS2," [PowerPoint slides] (2013). Retrieved from http://echodelivery.cvm.iastate.edu:8080/ess/eco/presentation/85d4095e-b12a-47e8-b897-15b537feaa25

Youngs, H. L. (2012). In Perspectives on Biofuels: Potential Benefits and Possible Pitfalls, Ch 3: The Effects of Stakeholder Values on Biofuel Feedstock Choices,. Washington, DC: American Chemical Society. Taylor and Francis. Downloaded by IOWA STATE UNIV on March 16, 2013 from: http://pubs.acs.org

Development of Wearable Monitoring Systems for Future NASA Deep Space Exploration Missions

Wei Zhan[1]
Jacob Smith[2]
Abraham Garcia[3]
Collin Davis[4]
Jin Kim[5]

[1]*Department of Engineering Technology, Texas A&M University, College Station, TX 77843.*
[2]*Oncor Electric Delivery, Waco, TX 76710*
[3]*System & Technology Group, IBM FalshSystems, Houston, TX 77042*
[4]*Blueleaf Systems, San Marcos, TX 78666*
[5]*Mangstor LLC, Austin, TX 78759*
Corresponding email: wei.zhan@tamu.edu

Abstract

Texas A&M University collaborated with NASA to develop a low-cost wearable device with the capability of measuring carbon monoxide, carbon dioxide, and oxygen around the user in the spacecraft. This device is able to alert the user through sound and vibration if any dangerous thresholds are surpassed. Data are wirelessly transmitted to a base station. This article discusses the design requirements, hardware and software design, testing of the prototype, and the systems engineering approach used for the development of the wearable monitoring device.

1. Introduction

When discussing wearable technologies, the first thing which comes to a person's mind is probably Google Glass. However, long before Google Glass, wearable technologies have been explored and implemented in other areas (Stein, 2003; Bonato *et al*, 2004; Bonato, 2005). One of the first wearable technologies developed, known as the Georgia Tech Wearable Motherboard, or the "Smart Shirt", was developed for medical and battlefield use (Gopalsamy, 1999). Miniature sensors were attached to the human body or part of clothing so that the patient/soldier can be monitored over extended periods of time. Accelerometers were installed as wearable sensors to monitor the movement of patients in rehabilitation or to enhance independent living for senior citizens (Kemp *et al*, 1998; Giansanti *et al*, 2003; Park and Jayaraman, 2003).

In addition, wearable technologies were used in research of bio-chemical analysis of body fluids during exercise (Morris *et al*, 2008). Heartbeat and temperature can also be monitored remotely for patients using wearable monitoring devices. The development of wearable technologies has opened up countless possibilities for monitoring a human being's physical condition in many applications.

A new area of application for wearable technology is monitoring the environment. This has direct application in space exploration. While in space, it is important to monitor the environment for safety of the astronauts. Earlier spacecraft monitoring systems measured many vital aspects of astronauts, including environment in the spacecraft and vital signs of each astronaut. The data recorded in the spacecraft is sent to mission control to be processed in order to ensure the astronauts' safety. Sensors of the monitoring system are hard-mounted to the spacecraft's structure which requires the crew to locate and physically go to a monitor on the spacecraft to determine environmental levels. Caution and warning signals are also centrally located in the spacecraft. In particular, with the time delay in communication increasing as NASA missions dwell deeper into space and the increasing complexity of spacecraft structures, these monitoring systems do not meet the need for keeping the astronauts safe during their space explorations.

NASA is aggressively pursuing research and development of wearable technologies for future deep-space exploration missions. The intent is that the astronauts will not have to go to locations where hard-mounted sensors and monitoring systems are located, nor go to the base station to look for necessary information. Instead, astronauts can move to any location inside the spacecraft with the monitoring system being attached to them at all times. This proves to be a more effective solution over the hard-mounted monitoring systems. The health of astronauts is one of the primary concerns for NASA. When dealing with zero gravity and being in a confined space, the environment is different than that of being on Earth. For example, in a space shuttle hot air does not rise and air circulation can be difficult to uphold. When astronauts are working, they may work around the same area and are constantly breathing out carbon dioxide. As a result, the space surrounding the astronauts can be filled with dangerously high levels of carbon dioxide. If the monitoring system is installed a few yards away, the level of carbon dioxide near the monitoring system may not reflect the safety of the environment to the astronaut. Therefore, when wearable technologies are implemented in space, a more precise measurement may be provided, ensuring an astronaut's safety all the more.

Texas A&M University collaborated with NASA to develop a low-cost wearable device with the capability of measuring environmental parameters around the user as a basis of research in NASA's exploration into wearable electronics. This device will be able to detect carbon monoxide, carbon dioxide, and oxygen around the user, as well as alert the user if any dangerous thresholds have been surpassed. In addition, this data will be wirelessly transmitted to a base station for further analysis and data logging. Figure 1 illustrates the deployment of the Environmental Monitoring System (EMS) device in a spacecraft.

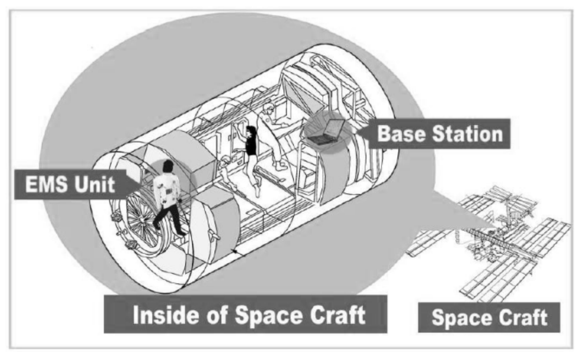

Figure 1. Deployment of the EMS device

This article presents the detailed design, testing, and the development process of the wearable EMS device. Section 2 presents the system requirements; detailed system design is discussed in Section 3; component level and system level tests are discussed in section 4; results are presented in section 5; conclusions and future work are discussed in section 6.

2. System requirements

The development of the EMS device was executed following the systems engineering approach. System design requirements were derived first, followed by a test plan and actual testing to verify that all design requirements had been met.

Due to its complexity, the project was also managed using many project management tools such as Critical Path Method, Work Breakdown Structure, Gant Chart, and the CPI SPI indexes for budget and time management. There are various processes that can be used to develop products (Brown and Eisenhardt, 1995; Muci-Küchler *et al*, 2007; Ulrich and Eppinger, 2011). The Texas A&M team followed the systems engineering approach (Reilly, 1993; Weaver and Vinarcik, 2006) during the development of the EMS device. Before designing the EMS device, a set of system design requirements were proposed by the Texas A&M team and approved by the Human Interface Branch of NASA. The EMS device is required to meet the following design requirements:

- EMS shall be comfortably wearable by astronauts.
- EMS shall be able to detect carbon monoxide, carbon dioxide, and oxygen around the user and alert the user if any dangerous thresholds have been surpassed, in which case audible alarms and vibration alarms shall be set. The thresholds should be adjustable by the user.
- EMS shall wirelessly transmit data to a base station within the spacecraft for further analysis and data logging. The range of wireless communication shall be at least 30 meters with direct line of sight.
- EMS shall be powered by rechargeable batteries that last at least 3 hours for continuous operation.
- EMS shall have a Graphical User Interface (GUI) for display to the astronauts. The GUI shall include sensor levels, thresholds, battery life, and wireless communication signal strength. In addition to the sensor outputs and thresholds displays, the base station shall have a GUI that allows users to add/delete astronauts to be monitored by EMS.
- EMS shall keep track of time when the wearable monitoring system is out of wireless communication range.
- EMS shall be expandable for future enhancement to include a radiation sensor. A hardware interface channel for Serial Peripheral Interface (SPI) of the micro-controllers should be reserved for the radiation sensor for future expansion.
- Total labor and parts cost of EMS shall be less than $1000.

3. System design

After the system design requirements were determined, the team at Texas A&M began designing the system architecture. A conceptual block diagram for the EMS device was created, as illustrated in Figure 2.

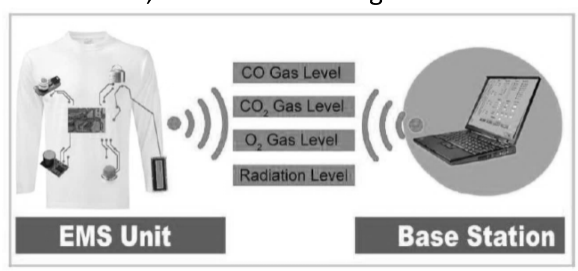

Figure 2. Conceptual block diagram of EMS

Based on the system requirements and the conceptual block diagram, extensive research was conducted to determine sensors and modules that were needed for the EMS device. It was determined that the EMS device needs an XBee module (Digital International Inc., 2012) for wireless communication (2.4 GHz) between the EMS device and the base station; an organic light-emitting diode (OLED) display screen; the micro-controller needs to have two universal asynchronous receiver/transmitter (UART) channels: one for the XBee module, and another for the carbon dioxide sensor; two SPI channels in the micro-controller: one for the OLED display, and the other for the radiation sensor Timepix (for future expansion); two analog-to-digital converter channels for sensing the battery voltage and reading the voltage signal from the carbon monoxide sensor; and three general input/output (I/O) pins for audible alarm, vibrator alarm, and alarm control button.

Based on the interface requirements, Freescale's MCF52259 ColdFire micro-the controller was selected for the EMS module. The functional block diagram is illustrated in Figure 3.

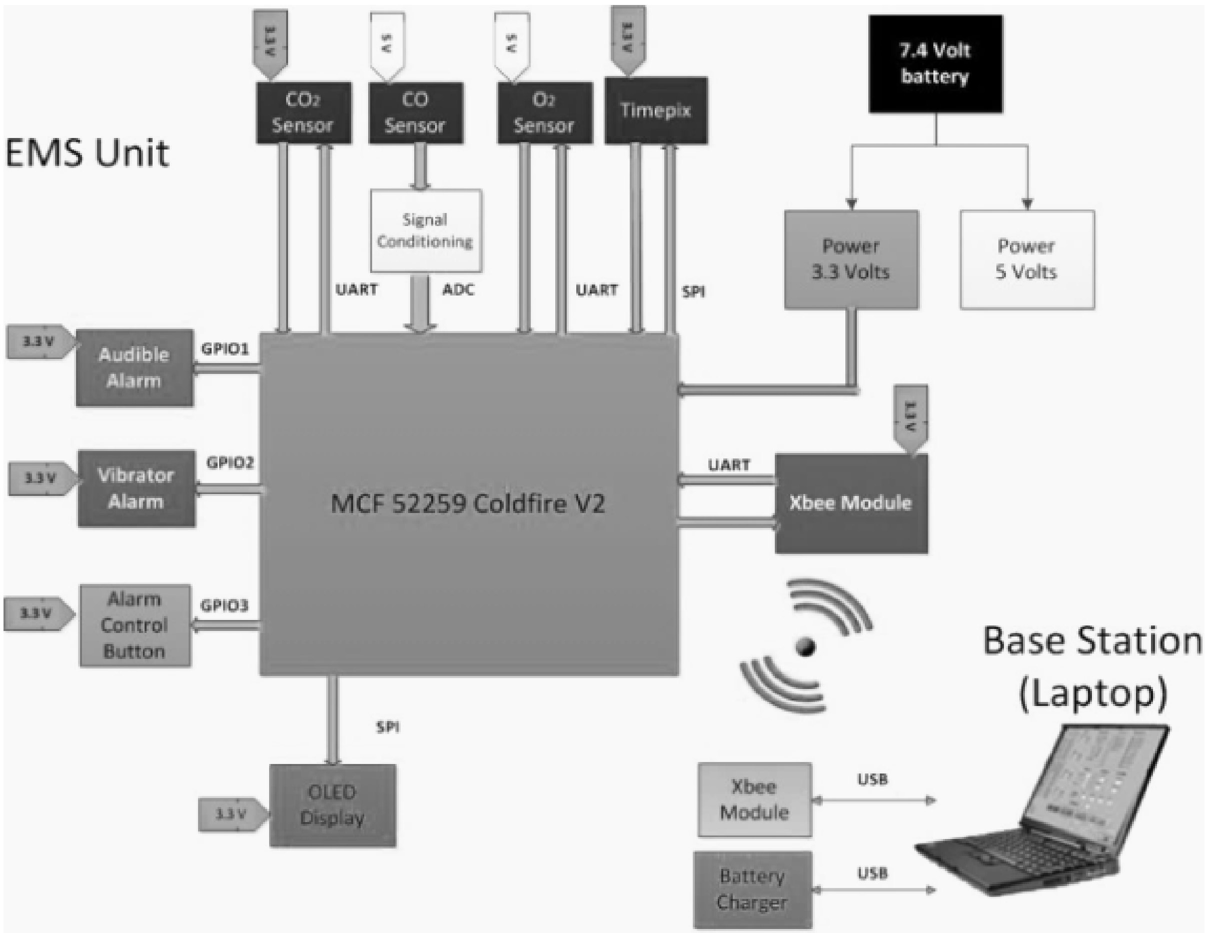

Figure 3. Functional block diagram of EMS

An electronic schematic was designed, simulated, and analyzed using Multisim (National Instruments, 2007). A two-layer printed circuit board layout was created in Ultiboard (National Instruments, 2007). The printed circuit board was manufactured by Advanced Circuits and populated by the Texas A&M team.

Embedded C code was designed for the EMS device. A LabVIEW GUI (National Instruments, 2003) for the base station, as illustrated in Figure 4, was developed so that the EMS devices and the base station can be set up easily for use by multiple astronauts. The flowchart for top-level LabVIEW software is partially shown in Figure 5. The GUI allows the user to set up the high and low limits for the oxygen sensor, the carbon dioxide danger limit, the carbon monoxide danger limit, and the radiation danger limit. Details of the software design can be found in (Smith *et al*, 2012).

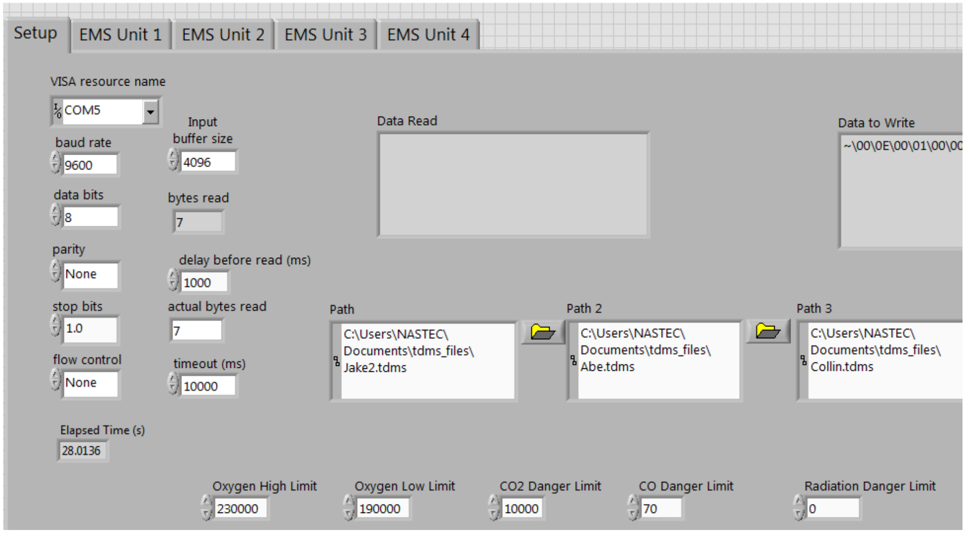

Figure 4. LabVIEW GUI for base station

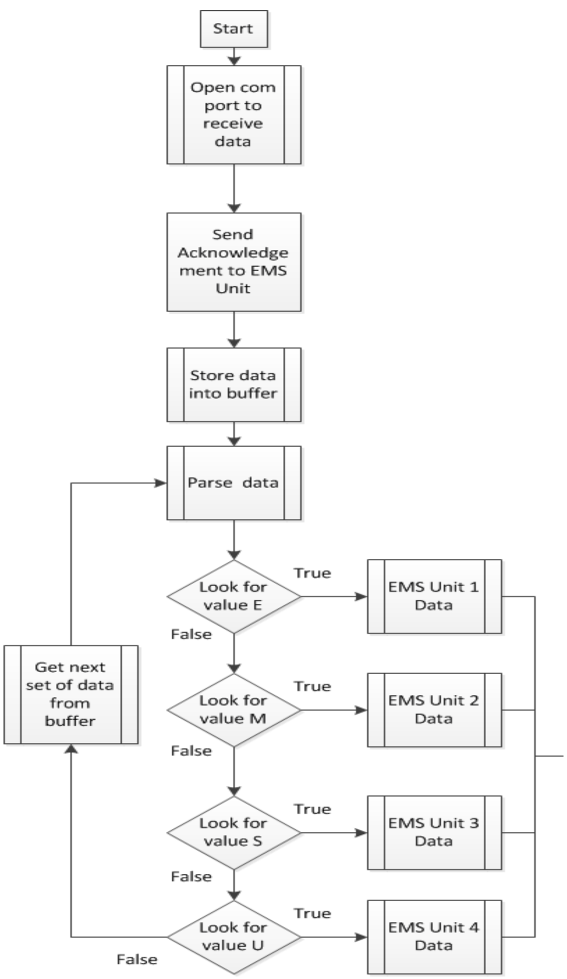

Figure 5. EMS software flowchart

4. Testing

After the system level requirements and main system architecture were developed, following the systems engineering approach, the team created a test plan which specifies system level, subsystem level, and component level tests which validate that all the design requirements are met. Each test procedure was described with specific information on test equipment and pass/fail criterion. These tests were conducted as soon as components, subsystem, or the entire EMS unit was available for testing.

Figure 6 shows part of the test matrix that relates each design requirement to tests that can be used to validate the requirements.

Before the integration of the EMS device, all important components and modules were thoroughly tested. The Texas A&M team used a bread board to test the carbon monoxide sensor, the carbon dioxide sensor, and the oxygen sensor. The tests were conducted in a NASA test chamber, as illustrated in Figure 7, with NASA space grade sensors and MES sensors taking measurements at the same time.

Func. Requirement / **Test**	Battery	User Interface	sensors	Zigbee Module	Alarm	Wearable EMS	LabVIEW	Data Storage
Running Time	x							
Recharge	x							
Display		x						
Gas Chamber			x					
Wireless communication				x				
Range		x		x				
Manually Trigger Alarms					x			
Movement						x		
Compatability with Base Station				x			x	
Data Logging								x
Data Log Retrieval							x	

Figure 6. Test matrix (partially shown)

The data from the NASA sensors were used to calibrate the EMS sensors, as shown in Figures 8 and 9. It can be seen that the EMS oxygen sensor consistently gives a slightly higher output than the NASA sensor. This was easily compensated by a constant offset implemented in the EMS software. The NASA carbon dioxide sensor's output was slightly lower than the EMS that of the EMS carbon dioxide sensor and the difference was not necessary constant. The NASA sensor actually had a higher level of noise than the EMS sensor at certain times. A small constant offset to the EMS sensor made the results closer to the NASA sensor output. The calibrated sensor outputs from EMS were used in the EMS device.

Before calibration, the differences between the NASA sensors and the EMS sensor were already small. After calibration, the differences were further reduced. Similar conclusions can be drawn for the carbon monoxide sensor. The radiation sensor is not implemented in the current version of the EMS device; only the hardware interface is provided for future expansion of EMS' functionalities. These results were reviewed by NASA engineers. Through this set of testing, the sensors were determined by NASA to have met the NASA requirements.

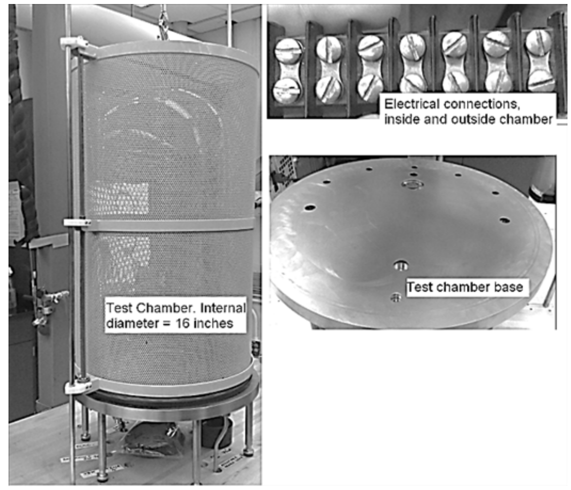

Figure 7. NASA test chamber

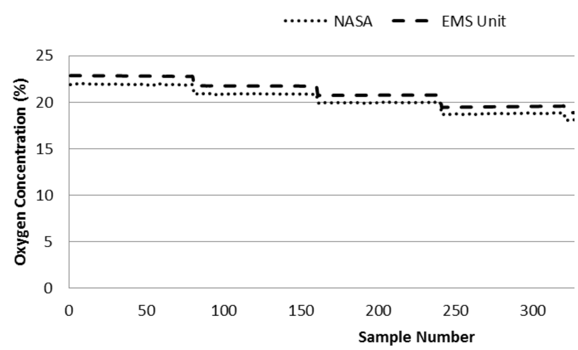

Figure 8. NASA and EMS oxygen output

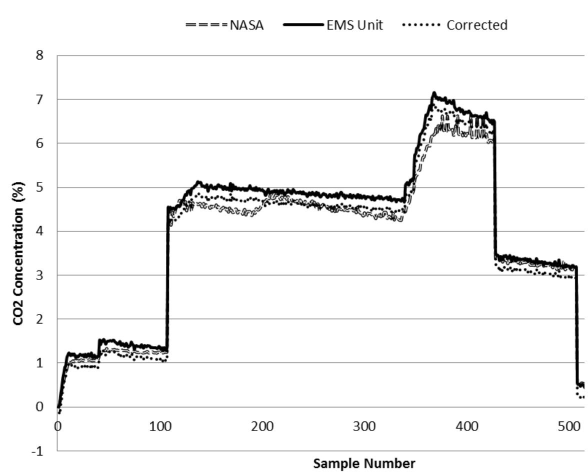

Figure 9. Carbon dioxide measurements

A number of other tests were conducted to verify that all design requirements had been met. Of these tests, one was the battery-life test. After the system integration was completed, the EMS device was set to run continuously until the battery voltage dropped below 6.8 V. Figure 10 shows the battery voltage as a function of time. The battery lasted over 3 hours, which met the system requirement.

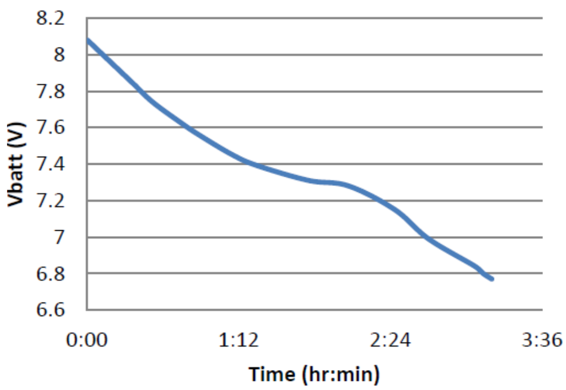

Figure 10. Battery life test

During the entire project, weekly review meetings were conducted where critical paths, project schedule, and budget were updated (Zhan and Morgan, 2011). Resources were reallocated when necessary to make sure tasks on the critical paths were completed according to schedule.

5. Results

After nine months of research and development effort by the Texas A&M team, a working prototype was built, thoroughly tested, and successfully demonstrated to NASA. The prototype is shown in Figure 11, with the display shown in Figure 12. The final product was worn to as far as 30 meters away from the base station. The device was able to communicate with the base station. Other design requirements were also verified with specific tests according to the test matrix and were determined to have been met.

The cost of a professionally populated EMS wearable device is below $400. This far exceeds NASA's target of $1,000. The low-cost design makes mass use of the devices by astronauts possible. A complete set of documentation, including user manual, design document, LabVIEW GUI, software code, circuit schematics, board layout, and test report, were submitted to NASA. After the demonstration, the prototype was also turned over to NASA for further research and development.

Figure 11. The EMS wearable monitoring system

Figure 12. EMS OLED display unit

6. Conclusions and future work

Following the systems engineering approach, a wearable monitoring EMS device was designed for NASA astronauts. System design requirements were derived first. The system architecture was selected after extensive research for off-the-shelf modules and components. Hardware and software was designed, integrated, and tested. All design requirements were verified. Project management tolls were used for managing the project.

During the developmental process, several areas for potential enhancement were identified: The EMS software can be wirelessly updated based on the data sent from the base station; a micro-controller with lower energy consumption can be used; different carbon monoxide sensors can be used to save energy. With these energy saving modifications, the battery life is expected to increase from three-and-a-half hours to over seven hours. Future work also includes the addition of the radiation sensor to the EMS module.

Acknowledgement: The authors would like to thank NASA for sponsoring the EMS development project.

References

Bonato, P. (2005). "Advances in wearable technology and applications in physical medicine and rehabilitation." *Journal of NeuroEngineering and Rehabilitation* 2:2.

Bonato, P., Hughes, R,, Sherrill, D.M., Black-Schaffer, R., Akay, M., Knorr, B., and Stein, J., (2004). "Using Wearable Sensors to Assess Quality of Movement After Stroke." *65th Annual Assembly American Academy of Physical Medicine and Rehabilitation, Phoenix (Arizona)*.

Brown, S. L. and Eisenhardt, K. M., (1995). "Product development: past research, present findings, and future direction," *Academy of Management Review*, Vol. 20, No. 2, pp. 343-378.

Digital International Inc., (2012). XBee ZigBee RF Module Development Kit Getting Started Guide. pp. 1-27.

Giansanti, D., Macellari, V., Maccioni, G., and Cappozzo, A. (2003). " Is it feasible to reconstruct body segment 3-D position and orientation using accelerometric data?" *IEEE Trans Biomed Eng* 50(4), pp. 476-483.

Gopalsamy, C., Park, S., Rajamanickam, R., and Jayaraman, S., (1999). The Wearable Motherboard™: The First Generation of Adaptive and Responsive Textile Structures (ARTS) for Medical Applications, *Virtual Reality*, vol. 4, pp. 152-168.

Kemp, B., Janssen, A.J., and van der Kamp, B. (1998). "Body position can be monitored in 3D using miniature accelerometers and earth-magnetic field sensors." *Electroencephalogr Clin Neurophysiol*, 109(6), pp. 484-488.

Morris, D., Schazmann, B., Wu, Y., Coyle, S., Brady, S., Fay, C., Hayes, J., Lau, K.T., Wallace, G., and Diamond, D., (2008). " Wearable technology for bio-chemical analysis of body fluids during exercise." *Conf Proc IEEE Eng Med Biol Soc.* pp. 5741-5744. doi: 10.1109/IEMBS.2008.4650518.

Muci-Küchler, K., Weaver, J., and Dolan, D., (2007)."Establishing Functional Requirements and Target Specifications: A Key Component of Product Development Projects," *Proceedings of American Society of Engineering Education Annual Conference*.

National Instruments, (2003). *LabVIEW User Manual*.

National Instruments, (2007). *NI Circuit Design Suite*.

Park, S. and Jayaraman, S., (2003). "Enhancing the quality of life through wearable technology." *IEEE Eng. Med. Biol. Mag*., 22(3), pp. 41-48.

Reilly, N. B., (1993). *Successful Systems Engineering*, Chapman & Hall.

Smith, J., Garcia, A., Davis, C., and Kim, J., (2012). "Environment Monitoring System," Texas A&M University Capstone Design Project Report.

Stein, J. (2003). "Wearable sensor technology for functional assessment after stroke." *IEEE Eng Med Biol Mag* 22(3), pp. 26-27.

Ulrich, K. T. and Eppinger, S. D., (2011). *Product Design and Development*, 5th Edition, McGraw-Hill, Irwin.

Weaver, J. and Vinarcik, M., (2006). "Combining Systems Architecture and Systems Engineering in an Engineering Management Program," *Proceedings of American Society of Engineering Education Annual Conference*.

Zhan, W. and Morgan, J. A., (2011). "Use of visual project management tools," *Journal of Management and Engineering Integration*, Vol. 4, No. 1, pp. 137-144.

Development of an Integrated Cost Management System for Small Business

Ekaterina Koromyslova, Ph.D.[1]
Carrie Steinlicht, Ph.D.[1]
[1]*South Dakota State University*
Ekaterina.Koromyslova@sdstate.edu; Carrie.Steinlicht@sdstate.edu

Abstract

Integrated Cost Management (ICM) has not been widely used by small businesses even though it has been shown to increase business effectiveness. Part of the reason for this is the lack of a comprehensive yet manageable ICM system for small manufacturing businesses. This study examines ICM methodology and concepts with the intent to build a framework for development of an ICM system that can be used by small manufacturers to effectively support decision making.

1. Introduction

Global competition is a driving force in manufacturing that compels companies to continually seek ways to build a competitive advantage in the marketplace. According to the U.S. Census Bureau, small manufacturing businesses provide 24% of all full-time employment in the U.S. (U.S. Census Bureau, 2010) Effectiveness of small manufacturing companies has a large impact on the U.S. economy and thus, it is important to determine ways that will help these companies compete.

Integrated Cost Management – a system approach to strategic cost decision-making based on sharing and integration of information across a company's business processes – is one way that could improve small manufacturer's competitiveness. However, a review of previous and current published research shows a lack of comprehensive ICM methodology for manufacturing enterprises. Much of the research that exists focuses on project cost management (Behrendt & Wulke, 2004; Nalewaik & Witt, 2009; Wulke & Kohl, 2004; Youngsoo & Sungkwon, 2004) or for cost management systems (Alarcon, Ashley, de Hanily, Molenaar, & Ungo, 2011; Anirban, 2001; Ellram & Siferd, 1998; Khoury, 2010; Seuring, 2002; Victoravich, 2010; Zbib, Rakotobe-Joel, & Rigoli, 2003). Less attention has been paid to ICM (Cooper & Kaplan, 1998; Cooper & Slagmulder, 2004; Kaplan & Cooper, 1998; Rwelamila & Hall, 1995; Saxena & Jain, 2012). There is very little evidence of ICM methods developed for small manufacturing businesses. Development of a structured systems approach to ICM will allow small manufacturing businesses to make better business decisions using best fit models and techniques.

2. Problem statement

The purpose of this study is to develop a framework for an ICM model that can be used by small businesses. To develop an appropriate framework, it is necessary to explore methods of cost management and determine the primary activities that must be considered in the scope of the ICM framework. It is also necessary to examine the tools and methods that are most important to a small business as well as the metrics that are the best indicators of performance. From this information, an ICM model will be developed and operationalized for testing.

3. Cost management methods

Much research has been done on cost management. The importance of cost management was recognized in the early 1900's with the work of Frederick Taylor. Since that time, there have been several methods developed and used as businesses evolved, technology was developed, and markets changed. The first cost management methods were used in the 1920's using standard costing. As markets and competition became more complex and eventually global, cost management methods evolved and in 1988, activity based costing was introduced by Cooper and Kaplan (1998). Computerization allowed the development of databases which gave rise to targeted strategic management processes (SMP's) during the 1990's. At the turn of the century, SMP's became integrated (Inst. of Management Consultants, 2000). New methodic approaches to cost management appeared which considered differences between cost cutting and cost optimization (Khoury, 2010). ICM is the newest approach to enterprise cost management. This new approach is possible because of the ability to collect and analyze large amounts of data quickly from all areas of the company and its partners. ICM is a systems approach that takes information from across the organization and examines interactions of cost factors to suggest actions that optimize cost outcomes. Cost management systems using ICM have been developed but are typically add-on modules to large ERP systems (Wulke & Kohl, 2004). These types of systems are often cost prohibitive for small businesses.

4. Relevant cost management activities

Researchers have done multiple studies on supply chain cost management and project cost management which examine different methods of cost analysis and management. Examples include Ellram (2002) who defined a simplified supply chain model and then described tools and procedures for supporting strategic cost management. Seuring (2002) describes several different supply chain cost management methods arguing that cost optimization can be achieved using supply chain partnerships. Zbib, Rakotabe-Joel, and Rigoli (2003) showed how cost management methods must fit the characteristics of the supply chain at that time. Behrendt and Wulke (2004) studied project cost management and showed how costs are typically collected at a lower organizational level than the level at which they are managed. They argued that actual costs should be summarized at a higher level for proper consideration in a cost analysis.

It is also important to classify costs for effective cost optimization. Studies by Victoravich (2010), Ellram and Siferd (1998), Christopher and Gattorna (2005), and others identify major cost classifications such as opportunity costs, costs of ownership, and true costs of inventory.

The primary purpose of cost classification and cost analysis is to identify the categories of costs which have the most impact on profitability and require managerial action. This study proposes that cost classification can be represented by five analysis levels that can be described as cost "filters" (Fig. 1). A company decision maker starts at the top level and sorts overall company costs into different groups and prioritizes them. The decision maker continues to move through the levels to the bottom. At the bottom level, the influence level, the costs are classified into the most important categories in an ICM system: hidden costs, conflicting costs, and opportunity costs.

There are many areas of enterprise activity that could be included in cost management analysis. These activities overlap across functions in an organization and influence other activities and costs associated with them. It is constructive to view enterprise activities as a value chain for cost management purposes

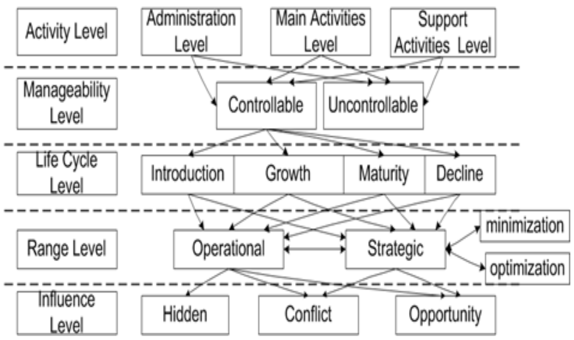

Figure 1. Cost structure analysis

(Anirban, 2011). Porter (1985) describes the value chain as a whole series of activities that add value in sequence. Each of these activities has inputs, transformation processes, and outputs. There are primary activities and support activities, each of which contributes to the overall cost and affects profits. Primary activities include inbound logistics, operations, outbound logistics, marketing and sales, and service. Support activities include infrastructure, human resource management, research and development, and procurement. Each of the activities is linked with other activities and these linkages are also important in the consideration of cost management.

In the proposed ICM system for small manufacturing companies, there are three activity levels that should be considered: the administrative level, the main activities level, and the support activities level (First level in Fig. 1). These three activity levels are detailed in Figure 2. The administrative level is a source of overhead cost that must be allocated. Cost management at the administrative level of an organization should use a cost driver analysis method because any decrease in allocated costs directly influences profit. By analyzing cost drivers, manageable sources of fixed costs (second level in Fig. 1) can be leveraged to minimize these administrative level costs.

When considering cost management in a small manufacturing company, most of the attention should be at the main activities level and then the support activities level. The main activities level includes production and

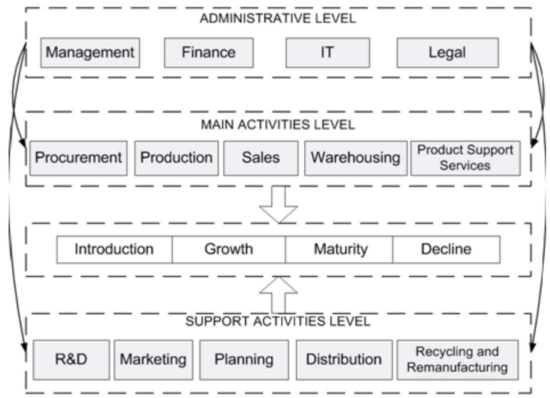

Figure 2. Cost of activity levels

operating processes relate to creating value for the customer. The support activities level includes required non-value added activities. Cost on these levels can be directly or indirectly associated with product and projected throughout the product life cycle, the third level of the cost structure in figure 1.

Each department is considered a profit center, which means that its performance is focused on increasing profit. This approach can help eliminate competition that develops between departments when they focus on cost reduction. When the focus is on cost reduction, costs are often passed on to other cost centers. When the focus is on increasing profit, efforts shift to making decisions that consider the system as a whole. The range level in the cost structure (Fig. 1) is concerned with the effect of strategic decisions versus operational decisions. By understanding the system wide effects and how they relate to overall company performance, cost can be optimized.

Different types of cost decision relationships and linkages (conflicting, indifferent, or synergistic) across the organization contribute differently to overall profitability (third level in Fig. 1). Since cost centers are linked in sequence, supply chain cost management methods can be applied (cost optimization via partnership) within a company, as well as project cost management methods (cost breakdown and summarization).

Thus, this type of cost classification within the scope of ICM can help to achieve an optimum value of total cost within the organization. By using this method, a company can consider the interrelationships of the decisions made by all parties within the company, and how these decisions fit with the goals and strategies of the company, as well as consider how these decisions will affect the customer or the market.

5. Cost analysis methods and techniques

A focus on the most influential and manageable costs in specific areas of enterprise activity assists in the choice of methods used in cost management. There are several studies available that have studied systems used in various contexts. Cooper and Slagmulder (2004) examined five different major techniques including target costing, product-specific kaizen costing, general kaizen costing, functional group management, and product costing. One of their conclusions was that integration of various techniques can help reduce costs throughout the product life cycle. Another important idea from this research is that effective cost management systems are designed for the specific context of the company. Production volume and product variety should influence the choice of the cost management system. In another study, Zbib, Rakotabe-Joel, and Rigoli (2003) examined four different companies that had implemented ICM techniques and also determined that context was important. Different cost factors could be used for defining target customers or products and for analysis purposes. In yet another study, Ellram and Siferd (1998) showed a relationship between total cost of ownership and the most relevant cost management methods and concepts. Anirban (2011) also describes how differing cost management tools can be applied to different activities in the value chain. Therefore, to effectively manage costs in a business, it is important to select tools appropriate for the context and activities that are part of the system.

Based on previous studies in the cost management field, the following ICM framework is suggested (Fig. 3). There are four main parts in this Integrated Cost Management Framework: cost management systems, models, methods, and a company's business activities.

Figure 3 contains a combination of three cost management systems (Strategic, Traditional, and Total Cost Management), two

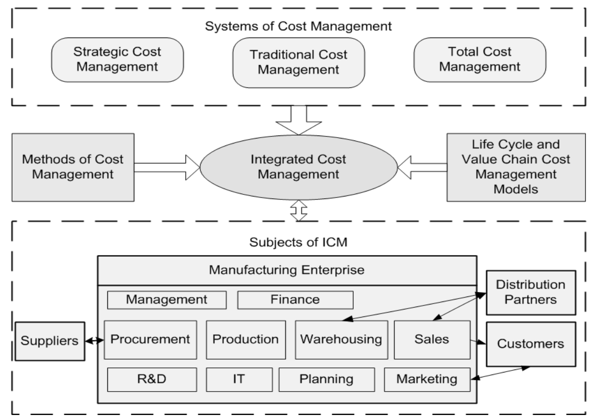

Figure 3. ICM schematic framework

management models (Life Cycle and Value Chain), and the most appropriate methods of cost management defined by each company individually. This combination should provide all the information necessary to properly analyze costs across the manufacturing enterprise.

Traditional cost management systems are accepted accounting based systems commonly used throughout industry. The Strategic analysis is included because ICM systems require a future orientation to meet goals. The third, the Total Cost Management is an integrated approach that applies specifically to project management which can serve as a basis for an ICM system for a small manufacturer.

The management models include the value chain orientation suggested by Porter (1985) and life cycle management which considers the life stage at which the product(s) exists to minimize resource use at the declining stage of a product's life cycle.

The main features of the ICM system are sharing of essential data between departments (which are considered profit centers), the company's top management, and its partners and customers; understanding how and where value for customers is created within a company and its supply chain; developing a way for integration of the different cost management systems and techniques which are a better fit for the company: complete or partial application of different cost management elements and their interconnections; and linking performance measurements across business processes (created value monitoring) and between organizational levels of a company (profit centers and higher level decision-makers).

6. Risk

Risk management is an important part of decision making. Cost management decisions carry with them an element of risk. Certain decisions are more risky than others. Cullen (2004) suggests that risk should be considered in terms of contingency planning or alternate approaches for mitigation of the risk. Others have used risk analysis, for instance using Monte Carlo simulation methods, to determine the most important risks that affect a decision (Alarcon, Ashley, Hanily, Molenaar, & Ungo, 2011).

In the proposed Integrated Cost Management framework, system enterprise risk is accounted for as one of the factors of decision making on the strategic level of cost optimization. Enterprise risk includes four types of risks: financial, market, operational, and information risk. The Composite Risk Index (CRI) is considered a control parameter for acceptance or rejection of an integrated cost alternative. CRI is calculated as a product of Impact of Risk Event and Probability of Occurrence. The acceptable level of the Index should be established by every company individually.

7. Metrics for ICM effectiveness

Despite the importance of effectiveness measures for ICM, there has been little research done in this area. Hyde, Regelman, and Kanagasabai (2008) offer a detailed methodology for development of a metrics system to measure performance in financial services. This methodology includes what and how to measure performance as well as how to use what is measured. In their research, the authors describe how different cost center objectives should use different metrics. They also show differences for short, medium, and long periods of time. Other research offers particular metrics that can be used by decision-makers (Nalewaik & Witt, 2009).

Because costs are analyzed at two levels of the organization, the operational level and the strategic level, it is necessary for the ICM system to use two levels of metrics: a profit center's performance metrics and metrics for the higher level decision-maker. The higher level metrics integrate performance information from production and operations levels, support strategic decision-making, and serve as "dashboard indicators" within the ICM system. The metrics should be balanced and should reflect not only financial information (e.g. profit, profit margin, ROI), but also production efficiency measurements (e.g., throughput, value added time ratio) and qualitative criteria (e.g. customer satisfaction).

8. Methodology of ICM framework formation

Every company determines its own approach to cost management based on existing systems, models and methods, and depending on a company's business processes and activities. Although there is no universal approach to ICM system formation, the following framework building methodology for an ICM system can be used by small businesses. The methodology is based on the integration and summarization of previous and current studies and includes cost analysis, cost management, and cost control steps to be taken by the small businesses. These steps should be done in order.

1. A cost structure analysis should be performed to figure out problem areas and potential areas for improvements paying special attention to opportunity costs, conflict costs, and hidden costs. Cost structure analysis and contribution margin analysis will reveal weak and unprofitable products.
2. Use a Pareto analysis to focus resources on the most important customers (products) and suppliers of materials for the products.
3. Life Cycle Stage should be determined for target products. Minimal resources should be utilized when a product is in the declining stages. Methods of cost reduction should be chosen correspondingly to life cycle stages.
4. A company should determine useful metrics for ICM and their interrelationships. Balanced higher level metrics should be included in a "dashboard" reporting and control system. The goal of the measurement system is a comprehensive analysis of the impact of costing decisions on the company's performance.
5. A risk management system, which determines a procedure for choosing actions for risk analysis, should be incorporated into an ICM system. A way for risk estimation and managing should be included.
6. The next step is to choose cost reduction methods. In this step, the company considers all the decisions made in the previous five steps and chooses cost reduction methods that are appropriate for the costs identified. The methods must be complementary to the company's business strategy. Predominantly, process improvement methods should be applied in terms of cost optimization, because they can help reveal and eliminate a company's hidden costs.
7. The final step of the ICM methodology allows integration of all obtained data and estimation of potential results of alternate cost management decisions. The objective function of the analysis is a sum of costs of all enterprise activities. These costs represent dependent variables. Independent variables are cost drivers which can be determined using a parametric cost analysis or empirically.

The optimal value of the objective function (integrated cost) is the minimal value that falls within the constraints defined for the ICM system. From the ICM framework an MS Excel simulation model can be created and validated using statistical software analysis. There should be a small magnitude of error between the two results; however, it should be insignificant.

9. ICM proposed model

The ICM Model is a decision making tool which allows a company to determine and estimate different costing alternatives and focus on the optimal combination of integrated components that provide the minimum value of total costs adjusted on the control parameters' constraints. The ICM Model includes three levels of components; Input, Variable Components, and Calculated Components (Fig. 4).

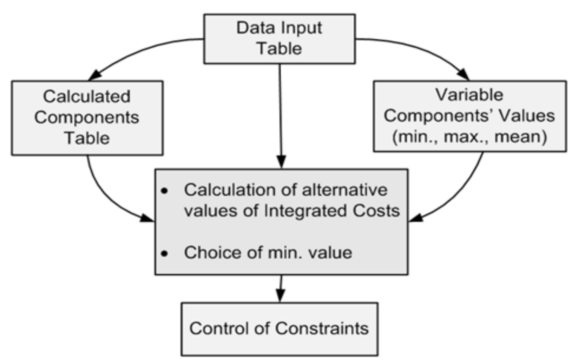

Figure 4. Simulation model structure

Realization of the ICM model in MS Excel provides a comprehensive and less expensive way for small businesses to manage their costs effectively.

Each profit center (department) has the same computer interface and inputs data, the independent variables' values, and the constraints' values. Then, the individual profit center analyses are combined at a higher decision making level to compare different combinations of cost alternatives in the Integrated Cost Alternatives analysis (Fig. 5).

An important part of the ICM Model is constraints, which determine control parameters for calculated components. There are three types of control. First is control of constraints including time, quality, capacity, and finance. The second is control of correct integration of profit centers' data. The third is control of "dashboard indicators" which are metrics of overall company performance.

Constraints are controlled by assuring that the minimum integrated cost value is achieved by the values of the variable components within

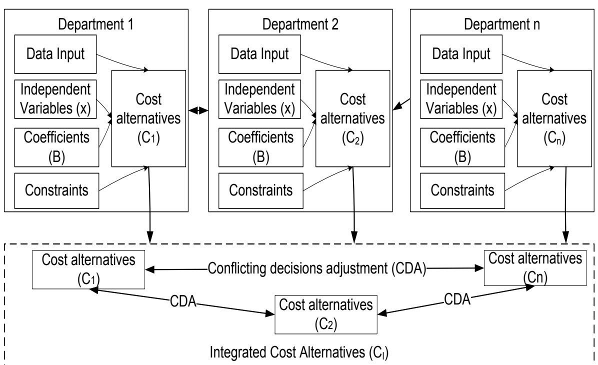

Figure 5. Profit centers' cost integration

the defined limits. If this condition is not satisfied, the next minimum integrated cost value should be considered, and so forth until the constraints' limits have been met. Also, because the profit centers' activities interconnect, some parameters of one profit center influence the parameters of another one, and vice-versa. So, the second stage of control is elimination or adjustment of conflicting decisions during the integration. The next control step is assuring that the chosen optimal value of total integrated cost provides the desired dashboard indicators. In other words, the indicators' values are not below minimum or above maximum acceptable levels.

The ICM Model simulation process can be represented by the following algorithm (Fig. 6). The obtained optimal result should be analyzed by the decision-maker, who interprets which combination of components provided the optimum.

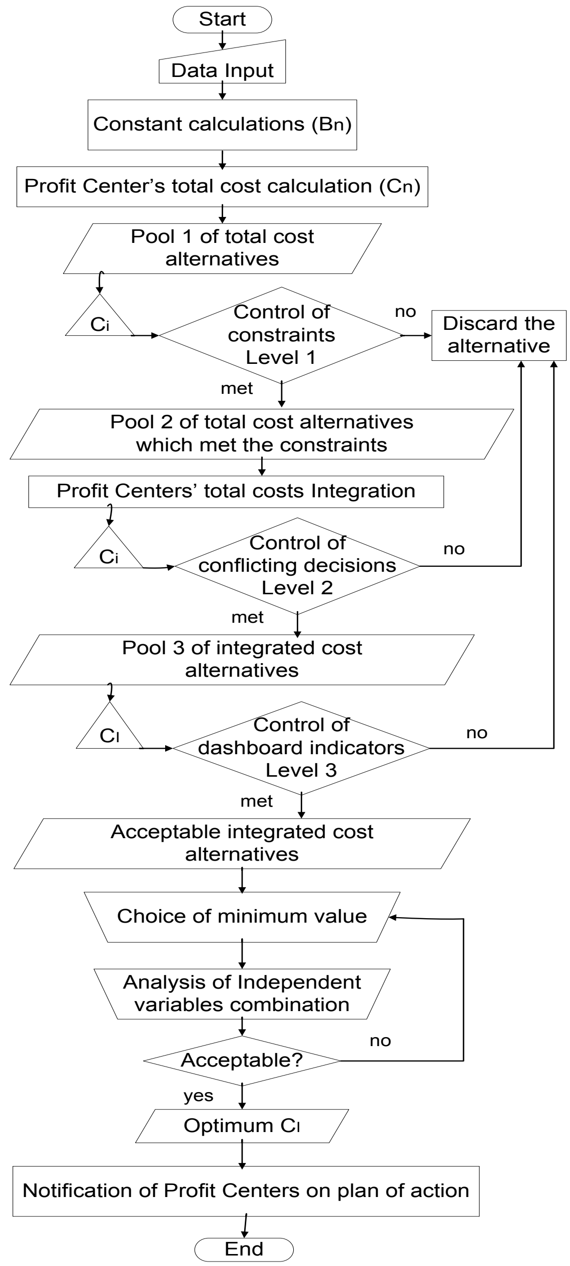

Figure 6. The ICM model algorithm

10. Preliminary results

Parts of this model have been tested at the procurement cost management stage in a company-manufacturer of kitchen equipment for public eateries. Preliminary testing indicates that this model will successfully indicate better solutions to cost problems in small manufacturing companies. The developed model provided thirteen percent decrease of procurement cost in comparison to the original approach used in the company. More data are needed to refine the model and additional parts are still in progress.

11. Conclusions

In this study a theoretical ICM framework has been developed and built for small manufacturing businesses. Finding the correct Integrated cost management approach is burdensome for small businesses, and the created ICM framework is designed to support business decisions by providing a clear methodological approach to cost optimization using fewer resources than traditional ERP based analyses.

In this research, various methods, techniques, and contextual conditions are examined for inclusion in a comprehensive ICM framework. Three cost management systems and two models have been adopted for this framework. Nevertheless, a choice of cost management methods has the flexibility to allow companies to use different factors appropriate to the specific company's context. This is especially important in the diverse market environments in which small manufacturers compete.

In the scope of the ICM framework for small businesses, the five-level cost classification, the measurement system, and the risk evaluation system have been developed. The cost classification requires five levels of cost structure analysis and results in extraction of costs targeted for exposure. The developed measurement system combines operational and strategic balanced metrics to monitor financial and nonfinancial company performance and shows whether the optimum integrated cost was achieved. The risk evaluation system is included in the ICM framework as a constraint factor. These analyses inform the developed ICM framework for small businesses.

In this study, an MS Excel simulation model is proposed to operationalize the ICM framework. The developed ICM framework is represented by the simulation model and should be customized for each company. The simulation model validity can be tested by the error magnitude evaluation in comparison with statistical software analysis.

Future work on this project will include using the model to analyze costs in existing small businesses and determining the effectiveness of the model.

12. References

Alarcon, L. F., Ashley, D.B., de Hanily, A., Molenaar, K. R., & Ungo, R. (2011). Risk planning and management for the Panama Canal expansion program. *Journal of Construction Engineering & Management*, 762-771.

Anirban, G. (2011). Total cost management: A new approach to cost control. *Advances in Management*, 63-65.

Behrendt, V. & Wulke, R. (2004). Cost management in scheduling applications: Using the right toolset for cost management. *Cost Engineering*, 13-15.

Christopher M. & Gattorna, J. (2005). Supply chain cost management and value-based pricing. *Industrial Marketing Management*, 115-121.

Cooper, R. & Kaplan, R. S. (1998). The promise and peril of integrated cost systems. *Harvard Business Review*, 109-119.

Cooper, R. & Slagmulder, R. (2004). Achieving full-cycle cost management. *MIT Sloan Management Review*, 45-52.

Cullen, S. (2004). Essentials of cost management. *AACE International Transactions.*

Ellram, L. M. (2002). Strategic cost management in the supply chain: A purchasing and supply management perspective. *Caps Research*.

Ellram, L. M. & Siferd, S. P. (1998). Total Cost of ownership: A key concept in strategic cost management decisions. *Journal of Business Logistics*, 55-84.

Hyde, P., Regelman, R., & Kanagasabai, K. (2008). The value of operations: Using metrics to measure performance in financial services. Retrieved from http://www.booz.com/media/file/The_Value_of_Operations.pdf .

Institute of Management Accountants. (2000). Designing an integrated cost management system for driving profit and organizational performance. *Strategic Cost Management Statements on Management Accounting*, Retrieved from http://www.imanet.org/PDFs/Public/Research/SMA/DesigningIntrCostMng.pdf .

Kaplan R. S. & Cooper, R. (1998). *Cost and effect; Using integrated cost systems to drive profitability and performance.* Boston, MA: Harvard Business School Press.

Khoury, G. R. (2010). Innovative cost optimization: A creative approach to finding new cost optimization opportunities. Retrieved from http://gkstrategic.com/pdf_image/Innovative%20Cost%20Optimisation%20-%20Gerald%20Khoury15.pdf.

Nalewaik, A. A. & Witt, J. (2009). Challenges reporting project costs and risks to owner decision makers. *Cost Engineering,* 15-18.

Porter, M. (1985) *Competitive Advantage: Creating and Sustaining Superior Performance*. New York: Free Press.

Rwelamila, P. D. & Hall, K. A. (1995). Total systems intervention: An integrated approach to time, cost and quality management. *Construction Management & Economics*, 235-241.

Saxena, L. & Jain, P. P. (2012). An integrated model of dynamic cellular manufacturing and supply chain system design. *International Journal of Advanced Manufacturing Technology*, 385-404.

Seuring, S.(2002). Cost management in supply chains – Different research approaches. In S. Seuring & M. Goldbach (Eds.), *Cost Management in Supply Chains*. Heidelberg: Physica-Verlag.

U.S Census Bureau. (2010). Statistics of U.S. Businesses (SUSB) Main. Retrieved from http://www.census.gov/econ/susb/.

Victoravich, L. (2010). When do opportunity costs count? The impact of vagueness, project completion stage, and management accounting. *Behavioral Research In Accounting*, 85-108.

Wulke, R. & Kohl, B. (2004). Cost management: Roadmap to project success - supplementing accounting systems for project cost management. *Cost Engineering*, 11-13.

Youngsoo, J. & Sungkwon, W. (2004). Flexible work breakdown structure for integrated cost and schedule control. *Journal of Construction Engineering and Management*, 616-625.

Zbib, I., Rakotobe-Joel, T., & Rigoli, R. (2003). Target costing: The key to supply chain excellence. *International Business and Economics Research Journal*, 27-34.

Milling of Stacks of Material Composed of Carbon Fiber Composites and Titanium Alloy for Aerospace

Jean-François Chatelain
José David Montoya
École de technologie supérieure (Université du Québec)
1100 Notre-Dame West, Montréal, Québec, Canada
jfchatelain@mec.etsmtl.ca; jose-david.montoya.1@ens.etsmtl.cas

Abstract

Carbon Fiber Reinforced Polymers (CFRP) composite materials are widely used today in the aerospace industry for their specific strength and stiffness, as well as their relative light weight, compared to metallic alloys. Even though composite parts are manufactured to near net shape, additional machining operations are required for assembly purposes, such as drilling to produce holes for screws, bolts or rivets. Unlike metallic materials, composite materials raise some specific problems during drilling, especially for stacks of material as CFRP over titanium plates. For this process, the machining conditions for both materials are incompatible. Damage in the form of delamination, cracks, and matrix burning is observed due to the evacuation of hot titanium chips, improper cutting conditions or tool wear. The production of titanium burrs at the tool exit is also an important issue. In this paper, an orbital milling process is proposed and optimized to generate holes by means of a milling tool being operated along a helical path into the workpiece. The objective of this study is to describe the effects of orbital milling on quality of holes in CFRP/titanium stacks and to propose key parameters and optimal cutting conditions for this process. It was found that the corner radius of tools and the helical step had a severe impact on the quality of holes. It was also found that different cutting conditions for each material as well as a finishing cycle at the end of the orbital milling cycle were required to produce best quality holes.

1. Introduction

Recent trends in the aerospace industry have seen increased use of composites and titanium alloys due to their exceptional mechanical properties. Composite materials are widely used not only for their higher specific properties (properties per unit weight) of strength and stiffness compared to metals, but also for their excellent resistance to fatigue and corrosion. Due to the dissimilar properties of titanium and CFRP, drilling parameters and drilling defects are very different in both materials. Surface delamination, thermal damage, fiber pull-out, and roughness variation along the hole are common defects encountered while drilling CFRPs (Abrao, 2007). For the titanium alloy, the most common defect is burr formation at the hole exit.

There are several factors affecting the extent of delamination in machining CFRP laminates. Wen-Chou worked on CFRP laminates, and found that increased delamination is related to tool wear, and that tool wear is related to machining temperature (Wen-Chou, 1997). Liu conducted a review of the literature and found that most of the studies examined show that increased delamination is related to greater feed rates (Liu, 2012). Hocheng et al. found, based on an analytic model, that delamination is directly related to thrust force (Hocheng, 2005). Another key factor in CFRP delamination is the tool geometry, as shown by Tsao in his study of step-core drills in CFRP laminates (Tsao, 2008). There are different approaches used to measure delamination. Faraz et al. propose a new criterion Fa based on a percentage of the delamination area and hole area, which avoids certain errors caused by fibers being pushed into and out of the hole, which could increase the delamination value (Faraz, 2009).

For titanium machining defects, Ramulu et al. found that burrs depend on cutting speed and feed rate. Under conditions of constant speed, the size of the burr decreases with an increase of the feed rate, while with a constant feed rate, the size increases with a cuting speed increase (Ramulu, 2001).

While multiple studies have examined the drilling of CFRP, only a few have been carried out on the CFRP/titanium stacks. Schulze mentioned that the advantage of orbital milling is that with it, damage in the workpiece is lower because process forces are directed towards the center of the workpiece. He also mentioned that different studies have found better quality holes using a helical milling-like process as compared to drilling (Shulze, 2011). Park et al. found that with the use of a metal bonded diamond core drill in CFRP laminates, hole delamination is improved (Park, 1995). Persson compared special tool geometries with dagger drills in CFRP with the KTH procedure, and found better results in hole quality and fatigue resistance (Persson, 1997). Yagishita found lower roundness using circular milling with a diamond coated drill bit (Yagishita, 2007). Finally, Brinksmeier showed that helical milling of Aluminum/CFRP/titanium composites leads to lower temperatures and lower forces compared to drilling. He also found that titanium chips do not cause temperature peaks on the CFRP surface, which improves surface quality, and lastly, he found that drilling CFRP laminates with a low cutting temperature is preferred over helical milling (Brinksmeier, 2002, 2011).

Regarding the cutting parameters used in machining these materials, a relatively high cutting speed (150-200 m/min) with a low feed rate (0.01 to 0.05 mm/rev) are recommended for drilling CFRP laminates in order to minimize delamination (Konig, quoted by Shyha, 2011), while low cutting speeds (10-30 m/min) with moderate feed rate (0.05-0.1 mm/rev) are recommended for machining titanium alloys, (Ramulu, quoted by Shyha, 2011).

This paper presents an approach to the helical milling of CFRP/titanium stacks, and focuses on CFRP surface delamination and titanium burr defects.

2. Methodology

The workpiece used was composed of CFRP and titanium plates. The CFRP was an autoclave-cured 24-ply laminate with a stacking sequence $[(90°,-45°,45°,0°,45°,-45°,45°,-45°,0°,-45°,45°,90°)]_s$ and 3.72 mm thick. The titanium plate was a 3.175 mm thick $TiAl_4V_6$. Tests were performed without lubrication, with a supporting back plate used to prevent the elastic deformation of the material. Holes were drilled using a 16x5 arrangement, with a distance of 15 mm between them, as shown in Figure 1, and tool wear was verified for every 5 holes. Holes were 6 mm in diameter, and were made with a 4 mm diameter tool. The tests were performed using a CNC machining center Huron K2X-10 with a Siemens SINUMERIK 840D controller. Holes were made with a Pocket cycle available within the controller. This cycle allows circular pockets to be made following a helical trajectory and a circular milling finishing pass at the bottom of the hole (Figure 2). The pocket cycle has different parameters which could be changed according to machining requirements.

The hole depth is defined by the _DP parameter, and was set at 1 mm below the bottom of the surface. The radius of the hole was set to 3 mm for the roughing sequence, while the finishing allowance was set by the _FAL parameter, with a 0.05-to-0.1 mm range. All machining components were set to up-milling mode. The axial feed rate was set by the _FFD parameter, while the circumferential feed rate was controlled by the _FFP1 parameter.

Finally, the helical step was set by the _DP1 parameter and the spindle speed configured before the controller started the cycle. Cutting forces were measured along the three axes components using a Kistler 9225B table. Individual testing was carried out, first with CFPR, and then with titanium. The optimized parameters found for each of the materials were then used to drill stacks by modifying the latter at the transition point between the two materials.

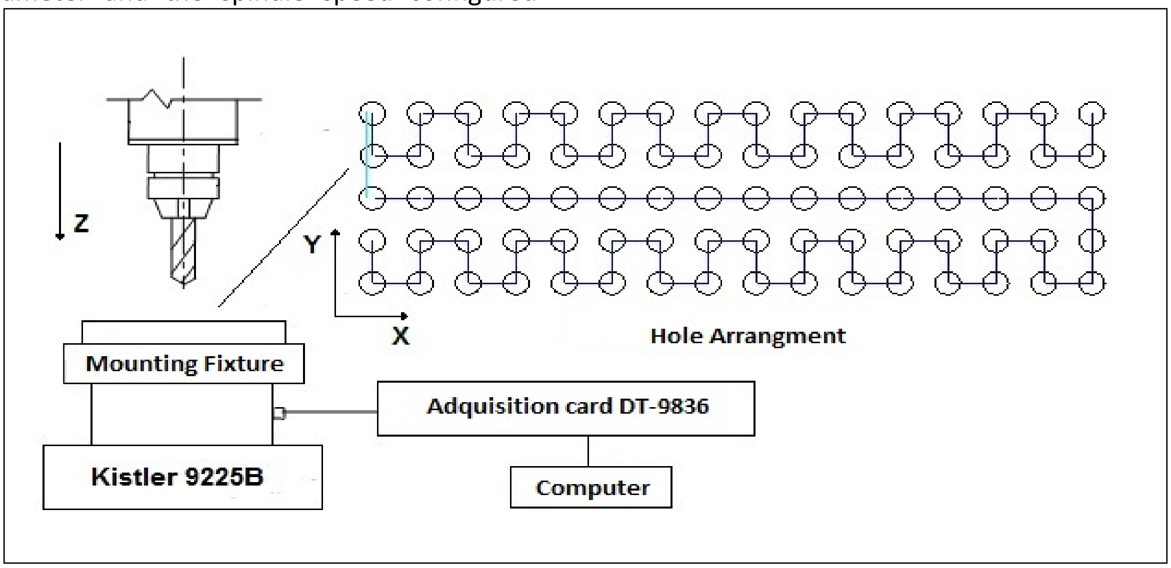

Figure 1. Experimental set-up

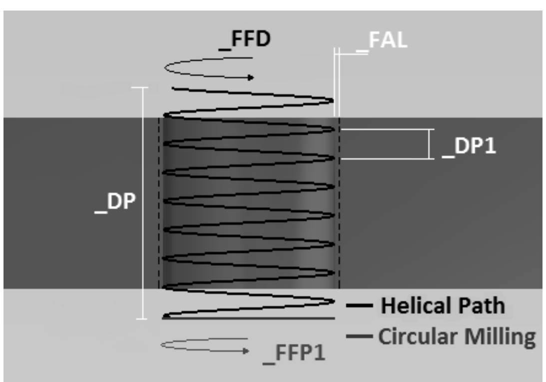

Figure 2. Parameters and tool path

Initial tests were performed with titanium alloy plates with a total of three different tools and a range of spindle speeds, axial feed rates, surface feed rates and helical steps, for two reasons: first, to select the more suitable tool for the testing, and secondly, to find the key parameters for the CNC controller cycle affecting the quality of the hole. The first tool tested (Type I, Figure 3) was a 4 mm diameter coated carbide drill bit, with four flutes, having a helix angle of 30° and a rake angle of 6°. The second tool tested (Type II) was a 4 mm diameter coated carbide drill bit, with four flutes, having a helix angle of 50° and a 0.5 mm corner radius. The third tool (Type III) was a 4 mm diameter coated ball end mill, with four flutes, having a helix angle of 20° and a rake angle of 6°. After preliminary tests, it was found that the most suitable tool to use for the rest of the study was the type I drill bit. We discuss the quality issues resulting from the preliminary tests for the three types of tools in the next section.

Following the preliminary tests, an optimization process, for the suitable tool, consisting of a design of experiments and an ANOVA analysis was performed to determine the factors, among those available with the cycle, that have a significant effect on the delamination of the CFRP laminate, on burr formation for the titanium plate, and on hole diameter for both materials. The influencing parameters were then varied in a study to find the best values, according to quality. This process was first performed for the titanium plates, alone, without a finishing cycle (Table 1). A total of 70 holes were machined to find appropriate axial feed rate and helical step values. Then, a study of the effect of the finishing tolerance was performed using the parameters shown in Table 2. The axial feed rate and helical step were kept constant with values equal to the best ones found in the previous study.

Following this process related to the titanium material, the optimization process was repeated for the CFRP laminates with the parameters shown in Table 3. As for the case of the titanium, a total of four tests were conducted, varying the finishing tolerance from 0 to 0.1 mm to study the finishing cycle influence on the quality of the hole, with the parameters shown in Table 4.

Finally, a total of 20 holes divided into four tests were performed within CFRP/titanium stacks. Ten holes were machined without the finishing cycle, and the rest with the finishing cycle. The machining tool was changed every 5 holes and tool wear was measured.

Figure 3. Tool types I, II and III

Table 1. Titanium Machining Test parameters

Test	Cutting Speed [m/min]		Axial Feed Rate [mm/min]		Helical Step [mm]		Number of Holes Per Test
#	Min	Max	Min	Max	Min	Max	
1	40		120	180	0.2	0.3	10
2			180	240	0.2	0.4	
3			240	300	0.3	0.5	
4			300	360	0.5	0.6	
5			300	360	0.2	0.4	
6			360	420	0.2	0.4	
7			420	480	0.2	0.6	

Table 2. Titanium Finishing Test parameters

Test	Cutting Speed [m/min]	Axial Feed Rate [mm/min]	Helical Step [mm]	Surface Feed Rate [mm/min]		Finishing Tolerance [mm]		Number of Holes Per Test
				Min	Max	Min	Max	
1	40	300	0.35	200	300	0.05	0.1	5
2				300	400	0.05	0.1	
3				200	300	0		
4				300	400			

Table 3. CFRP Machining Test parameters

Test	Cutting Speed [m/min]		Axial Feed Rate [mm/min]		Helical Step [mm]		Number of Holes Per Test
	Min	Max	Min	Max	Min	Max	
1	75	107	800	1000	0.25	0.5	10
2	107	138	600	800	0.25	0.5	
3	107	138	600	800	0.5	0.75	
4	75	107	800	1000	0.5	0.75	
5	75	107	800	1000	0.75	1	
6	107	138	600	800	0.75	1	

Table 4. CFRP Finishing Test parameters

Test	Cutting Speed [m/min]	Axial Feed Rate [mm/min]	Helical Step [mm]	Surface Feed Rate [mm/min]		Finishing Tolerance [mm]		Number of Holes Per Test
				Min	Max	Min	Max	
1	138	800	0.7	200	300	0.05	0.1	5
2				300	400	0.05	0.1	
3				200	300	0		
4				300	400			

Table 5. Cutting parameters CFRP/Titanium stacks

Material	Axial feed rate [mm/min]	Cutting Speed [m/min]	Helical Step [mm]
Titanium	300	40	0.35
CFRP	800	138	0.7

All parameters were kept in the same order to visualize the finishing cycle and tool wear influence on the results (Table 5). To measure the delamination, only the defects on the first plies of each side of the composite were considered, and the factor Fa was used, as proposed by Faraz et al. (Faraz, 2009). Areas were measured using the ImageJ software, as shown in Figure 4. This software allows the measurement of the area in pixels of different contours in any image. Burr height was measured with a Mitutoyo electronic height gauge at four positions around the circle, and the average for each hole was taken. Finally, a Mitutoyo Coordinate Measuring Machine was used to measure the hole diameter. It was measured in eight positions in the periphery of

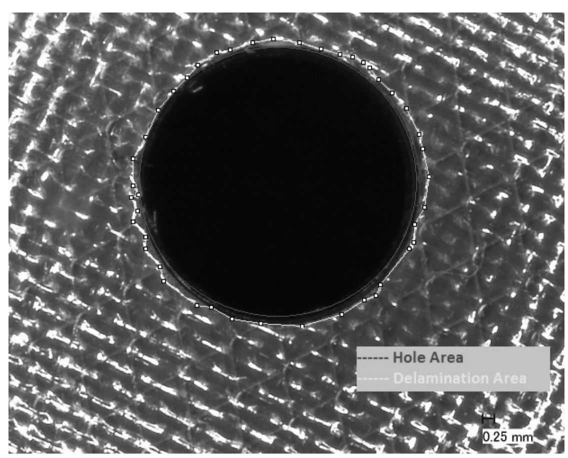

Figure 4. Delamination measurement

the hole, separated by 45 degrees at three different heights: 0.5 mm from the surface, 0.5 mm from the bottom, and in the middle of the hole. Figure 5 shows the measuring configuration for the CFRP/Titanium stacks.

3. Results

3.1. Key factors in the process

A total of three different tool geometries were used at the beginning of this experiment. Burr formation was the only criterion used to

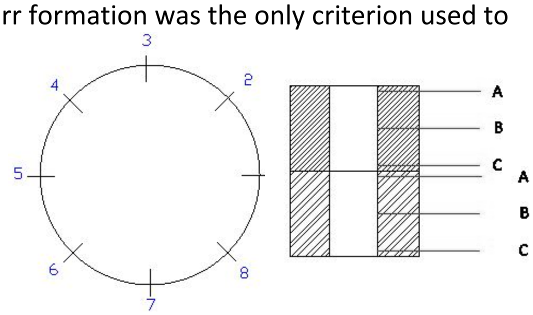

Figure 5. Diameter measurement

select the tool, and it was found that drill bits with a corner radius produced burrs in the titanium alloy. Tool geometry without a corner radius was capable of producing holes without burr formation, and was therefore used for all the remaining tests. Initial tests also showed that the circular milling feed rate did not have an influence on the quality of the hole, and was set at a value of 250 mm/min for the rest of the experiment. Finally, the optimization process allowed us to find a cutting speed of 40 m/min, capable of producing holes in the titanium alloy without burr formation, and which, consequently, was used for the rest of the tests.

3.2. Titanium Alloy Plates

The ANOVA analysis for the titanium plates revealed no significant influence on the burr height by the axial feed rate or helical step. However, the same analysis also revealed that the helical step had an influence on the hole diameter; when the helical step was increased, the hole diameter also increased, as shown in the table showing the ANOVA results (Figure 6). The axial feed rate does not show an influence on the hole diameter. As burr formation was not present, optimal parameters were selected to obtain a closer value of the nominal diameter. As shown in the Box-and-Whisker Plot (Figure 6), the helical step that would produce a hole diameter near the value of 6 mm is located between a value of 0.3 to 0.4 mm, which is why 0.35 mm was selected as an optimal value for the helical step. Moreover, as shown in the same figure, the axial feed rate that would produce a value closer to the 6 mm diameter was situated between 300 and 360 mm/min, and 300 was selected as it presented less variability in results.

Source	Sum of Squares	Df	Mean Square	F-Ratio	P-Value
Principal Factors					
A : Helical Step SP1	0,0030	5	0,00060	24,71	0,0000
B: Axial Feed Rate FFD	0,0002	10	0,00002	0,65	0,7615
RESIDUAL	0,0010	44	0,00003		
TOTAL (CORR)	0,0050	59			

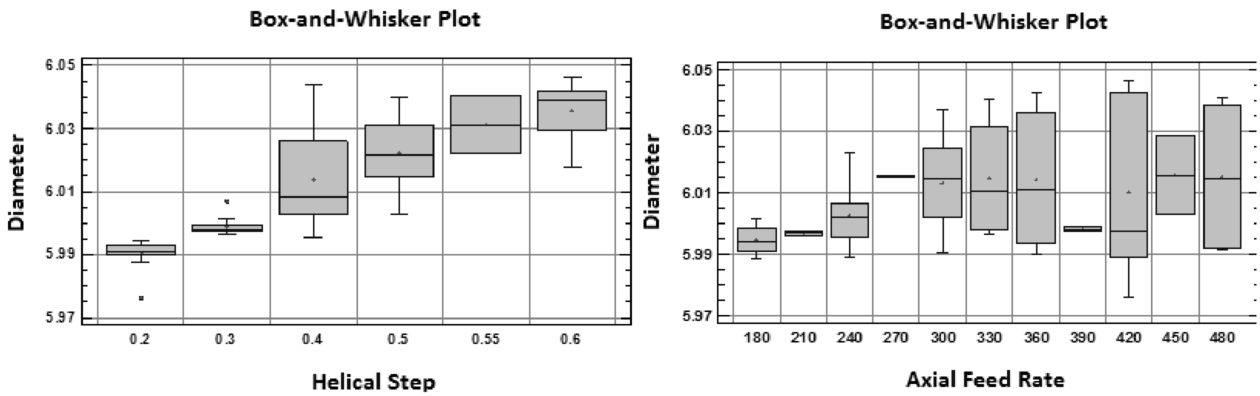

Figure 6. ANOVA and Box-and-Whisker Plot for Helical step and axial feed VS diameter (titanium alloy)

3.3. CFRP Laminates

No significant delamination was present during all tests. The ANOVA for the CFRP laminates did not reveal any influence of the cutting speed, axial feed rate, and helical step on the hole diameter, as the P-Values are much larger than 0.05, as shown in Table 6. The measured values of hole diameter in CFRP are reported in Table 7. As there was no significant delamination, and no significant difference in the results of the diameter value, the maximum cutting speed of 138 m/min was selected as an optimal parameter to improve machining time. However, a helical step of 0.7mm and axial feed rate of 800 mm/min were selected, which are below the maximal values, in order to protect the tool from excessive wear caused by the abrasive CFRP (Table 5).

Table 6 ANOVA for Helical step, cutting speed and axial feed VS diameter (CFRP)

ANOVA Table for Hole Diametrer by Helical Step					
Source	**Sum of Squares**	**Df**	**Mean Square**	**F-Ratio**	**P-Value**
Between groups	0,00004	6	0,000007	0,40	0,8779
Within groups	0,00092	53	0,000020		
Total (Corr.)	0,00096	59			
Groups as Values of helical step in mm (0.25, 0.375, 0.5, 0.625m 0.75, 0.875, 1)					
ANOVA Table for Hole Diameter by Cutting Speed					
Source	**Sum of Squares**	**Df**	**Mean Square**	**F-Ratio**	**P-Value**
Between groups	0,00012	4	0,00003	1,93	0,1179
Within groups	0,00084	55	0,00002		
Total (Corr.)	0,00096	59			
Groups as Values of cutting speed in RPM (6000, 7250, 8500, 9750, 10000)					
ANOVA Table for Hole Diameter by Axial Feed Rate					
Source	**Sum of Squares**	**Df**	**Mean Square**	**F-Ratio**	**P-Value**
Between groups	0,00010	4	0,00003	1,63	0,1801
Within groups	0,00086	55	0,00002		
Total (Corr.)	0,00096	59			
Groups as Values of axial feed rate in mm/min (600, 700, 800, 900, 1000)					

Table 7. CFRP Laminate diameter tests results

Test	Diameter [mm]	Standard Deviation
1	6,015	0,004
2	6,011	0,005
3	6.013	0.004
4	6.011	0.004
5	6.013	0.005
6	6.012	0.005

3.4. Production of burrs

Regarding the quality of the holes in the titanium alloy, it was found that the burr height depended on two factors. First, the geometry of the drill bits seemed to affect the burr height. Burrs were obtained in all tests with ball-nose drill bits in different sets of combinations of cutting speed and feed rate. They were also noted using drills bits with corner radii. The best results were obtained using a drill bit without a corner radius. Secondly, tool wear could increase burr height. This could be explained by the fact that the tool would exert a greater push force as wear increased. When machining CFRP/titanium stacks, burr height also increased with every hole, as the tool wear increased (Table 8). However, the finishing cycle following the orbital motions was capable of eliminating all burrs.

3.5. Delamination

Tests of the CFRP laminates showed no significant delamination, indicating good results for this method. However, delamination at the hole entrance was observed in the CFRP/titanium stacks, probably caused by the evacuation of titanium chips during machining. Delamination values for these tests are shown in Table 8. Figure 7 shows a hole drilled in the CFRP laminate and another drilled in the CFRP/titanium stack. The CFRP hole wall in the stack is gray in color, probably indicating titanium chips adhering to the surface of the hole wall. Delamination is also observed. This delamination was eliminated with the introduction of the finishing cycle when reaching the bottom of the hole, as shown in Figure 8.

3.6. Hole diameter

Hole diameter variations could be caused by the difference in properties of the two materials (Denkena, 2008). With a nominal diameter of 6 mm, the results for the CFRP/titanium stacks tests show that the mean holes diameter for CFRP was 6.0125 mm, and the mean titanium hole diameter was 5.9985 mm. Tests including the finishing cycle show that the diameter was lower than 6 mm for both materials: 5.9665 mm for the titanium and 5.984 for the CFRP. This may be partly due to the tool deflection difference between materials, but there also seem to be a CNC dynamic effect of the cycle, as tests were conducted in an Acrylonitrile Butadiene Styrene material, and similar results were observed in this soft material.

Table 8. Burr height and delamination in stack without finishing cycle

Hole	Burr height [μm]	Delamination [%]
1	40	0.0814
2	95	0.0711
3	165	0.1162
4	135	0.0859
5	245	0.0670

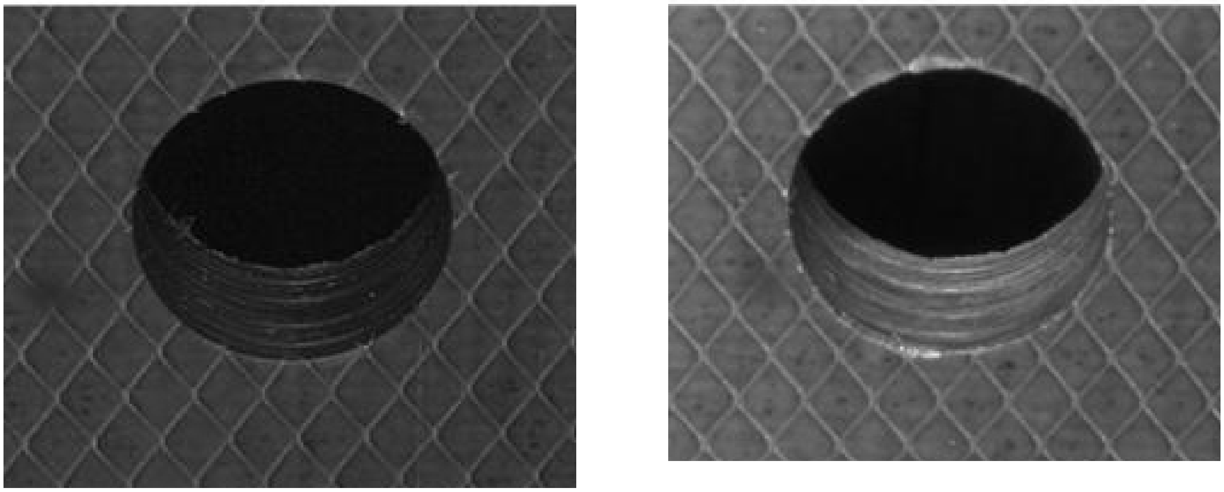

Figure 7. CFRP plate hole wall and CFRP/Titanium stack hole wall comparison

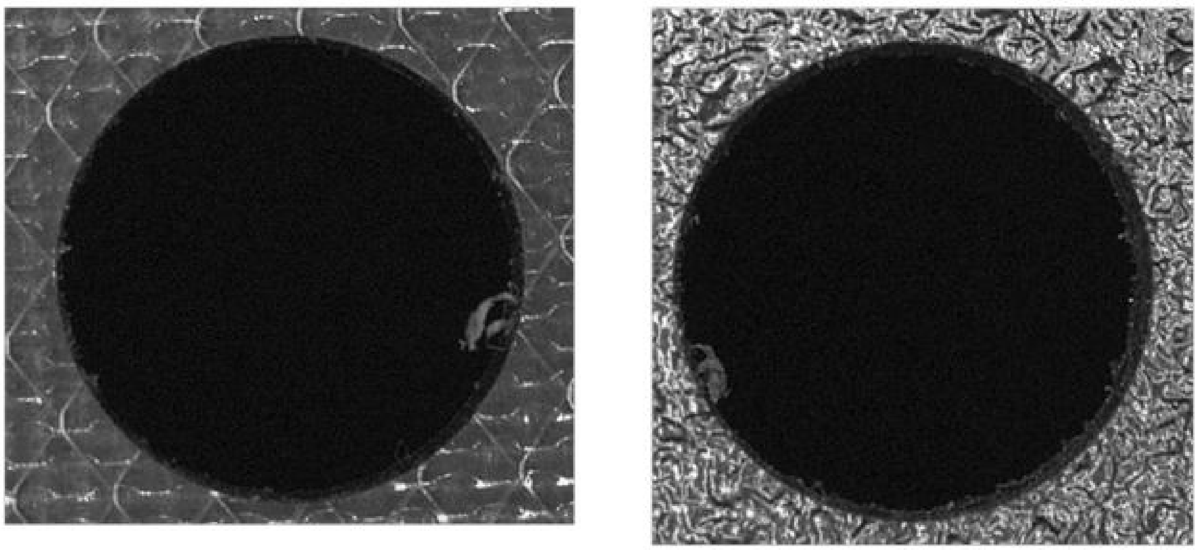

Figure 8. Final Results with optimal parameters and finishing cycle (top surface and bottom surfaces)

4. Conclusions

Hole drilling in stacks of different materials is affected by diverse factors. This paper focuses on how those factors affect delamination, burr formation and hole dimensions. Drill bits of 4mm were used in helical milling machining to produce 6 mm holes in CFRP/titanium stacks. The hole dimension was inspected using a CMM, and the surface integrity, using an electronic microscope.

A relationship was found between the tool geometry and burr size as well as between the tool wear and burr size. A drill bit without a corner radius is preferred for helical milling of titanium thanks largely to the difference in the pushing force related to the tool geometry. A single set of machining parameters for machining both materials successively was difficult to find due to the differences in materials characteristics. When machining CFRP/titanium stacks, the titanium chips evacuation was found to produce delamination at the hole entrance. Also, it was found that the diameter of the CFRP holes was greater than those of the titanium plate, and this could be attributed to the difference in material properties. Finally, the finishing cycle in orbital milling is an effective way to remove burrs and delamination and obtain excellent quality holes with no delamination and burr.

5. Acknowledgment

This work was funded by the Consortium for Research and Innovation in Aerospace in Québec (CRIAQ) and its partners. We are grateful to Mr. Éric Marcoux who conducted all the machining experiments.

6. References

Abrão, A. M., P. E. Faria, J. C. Campos Rubio, P. Reis and Paulo Davim J. (2007). Drilling of fiber reinforced plastics: A review. *Journal of Materials Processing Technology*, *186* (1–3), 1-7.

Brinksmeier, E., Janssen, R. (2002). Drilling of Multi-Layer Composite Materials consisting of Carbon Fiber Reinforced Plastics (CFRP), Titanium and Aluminum Alloys. *CIRP Annals - Manufacturing Technology*, *51*(1), 87-90.

Brinksmeier, E., Fangmann, S., Rentsch, R. (2011). Drilling of composites and resulting surface integrity. *CIRP Annals- Manufacturing Technology*, *60*(1), 57-60.

Denkena, B., Boehnke, D., Dege, J.H. (2008). Helical milling of CFRP–titanium layer compounds. *CIRP Journal of Manufacturing Science and Technology*, *1(*2), 64-69.

Faraz, A., Biermann, D., Weinert, K. (2009). Cutting edge rounding: An innovative tool wear criterion in drilling CFRP composite laminates, *International Journal of Machine Tools and Manufacture*, *49* (15), 1185-1196.

Hocheng, H., Tsao C.C. (2005). The path towards delamination-free drilling of composite materials. *Journal of Materials Processing Technology, 167*(2–3), 251-264.

Liu, D., Yong Jun T., Cong, W. L. (2012). A review of mechanical drilling for composite laminates. *Composite Structures*, *94*(4), 1265-1279.

Park, K.Y., Choi, J.H., Lee, D.G. (1995). Delamination-free and high efficiency drilling of carbon fiber reinforced plastics. *Journal of Composite Materials*, *29*, 1998-2002.

Persson, E. Eriksson, I., Zackrisson, L. (1997). Effects of hole machining defects on strength and fatigue life of composite laminates. *Composites Part A*, *28*, 141-151.

Ramulu, M., Branson, T., Kim, D. (2001). A study on the drilling of composite and titanium stacks, *Composite Structures*, *54*(1), 67-77.

Schulze, V., Becke, C., Weidenmann, K., Dietrich, S. (2011). Machining strategies for hole making in composites with minimal workpiece damage by directing the process forces inwards. *Journal of Materials Processing Technology*, *211*(3), 329-338.

Shyha, I. S., Soo, S. L. Aspinwall, D. K., Bradley, S., Perry,R., Harden, P., Dawson, S. (2011). Hole quality assessment following drilling of metallic-composite stacks. *International Journal of Machine Tools and Manufacture, 51*(7–8), 569-578.

Tsao, C.C. (2008). Investigation into the effects of drilling parameters on delamination by various step-core drills, *Journal of Materials Processing Technology, 206*(1–3), 405-411.

Wen-Chou, C. (1997). Some experimental investigations in the drilling of carbon fiber-reinforced plastic (CFRP) composite laminates. *International Journal of Machine Tools and Manufacture*, *37*(8), 1097-1108.

Yagishita, H. (2007). Comparing drilling and circular milling for hole making in carbon fiber reinforced plastic (CFRP) laminates. *Transactions of the North American Manufacturing Research Institute of SME*, *35*, 153-160.

Improving the Mechanical Properties of Acetal Homopolymer Material to Boost its Quality

Tamer A. Mohamed[1]
[1]*Associate Professor, Mechanical Engineering Department, Faculty of Engineering, The British University in Egypt*
N.S.M. El-Tayeb[2]
[2] *Professor, Mechanical Engineering Department, Faculty of Engineering, The British University in Egypt*
tamer.mohamed@bue.edu.eg ; nabil.eltayeb@bue.edu.eg

Abstract

This paper studies the effect of a burnishing process on the mechanical properties of the material. It is designed to apply burnishing on a flat surface of Acetal Homopolymer material, by studying several burnishing factors that are expected to affect the mechanical properties of the material such as toughness and the material ultimate and breaking strengths. Enhancing these mechanical properties, improves the material grade and alleviates its quality. The controllable factors that are expected to enhance the mechanical properties of the material are the number of tool passes during burnishing; burnishing depth, and burnishing feed rate. Due to the expensive nature of running the experiment, a 2^k factorial experimental design with nine centre points and three replicates are used to minimize the number of runs. Polynomial models of second order are proposed for prediction and optimization purposes.

Keywords: Acetal Homopolymer material, Mechanical Properties, Multiple non-linear regression, Factorial Design

1. Introduction

Linear and non-linear regression modeling has been used extensively in research in order to produce mathematical models for predicting values of response factors such as function of design controllable factors. In addition, these mathematical models can sometimes be used in optimizing the response variable in order to maximize/minimize its value.

Choudhury and Baradie (1999) have described the development of response models namely, tool life, roughness, and cutting force for turning Inconel 718 utilizing factorial design. First and second order predictive models have been developed to assist in choosing the process cutting conditions for higher metal removal rate without sacrificing surface finish. Krajnik et al. (2005) have developed and tested an empirical model to be used for prediction and optimization of the plunge centerless grinding process. The model assisted in determining the optimum centerless grinding system set up and operating conditions that minimize surface roughness. George et al. (2004) have studied the machinability of carbon-carbon composite by creating the model equation (empirical relations) for the machining variables, versus the machinability of the composite.

Onwubolu and Kumar (2006) have studied some drilling control parameters and their effects on the axial force and torque of the cutting tool (responses). These parameters are speed, feed rate and drill diameter. The model was useful in calculating ideal process parameters to reach the preferred quality of the process. Sharif el al. (2006) presented an idea of developing predictive mathematical models for surface roughness of titanium alloy (Ti-6Al-4V) when end milling using uncoated solid carbide tool under flood conditions. An optimized version of the mathematical model revealed that for this type of alloy; lower surface roughness can be achieved by higher cutting speed, low feed rate and high radial rake angle. Furthermore, El-Tayeb et al. (2009) have investigated a mathematical model and a response surface methodology for the friction coefficient in terms of speed, load and sliding distance of a newly developed titanium alloy Ti-5Al-4V-0.6 Mo-0.4 Fe (Ti54) sliding against tungsten carbide. The output of Ti54 alloy was compared with Ti-6Al-4V (Ti64). The wear behavior of SiC particles of reinforced aluminum composite was studied by Sahin (2003) using established linear equations utilizing pin on a disc wear machine. These equations helped in the prediction and minimization of the wear rate at different levels of the process variables.

Although conventional machining is commonly used in industry, research nowadays has shown a lot of attention to super-finishing machining operations such as burnishing which improves the surface characteristics by performing plastic deformation of surfaces (Loh et al., 1989). Burnishing is a way to make a smooth surface of the material. It is a post machining (finishing) and strengthening process (Yeldose, and Ramamoorthy, 2008) based on plastic deformation. This process occurs by applying high pressure to metallic or non-metallic surfaces using a hard and smooth roller or ball burnishing tool (El-Taweel and El-Axir, 2009; Luo et al., 2006; Shiou and Cheng, 2008). It is commonly known as a cold working process in which the pressure exceeds the yield strength of the material. Unlike many other conventional finishing processes which depend on chip removal such as grinding, lapping and honing, burnishing is a chipless post machining process by which, scratches, tool marks, pits and porosity for non-metallic surfaces are eliminated (El-Taweel and El-Axir; El-Tayeb et al., 2008; Luo et al., 2006; and Korzynski, 2009).

The principle of burnishing is based on compressing the peaks of the surface permanently into the valleys, in other words, it is a cold forming process, in which the metal near a machined surface is displaced from protrusions to fill the depressions. In addition to producing high quality surface finish and as a result of producing compressive residual stress, the burnishing operation has a significant positive effect on hardness, corrosion resistance and fatigue life (El-Axir 2000). A comprehensive non-exhaustive literature review shows that a burnishing process has a proven record of improving wear resistance (Michael et al, 1989), hardness (Fattouh et al., 1988), and surface quality (Lee et al., 1993). The controllable factors that are mostly tested in burnishing experiments are burnishing force, feed rate, burnishing depth, ball material, number of passes, workpiece material and lubrication (Loh et al., 1989).

Recent studies of burnishing operations involve the deduction of a mathematical model for prediction purposes, among those are the following: A mathematical model was established by Hassan et al. (1998) for the surface finish for ball burnishing of brass components to correlate the most significant design variables (burnishing force and number of tool passes) with the surface roughness. Another burnishing study was performed by Al-Axir (2000) where a mathematical prediction model for predicting surface micro-hardness and roughness of St-37 after roller-burnishing under lubricated conditions. Spindle speed, burnishing forces, feed, and number of passes were to have the most significant effect on both the surface micro-hardness and roughness.

By this way it is believed that burnishing increases the hardness, mechanical properties and fatigue. However, if the burnishing exceeds a certain limit it can separate the core of the material and the surface; which results in undersurface cracks and this can have consequences in material failure.

This research intends to study the effect of the burnishing controllable factors, i.e. the number of tool passes during burnishing; burnishing depth, and burnishing feed rate, on ultimate strength, breaking strength, and toughness. A 2^k factorial experimental design with nine centre points and three replicates are implemented to minimize the number of runs. Polynomial models of second order are proposed to express the relationship between the significant controllable factors and the response factors.

2. Experimental details

In brief, a burnishing process is a post machining operation based on plastic deformation. In this process, the surface of the workpiece is compressed by the application of a highly polished and hardened ball or roller.

2.1. The experimental procedure

This experiment is designed to apply burnishing techniques on a flat surface of Acetal Homopolymer material, by varying several factors that are assumed to affect the mechanical properties of the material such as, strength and toughness. There are four main tools that are used to achieve this experiment which are namely dial gauge, universal testing machine, horizontal milling machine and a roller burnishing tool. The universal testing machine and horizontal milling machine are available in the engineering workshop at the British University in Egypt. The roller burnishing tool is a very simple design to achieve the roller burnishing task. This tool consists of two parts, the first part is a 12 mm Roller, and the second part is an adaptor where the roller is attached. Comprehensive classifications of burnishing tools and their direct application are presented by Shneider (1989).

2.2. The tested material (Derlin)

Acetal Homopolymer had been selected for the current study as a tested material. The Acetal Homopolymer sometimes is named as Derlin or POM- H. The Acetal is one of the strongest and stiffest of thermoplastic materials. Acetal Homopolymer material is available in several viscosity ranges that meet a variety of processing and end-use needs. This material (Derlin) is commonly used in bearings, precision gears, rollers, and transport conveyors. Sheets of the Acetal Homopolymer material were received in the dimensions of 107mm x 165mm x 5mm, as shown in Figure 1.

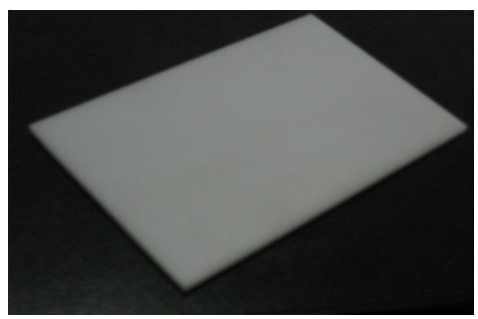

Figure 1. The Selected Material, Acetal Homopolymer (107mm x 165mm x 5mm)

Acetal Homopolymer and Derlin, combine many advantages in mechanical, tribological properties, which make it ideal for many industrial wear and mechanical applications. Automotive applications of Acetal Homopolymer resins includes fuel-system and seat-belt components, steering columns, window-support brackets, and handles. Since it has the low moisture absorption properties, it can be manufactured for the parts that are exposed to a moist or wet environment, such as pump and valve components. Besides, the Acetal Homopolymer also is used in the aerospace field. Industrial application of Acetal Homopolymer includes couplings, pump impellers, conveyor plates, gears, sprockets and springs. Other applications of Acetal Homopolymer includes electrical insulator parts, furniture, toys, and etc.

2.3. The experimental setup

The setup of the experiment is shown in Figure 2 in which the Acetal Homopolymer work piece is fixed onto the table of the machine by four clamps, while the roller burnishing tool is attached to the shaft. A dial gauge is used to measure the penetration depth of the tool. The table can move vertically to adjust the required burnishing depth with the aid of the dial gauge and horizontally, so that the other burnishing parameters can be achieved.

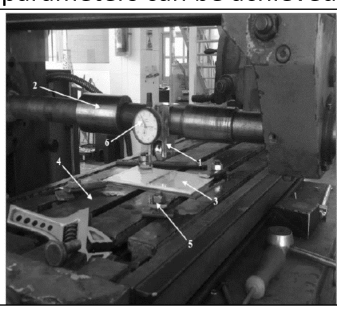

1. Roller Burnishing Tool
2. Shaft
3. Acetal Homopolymer Work piece
4. Table of the Milling Machine
5. Fixation Clamps
6. Dial Gauge

Figure 2. Fixation of the Tool and Workpiece on the Machine

3. Design and Response Variables

Based on the literature, three controllable factors namely, number of passes; burnishing depth; and feed rate are commonly used when studying the effect of burnishing operations. It is worth mentioning that the number of passes is a discrete variable whereas the other two controllable variables are considered continuous variables. The mechanical properties of the burnished specimen are very important in our research. More specifically, this research focuses on the effect of the burnishing controllable factors on ultimate strength (the maximum strength that the specimen can withstand), breaking strength (the stress at which the specimen breaks) and toughness (ability of specimen to resist fracture). In order to measure the response factors, a tensile test was performed after preparing the specimen according to ASTM standards to achieve accurate results. The burnishing conditions and their coded levels are summarized in Table 1.
Once the burnishing operations are finished, the burnished specimens were tested up to failure points using the universal testing machine and data of the stress and strain are recorded in Table 2.

Table 1. Summary of Burnishing Conditions

Design Variables	**Variable Type**	**Symbols**	**Factor Levels**		
			-1	**0**	**1**
Number of Passes	Discrete	*N*	2	3	4
Burnishing depth (mm)	Continuous	*d*	0.4	0.6	0.8
Feed Rate (mm/min)	Continuous	*f*	80	100	120

4. Experimental Design Methodology

The concept of experimental factorial design is more efficient compared to the conventional technique of studying one factor at a time known as 1-FAT design. More specifically, factorial design results in less experimental effort by testing a smaller number of samples beside the fact that it allows the studying of both the main factors effect and the interactions effect (Montgomery, 2012).

In this research, 33 sets of experiments are performed using a randomized order according to the experimental design matrix shown in Table 2. The experiment consists of 2^k factorial (coded as $\pm$ 1 notation) augmented by 9 centre points (0, 0,...0) to improve the accuracy in developing a higher order prediction mathematical model.

Table 2. Experimental Conditions and Results for the Acetal Homopolymer Material

		Controllable Factors			Response		
Serial	**Run**	**Number of Runs**	**Burnishing depth (mm)**	**Feed rate (mm/min)**	**Ultimate Stress MPascal**	**Breaking Stress MPascal**	**Modulus of Toughness**
1	7	2	0.4	80	0.060154	0.054615	0.0391
2	5	2	0.4	80	0.059538	0.052923	0.034532308
3	3	2	0.4	80	0.059692	0.052308	0.0388
4	16	4	0.4	80	0.059692	0.053692	0.028055385
5	11	4	0.4	80	0.059538	0.054	0.029769231
6	21	4	0.4	80	0.06	0.053692	0.02412
7	23	2	0.8	80	0.060769	0.055231	0.0316
8	8	2	0.8	80	0.061077	0.055538	0.031149231
9	20	2	0.8	80	0.06	0.054	0.0396
10	19	4	0.8	80	0.059846	0.052462	0.032915385
11	1	4	0.8	80	0.060462	0.053846	0.031560923
12	18	4	0.8	80	0.060154	0.053538	0.032483077
13	22	2	0.4	120	0.062	0.058462	0.04712
14	17	2	0.4	120	0.061385	0.058462	0.042969231
15	6	2	0.4	120	0.061231	0.056308	0.053270769
16	9	4	0.4	120	0.061231	0.055385	0.034901538
17	15	4	0.4	120	0.061538	0.056923	0.038153846
18	24	4	0.4	120	0.060923	0.053846	0.034116923
19	14	2	0.8	120	0.061231	0.056769	0.039187692
20	10	2	0.8	120	0.061077	0.055692	0.045196923
21	25	2	0.8	120	0.060769	0.057692	0.040107692
22	2	4	0.8	120	0.061538	0.056154	0.045538462
23	26	4	0.8	120	0.061385	0.054769	0.042969231
24	13	4	0.8	120	0.061692	0.056615	0.039483077
25	4	3	0.6	100	0.061077	0.056154	0.034203077
26	12	3	0.6	100	0.061538	0.057385	0.035692308
27	27	3	0.6	100	0.061538	0.056615	0.033230769
28	28	3	0.6	100	0.062308	0.06	0.027041538
29	29	3	0.6	100	0.062308	0.058923	0.028536923
30	30	3	0.6	100	0.062154	0.058769	0.024612923
31	31	3	0.6	100	0.062462	0.058462	0.024984615
32	32	3	0.6	100	0.061692	0.059538	0.026404308
33	33	3	0.6	100	0.061231	0.058923	0.026941538

5. Results and Discussion

Using the experimental data results from the factorial design, fitting a linear model was found to be not significant revealing very weak regression coefficients. As a result, a higher order polynomial model was fitted in a forward pattern starting from linear, quadratic, cubic, quartic, fifth and sixth order prediction equations. Moving from one order to another is done based on an improvement in the regression coefficients which reveals better prediction accuracy. Fortunately, a second order prediction model was found satisfactory with respect to the regression numerical measures for all the response variables. Thus polynomial models of second order are proposed to express the relationship between the significant controllable factors and the response factors. A number of numerical measures assists in determining the accuracy of the proposed model. These measures will be shown in Subsection 5.1-5.3. When all the controllable factors are assumed to be measurable, the prediction equation (model) for the response factor can be expressed in terms of the controllable significant factors as follows:

$y = f(x_1, x_2, x_3, \ldots x_m)$.

Generally speaking the prediction model can be written as

$$y = \beta_0 + \sum_{i=1}^{k} \beta_i x_i + \sum_{i=1}^{k} \beta_{ii} x_i^2 + \sum_{i=1}^{k}\sum_{j=1}^{k} \beta_{ij} x_i x_j + \varepsilon$$

where the random errors ε are uncorrelated, normally distributed with zero mean and variance σ^2. The set of β_0, $\beta_i (i = 1,2 \ldots k)$, and $\beta_{ij}\ i = 1,2,\ldots k, j = 1,2,\ldots k)$ are unknown but are estimated using the least squares method utilizing the factorial experimental data. The following subsections explain in detail the prediction models for the three response factors.

5.1. Ultimate Tensile Strength Model

The material ultimate tensile strength based on the 33 runs of the experiment in actual values format can be derived using 2nd order least square modeling as:

Ultimate Strength=
*+0.045748 - +6.60256E-003*N + +5.12821E-003*d + +5.83333E-005*f- 4.48718E-005*d*f - 1.10684E-003*N²*

……………………. (1)

The analysis of variance at a 95% confidence interval has shown that the ratio of lack of fit to the pure error was 1.70, whilst the F-statistics was 3.01. The lack of fit F-value of 1.70 implies that the Lack of Fit is not significant relative to the pure error. There is a 19.29% chance that a Lack of Fit F-value that large could occur due to noise. These results are shown in the reduced ANOVA presented in Table 3. Therefore the model expressed in Equation (1) was adequate to describe the ultimate tensile strength in terms of the design variables (number of passes; burnishing depth; and feed rate). To better visualize Equation (1), three contour plots were generated each at a different number of passes (2, 3, and 4), which are shown in Figure 3.

(a) N = 2

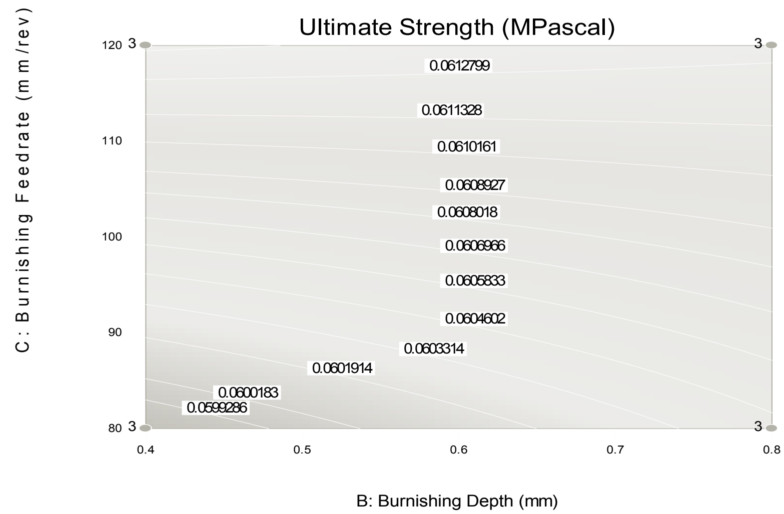

(b) N = 3

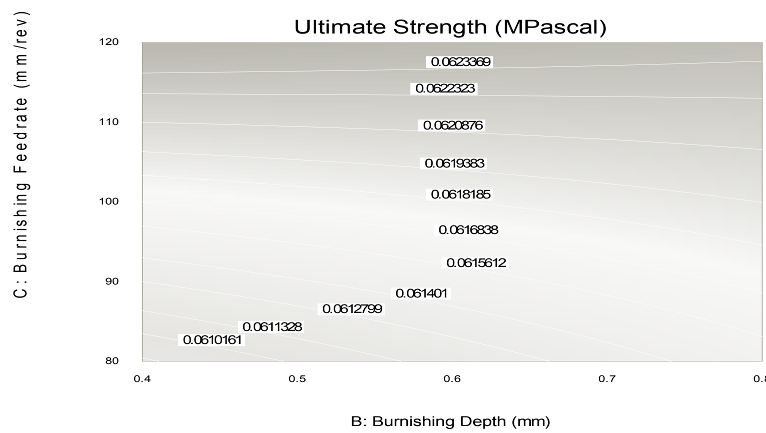

(c) N = 4

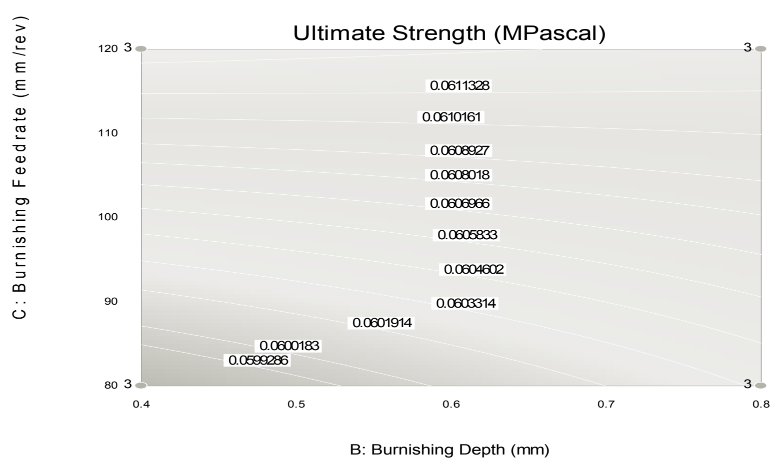

Figure 3. Ultimate Tensile Strength Contour Plots in the Burnishing depth and Feed rate Plane for Different Number of Passes: (a) 2, (b) 3, (c) 4

Figure 3 (a) shows that at a ow number of passes (N=2), ultimate tensile strength increases by increasing burnishing depth. It also increases by increasing burnishing feed rate. The same conclusion can be achieved from Figure 3 (b) and (c) at N=3 and N=4. Maximizing Equation (1) can be achieved by keeping the number of passes at 3, Burnishing depth at 0.5 mm, and Feed rate of 120 mm/min. It is worth saying that in optimizing Equation (1), the number of passes is restricted as being a discrete variable.

To further test the adequacy of the model, regression measures are computed for the model to ensure that the model shown in Equation (1) caught most of the variability in the data and no other term is left outside the model. The regression measures for the ultimate tensile strength are shown in Table 3.

Table 3. Regression Measures for the Ultimate Tensile Strength Model

R-Squared	0.7992
Adj R-Squared	0.7621
Pred R-Squared	0.7089
Adeq Precision	11.704

R-squared is a measure of the percentage of the variability in the data that the model explains. It is a measure of the amount of variation around the mean explained by the model. Whenever R-squared approaches 1, that means that the model is adequate. An R-squared of 0.7992 which is shown in Table 3 means that there is a strong relationship between the dependent variable (ultimate tensile strength) and the independent variables (number of passes; burnishing depth and feed rate). This relationship is illustrated by Equation (1). However, experimenters should be focusing on the adjusted R-squared and predicted R-squared values. The regular R-squared can be artificially inflated by simply continuing to add terms to the model, even if the terms are not statistically significant. The adjusted R-squared and the predicted R-squared will decrease when there are too many insignificant terms. The adjusted R-squared is the R-squared adjusted for the number of parameters in the model relative to the number of points in the design, whereas the Pred. R-squared is a measure of how good the model predicts a response value. A rule of thumb is that the adjusted and predicted R-squared values should be within 0.2 of each other. Table 3 shows that the Pred R-squared of 0.7089 is in reasonable agreement with the Adj R-squared of 0.7621, i.e. the difference is less than 0.2. Thus it can be concluded that model does not contain too many insignificant factors. The fourth measure in Table 3 is for the Adequate Precision that is the signal-to-noise ratio. It compares the range of the predicted values at the design points to the average prediction error (Abraham and Ledolter, 2006). Ratios greater than 4 indicate adequate model discrimination. The mathematical model in Equation (1) was found to have an adequate precision of 11.704 which indicates that the model is adequate and can be used in prediction.

5.2 Breaking Tensile Strength

The material breaking tensile strength based on the 33 runs of the experiment in actual values format can be derived using 2nd order least square modeling as:

$$\textit{Breaking Strength} = +0.021378 + 0.018571*N + 5.64103E\text{-}003*d + 9.67949E\text{-}005*f - 5.28846E\text{-}005*d*f - 3.18590E\text{-}003*N^2 \quad \text{.................... (2)}$$

Same as in Equation (1), Equation (2) is derived in terms of the actual factors and can be used to make predictions about the response for given levels of each factor. Here, the levels should be specified in the original units for each factor.

Before the start of using Equation (2) in prediction, it is very crucial to test its accuracy using lack of fit measures (shown in the analysis of variance output) and the regression coefficients. From the analysis of variance results, it was found the p-value for all the terms in the model is less than 0.05. This is desirable as it indicates that the model terms in Equation (2) have a significant effect on the response. The analysis of variance results also demonstrate that the model is highly significant and that the lack of fit is not significant. The lack of fit revealed a p-value of 0.1797 (>0.05) thus the model is adequate and includes all the significant terms. A similar conclusion is drawn from the regression measures computations presented in Table 4.

Table 4. Regression Measures for the Breaking Tensile Strength Model

R-Squared	0.7547
Adj R-Squared	0.7093
Pred R-Squared	0.6383
Adeq Precision	10.575

Results of the combined effect of burnishing number of passes; burnishing depth; and feed rate on the breaking tensile strength of the Acetal Homopolymer material are presented in the contour plots shown in Figure 4 (a), (b), and (c). From this plot, the combination of the design variables can be found to achieve any pre-determined value of the breaking tensile strength.

Non-linear maximization of the mathematical model presented in Equation (2) reveals that the maximum breaking tensile strength can be achieved at *N=3 passes, d=0.4 mm, and f = 120 mm/min.*

5.3 Modulus of Toughness

Modulus of toughness is the ability of the material to resist fracture. Improving/increasing the modulus of toughness enhances the material quality and consequently increases its grade. Modulus of toughness can be calculated as a function of the ultimate load applied; initial cross sectional area; the specimen maximum elongation; and the initial length of the specimen. The modulus of toughness can be numerically formulated as shown in Equation (3) :

$$MT = \frac{\frac{F}{A}}{\frac{\Delta L}{L}} \qquad \text{……………………(3)}$$

Where *F* is the ultimate applied load in Newton, *A* is the initial cross sectional area of the specimen in mm^2, ΔL is the final elongation at the breaking point in mm, and *L* is the initial length of the specimen in mm.

Using the experimental data and Equation (3), the modulus of toughness is calculated for each combination of the design variables and presented in the last column of Table 1. Using this data, a mathematical prediction model is derived utilizing the least square quadratic model as shown in Equation (4).

Modulus of Toughness =
+0.11291-0.060698**N*-0.039056*E-003*d*
*+2.27771E-005*f* +0.013497*E-005*N*d*
+8.29054*E-003*N*^{2}
……………………(4)

The adequacy of this mathematical model was tested using both analysis of variance lack of fit test, and coefficient of regression measures. All of these tests were found satisfactory and thus the mathematical model can be safely utilized for prediction of the modulus of toughness for any combination of the design variables. Optimizing Equation (4) is beneficial to decide where to set the values of the design variables (Number of passes, burnishing depth, and burnishing feed rate) to maximize the modulus of toughness. Non-linear optimization of Equation (4) revealed that the maximum Modulus of Toughness can be achieved at *N* = 2 passes; *d* = 0.4 mm; and *f* = 120 mm/min.

In the previous analysis, the optimization process optimizes (maximizes) each response variable (ultimate tensile strength; breaking tensile strength; and modulus of toughness) separately. Optimizing all the response variables (assuming equal importance) revealed that setting *the burnishing number of passes* at

3 passes; burnishing depth = 0.4 mm; and burnishing feed rate = 120 mm/min helps maximize all of the response variables together.

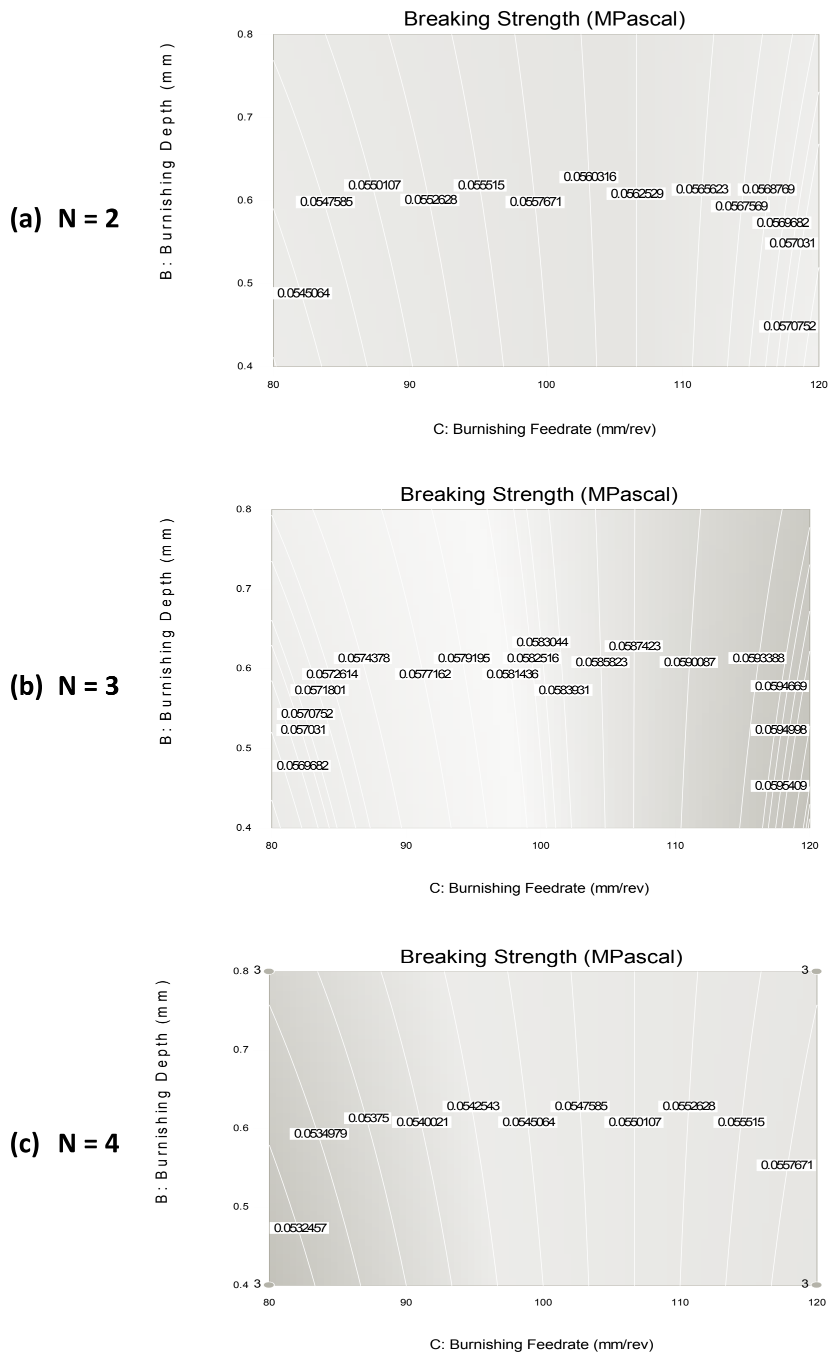

Figure 4. Breaking Tensile Strength Contour Plots in the Burnishing depth and Feed rate Plane for Different Number of Passes: (a) 2, (b) 3, (c) 4

6.0 Conclusions

Machined polymeric surfaces may have inherent surface irregularities. Owing to their excellent characteristics such as corrosion resistance, high strength-to-weight ratio, low electrical and thermal conductivity, design flexibility, and ease in processing, polymeric materials have gained rapid popularity in many industries to replace metallic components in the production of bearing and sliding components such as bearings, gears, cams, wheels.

The model developed can be used by those who are interested in the burnishing process as a cold-forming technique to produce better mechanical properties for the polymeric surfaces. Also this model can be used by those who intended to predict the burnishing process variables to achieve certain mechanical components. The model can be applied to a range of the conditions used in this article. The advantage of this approach over others is that it is a systematic approach which involves planning of experiments, collection and analysis of data. It is basically a model formulation procedure to investigate how important factors affect the response of the experiment. It aims to a development of 1st or 2nd order polynomial models that includes the parameters under consideration and their statistical significance.

It should be realized that most of the published work revealed that the burnishing process was commonly applied to metallic and non-ferrous components, but the current work intended to extend the application of this process to polymeric materials.

Using the experimental data results from the factorial design, fitting a linear model was found to be not significant revealing very weak regression coefficients. However, fortunately, a second order prediction model was found satisfactory with respect to the regression numerical measures for all of the response variables. Thus polynomial models of second order are proposed to express the relationship between the significant controllable factors (Number of passes, burnishing depth, and burnishing feedrate) and the response factors (Ultimate strength, Breaking strength, and Modulus of toughness). These mathematical models are very helpful in prediction of the response variables at any value of the controllable factors. In addition, by optimizing the prediction mathematical model, the material properties can be improved, and thus its grade can be enhanced, its quality can be alleviated.

It is worth mentioning that the mathematical prediction model developed in this research can only be used for the Acetal Homopolymer material, however, prediction models can be developed for other polymeric surfaces in the same experimental way.

Future research can focus on quantifying the increase in cost and selling price pertaining to use of the burnishing process to enhance the mechanical properties of the polymeric surface of the Acetal Homopolymer material.

References

Abraham, B. and Ledolter, (2006). Introduction to Regression Modeling. Thomson

Choudhury, I. and El-Baradie, M. (1999). Machinability assessment of inconel 718 by factorial design of experiment coupled with response surface methodology. *Journal of Materials Processing Technology, 95*, p. 30-39.

El-Axir, M.H. (2000). An Investigation into roller burnishing, International Journal of Machine Tools and Manufacture, 40, 1603-1617.

El-Taweel, T.A.; El-Axir, M.H., (2009) Analysis and optimization of the ball burnishing process through the Taguchi technique*, International Journal of Advanced Manufacturing Technology, 41(3-4)*, 301-310

El-Tayeb, N.S.M., Low, K.O., and Brevern, P.V. (2008). The influence of roller burnishing process on hardness and roughness of cylindrical polymer surfaces, *Proceedings of the Institution of Mechanical Engineers, Part J: Journal of Engineering Tribology, 222(7*), 947-955.

El-Tayeb. N.S.M., Yap, T.C., Venkatesh, V.C., and Breven, P.V. (2009). Modeling of cryogenic frictional behaviour of titanium alloys using Response Surface Methodology approach. *Materials and Design, 30*, 4023-4034.

Fattouh, M., El-Axir, M.H., Serage, S.M. (1988) Investigation into the burnishing of external cylindrical surface of 70/30 Cu-Zn-alloy, *Wear, 127*.

George, P., Raghunath, B., Manocha, L. and Warrier, A.M. (2004). Modelling of machinability parameters of carbon–carbon composite—a response surface approach. *Journal of Materials Processing Technology, 153–154,* 920–924.

Hassan, A.M., Al-Jalil, H.F., and Ebeid, A.A. (1998). Burnishing force and number of ball passes for the optimum surface finish of brass components. *Journal of Materials Processing Technology, 83,* 176-179.

Korzynski, M. (2009). A model of smoothing slide ball-burnishing and an analysis of the parameter interaction. *Journal of Materials Processing Technology, 209(1),* 625-33.

Krajnik, P. Kopac, J. and Sluga, A. (2005). Design of grinding factors based on response surface methodology. *Journal of Materials Processing Technology, 162-163,* 629-636.

Lee, S.S.G., Tam, S.C., Lob, N.H. (1993). Ball burnishing of 3 16L stainless steel, *Journal of Materials Processing Technology, 37*, 241.

Loh, N.H., Tam, S.C. Miyazawa, S. (1989). A study of the effects of ball-burnishing parameters on surface roughness using factorial design. *Journal of Mechanical Working Technology, 18,* 53–61.

Luo, H., Liu, J., Wang, L., and Zhong, Q. (2006). The effect of burnishing parameters on burnishing force and surface micro-hardness. *International Journal of Advanced Manufacturing Technology, 28(7-8)*, 707-713.

Michael, P.C., Saka, N., Rabinowicz, E. (1989). Burnishing and adhesive wear of an electrically conductive polyester–carbon film, *Wear, 32*, 265.

Montgomery, D. C. (2012). Design and Analysis of Experiments: John Wiley & Sons. 978-1118146927.

Onwubolu, G. C. and Kumar, S. (2006) Response surface methodology-based approach to CNC drilling operations. *Journal of Materials Processing Technology, 171,* 41–47.

Sahin, Y. (2003) Wear behaviour of aluminium alloy and its composites reinforced by SiC particles using statistical analysis. *Materials and Design, 24,* 95-103.

Sharif, S., Mohruni, A.S., Noordin, M.Y., and Vekatesh, V.C. (2006). Optimization of surface roughness prediction model in end milling titanium alloy (Ti-6Al4V). *Proceedings of ICOMAST2006, International Conference on Manufacturing Science and Technology, Melaka, Malaysia,* 55-58.

Shiou, F.J.; Cheng, C.H. (2008). Ultra-precision surface finish of NAK80 mould tool steel using sequential ball burnishing and ball polishing processes. *Journal of Materials Processing Technology,* 201(1-3), 554-559.

Yeldose, B.C. and Ramamoorthy (2008). An investigation into the high performance of TiN-coated rollers in burnishing process, *Journal of Materials Processing Technology, 207(1-3),* 16, 350-355.

Finite Element Analysis of an Automobile Engine Hood

S. M. Darwish[1], Sh. M. Elseufy[1], A. Ahmad[2]

[1]Advanced Manufacturing Institute, King Saud University,
P.O. Box 800, Riyadh 11421, Saudi Arabia
[2]Department of Engineering Technology, Northwestern State University of Louisiana,
Natchitoches, LA 71497, USA

Correspondence: sseufy@ksu.edu.sa

Abstract

An automobile's engine hood is important. It performs several functions, for example, during maintenance of engine area, the hood mechanisms should enable manipulation, and during everyday operation or in case of crashes, the engine hood must be rigid to enable safety; hence it is important to perform engine hood global and local stiffness analysis. This paper applies finite element analysis techniques to evaluate global and local stiffness for the first Saudi Arabian designed SUV; thus checking hinges, lateral firmness, closed and open spring latches, among other engine hood components. Target global and local stiffness values were determined based on the analysis of a similar SUV (i.e., Mercedes G class 500). The results of the finite element analysis indicated that the bump stopper bracket thickness should be increased from 1.2 to 1.5 mm and some parts' geometries should be redesigned in order to improve stiffness. Overall, this paper provides a unified framework to evaluate stiffness of important automobile parts (such as engine hoods) via finite element analysis, and establishes a mechanism for parts' redesign to ensure that pre-established design targets are met.

1. Introduction

The shape of auto panels is usually complex, the flow regularity and character of deformation are difficult to master, so to control the metal flowage to get a qualified work piece is a difficult problem in auto panels' process and mold design (Qiu, Huang, et al., 2007). Finite Element Analysis (FEA) is a technique to discretize differential operators. FEA is widely used in computational mechanics, where meshing is used to create a net of elements that are used to simulate models of complicated work pieces (Cerrolaza, and Osorio, 2012), such as engine hoods. When compared to experimental work, FEA saves effort, time and costs (Kajtaz, Subic, et al., 2010). [1] Firstly, Noise, Vibration and Harshness (NVH) analysis is used to detect natural frequencies and to provide a general outlook about stiffness in the engine hood, and to check whether engine hood frequencies fulfill predetermined targets (Zhang, and Shen, et al., 2013). NVH is not only important for such checks, but also essential for checking FEA mesh assumptions and revealing any improperly attached part in the body, since the number of natural frequencies depends on the number of free bodies in the system (Zhang, and Shen, et al., 2013), (Lanczos, 1950).

Dynamic modal analysis entails determining the lowest natural frequency of the car engine hood. This is accomplished using the Lanczos algorithm, an iterative algorithm that is an adaptation of power method for finding the singular value decomposition of a rectangular matrix (Lanczos, 1950). The power method is used for finding the largest eigen-value of a matrix (Humar, 2012).

The NVH requirements for the car engine hood were defined through determining the lowest natural vibration frequency for the engine hood in the closed position (Hughes, 2000). Towards that end, an eigen-value analysis of the engine hood was conducted and the eigen-modes and their corresponding eigen-frequencies were obtained using the Lanczos numerical eigen-solver.

Previous research aimed at reducing vehicle weight without sacrificing its safety. This can be achieved by either redesigning its structure or using light-weight materials with the same stiffness. A previous design optimization experiment for a sandwich hood structure is performed using a study vehicle and FEA models; the results showed that the total mass of this optimized sandwich hood design is about 27% more than that of the original hood of the study vehicle (Liu, Xia, et al., 2009). In another study on engine hood material, a composite and aluminum killed steel were compared using numerical analysis software; which led to engine hood's weight reduction of around 30% (Kwak, Jeong, et al., 1997). Structural topology optimization was applied to a hood's inner panel with the properties of lightweight material, which realized performance improvement and weight reduction to the inner panel; the result demonstrates the feasibility of structural topology optimization in realizing lightweight design for inner panes and similar parts (Yanping, and L. Haijiang, 2010). Structural analysis for a Sedan car hood's stiffener was conducted, where three proposed design concepts were compared in terms of local, global, torsional and natural frequencies (Ramesh, Srikari, et al., 2012).

This paper presents the results of different types of FEA that were performed on the first Saudi Arabian designed car's engine hood. The paper proceeds by describing the approach, the results of the engine hood analysis, the results of the local stiffness analysis, and the results of the global stiffness analysis. The paper concludes by identifying several redesign recommendations for the first Saudi Arabian car's engine hood.

2. Results and discussion

2.1. Procedure

FEA was used for local and global stiffness analysis for engine hood parts (i.e., latch, bump stopper fixation, opened and closed gas spring, and hinges), comparing each result with targets established from a similar vehicle (i.e., Mercedes G class 500).

The FEA had three steps:

1) Preprocessing to prepare the engine hood model by creating meshes, simulating materials and boundary conditions for each case analysis. Particular attention is paid for spot welding simulation (e.g., selecting spot points locations between parts, selecting elements for each part and creating spot elements) in FEA generally and in HyperMesh software (Fang, Hoff, et al., 2000), (Donders, Brughmans, et al. , 2005).
2) Solving to calculate each engine hood case study by running the NASTRAN solver software.
3) Post-processing to view the results using the HyperView software, study them and produce a feedback report

2.2. Engine hood analysis

Static analysis, which is a test of the strength of the car engine hood, was conducted by applying forces at carefully selected points in various components of the engine hood for determining resulting displacement and stresses. This can also be divided into static global and closure-force FEA. In the former, the effect of force on the whole engine hood is analyzed while in the latter, certain closures in the engine hood are analyzed. Stress results are compared with the elastic limit of the material of the various components. The stress must be lower than the material elastic limits with a certain factor of safety (Shchepinov, and

Pisarev, 2009). Displacement results are used for calculating stiffness of components at specific points through dividing the applied force by corresponding displacement. The calculated stiffness is compared to a set of target values. If some tests' results do not match targets, modifications must be suggested to some components such as web addition or component thickness increase or some related parameters' change. Any suggestions must be thoroughly studied since it may affect other criteria, i.e. increase overall car weight or decrease stiffness of some other parts. Tests must be performed several times to verify validity of the suggested modifications until matching targets is reached all over the engine hood.

A mesh was made by HyperMesh according to the general rules of meshing: elements must be of global size 8 mm and not to exceed 16 mm (Altair Engineering, Inc., 2007). Elements are of shell types, quadratic but triangular elements are also allowed such that not to exceed 10% of the number of elements. Meshing was made roughly at first and it was refined step by step until it reached an optimum. The numbers of nodes, elements and connectors are shown in Table 1. Connections between various components are achieved by modeling of welding mechanical fixations and prepared for NASTRAN solver (Nastran, 2010).

Table 1. Mesh General Statistics

Element	Total #
Nodes	49027
Elements	49373
Spot weld	162
Rigid bars	438
Spiders	6

FEA revealed several problems with the engine hood, which were treated by redesign recommendations, such as decreasing an opening, and duplicating hinges, but modifying material also remains as an option. Strength to weight ratio of engine hood components has an opportunity to be increased by changing the material used. The different materials used are shown in Table 2.

Table 2. Car Engine Hood Materials

Material	Mass (kg)
FeE275	7.85
FeP04	11.99
Low stiff glue	0. 4
Total	20.24

Welding elements were performed according to designer experience (Palmonella, Friswell, et al., 2004), taking into consideration its behavior under dynamic analysis (Palmonella, Friswell, et al., 2005), and strength under various loadings (Chao, 2003). The car engine hood components are given in Table 3.

Table 3. Engine Hood Components

Name	Th. (mm)	Mass (kg)	El. No.	Image
Outer Panel	0.8	10.5	25720	
Inner Panel	0.8	7.85	19124	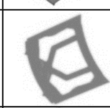
Latch Bracket	1.2	0.41	756	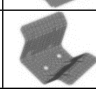
Spring Bracket	1.6	0.06	120	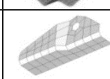
Hinges	3.5	0.69	494	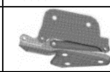
Hinge Bracket	1.2	0.35	608	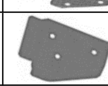
Latch Lock	2	0.04	192	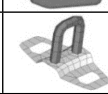
Glue	-	0.03	1698	Solid El.

2.3. Local stiffness analysis

Local stiffness analysis represents the stiffness of each possible loading point of a structure; it gives the stiffness of local fixing point or loading point. An engine hood local analysis has five main check points to be considered, which are:

1. Latch
2. Bump stopper fixation
3. Gas spring opened
4. Gas spring closed
5. Hinges

The boundary conditions considered are:

1. A force of 100 N at the hinge location, bump stopper fixation and the latch.
2. A force of 300 N at the gas spring in the two cases closed and opened engine hood.
3. Fixing the engine hood at some points as shown in Figure 1.

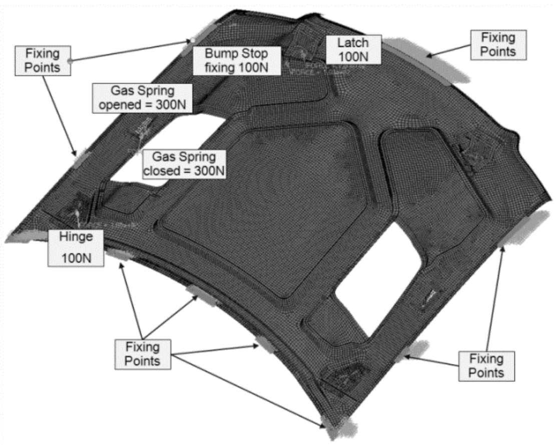

Figure 1 Local Stiffness Analysis

Nastran FEA program was used to solve these cases, results for latch, hinge, opened and closed stabilizers were developed using HyperView. The results were reviewed several times to improve the stiffness for each check point. Table 4 shows that the stiffness latch fixation (448 N/mm) exceeds the target (200 N/mm), similarly; the stiffness hinge fixation (1081 N/mm) exceeds the target (1000 N/mm), gap spring closed (577 N/mm) exceeds the target (500 N/mm) and gap spring opened 5º (2500 N/mm) exceeds the target (2200 N/mm). However the bump stopper fixation (195 N/mm) was lower than the target (200 N/mm) so; it is suggested to increase the part thickness from 1.2 to 1.5mm or improve the geometry design.

Table 4. Local Stiffness Analysis Results

Analysis	Image	Load N	Dis. mm	Stiff N/mm	Target N/mm
Latch fixation	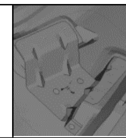	100	0.22	448	200
Hinge fixation	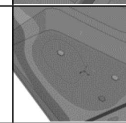	100	0.09	1081	1000
Gap spring closed	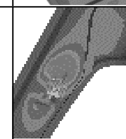	300	0.52	577	500
Gap spring open 5°	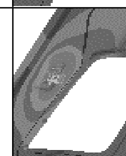	300	0.12	2500	2200
Bump Stopper fixation	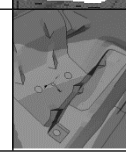	100	0.51	195	200

2.4. Global Analysis

Global analysis is defined as the general structure stiffness under certain boundary conditions; it gives the global performance of the component understudy (Tao, 2006). The following tests were applied on the engine hood:

- Torsional stiffness with lateral constrain
- Lateral stiffness (5° opening)
- Offset with seal and spring
- Misuse (i.e., full opening)

2.4.1. Torsional stiffness with lateral constrain (Closed)

Boundary condition:

▲ (X ,Y ,Z ,Rx ,Ry ,Rz) are hinge constraints

▲ Constraint in Z direction on rubber stopper left

● Loaded point is on latch left by 50 N as shown in Figure 2.

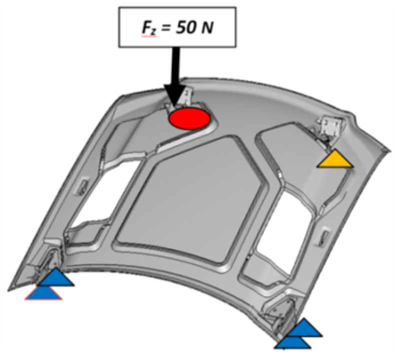

Figure 2 Lateral Constrain

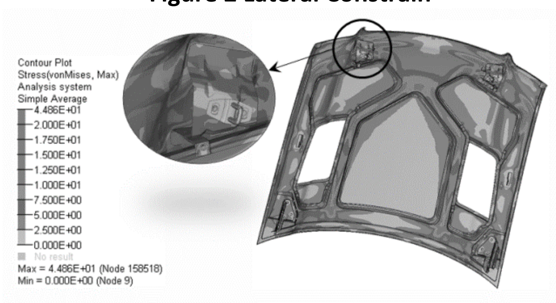

Figure 3 Stresses in Elastic Zone

The material (FeEP4) used in this area had elastic behavior until 160 Mpa, according to the FE results the Max stress is 45 Mpa within limit, so it is possible to reduce weight (see Figure 3).

2.4.2. Lateral stiffness (5° opening)

Boundary condition:

- (X ,Y ,Z ,Rx ,Ry ,Rz) are hinge constraints
- Constraint in Z direction (local axe) on right/left latch.
- Loaded point is on latch left.

Engine hood is 5° opening and Hinges mechanism is free to rotate around its own axle.

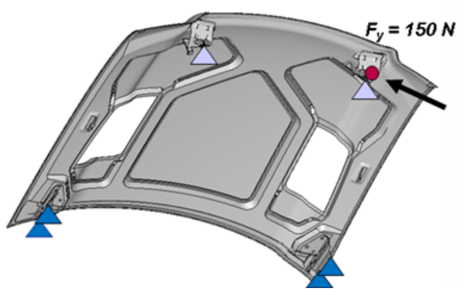

Figure 4 Engine Hood Opened 5°

As shown in Figure 4, the hinges constrained at the 6 degree of freedom and the latches constrain at Z direction only, the left latch loaded with 150 N, this case gives the following results:

Maximum ΔX, ΔZ reaches our goals but ΔY at loaded node failed 3.72mm.

Ky = Fy/ Δy = 150/3.72 = 40 [N/mm]

(Target Ky >50 [N/mm]), Where

Ky is the stiffness of this node in y direction.

Δy is the node deflection in y direction.

Fy is the force applied on node at y direction.

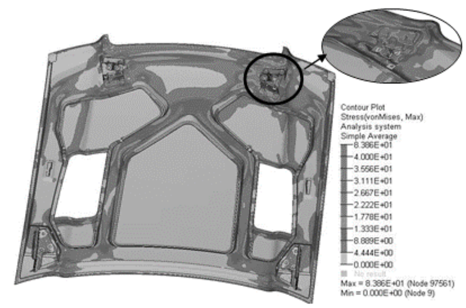

Figure 5 Stress in Open Engine Hood

The maximum stresses in this case appear on the latch area (Figure 5) and engine hood hinges (Figure 6), it records maximum stress of 84 Mpa within the plastic strain limit (material FEEP04, 160MPa) on the latch bracket.

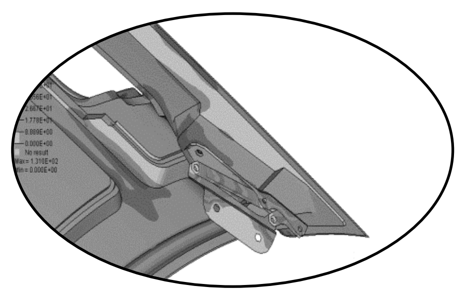

Figure 6 Stress on Engine Hood Hinges

For the hinges material it comes in plastic strain limit but the mean improvement should come from the hinges shape; the multipoint concept has a lack of stiffness in lateral bending. Hinges arms should be stiffened and a local reinforce should be added in the two latches fixings.

2.4.3. Offset with seal & spring (Closed)

Boundary condition:

- (X, Y, Z, Rx, Ry, Rz) hinge constraint

Constraint in Y, Z directions on latch refers to a local system with X axes along longitudinal axes of striker hood

Assume that seal load = 10 N/dm

Assume that rubber stop stiffness = 10.5 N/mm (refers to a local system)

- Loads applied on gas spring attaching point along gas spring longitudinal axes direction. Load's value is equal to gas spring force in open position.
- Hinges mechanism is free to rotate around its own axle.
- Engine hood is in horizontal position.

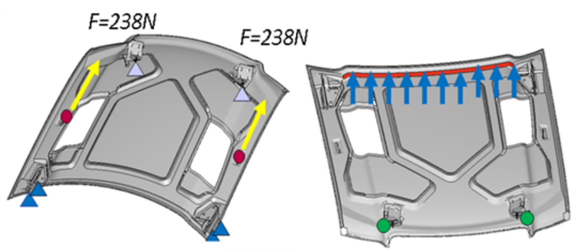

Figure 7 Seal and Spring

Deflection occurs for closed engine hood in X (0.72mm), Y (0.2mm), Z (0.72mm) which is in target limits, so the engine hood materials lie in the elastic zone (see Figure 7).

2.4.4. Engine hood Full opening 42°

Boundary condition:

(X, Y, Z, Rx, Ry, Rz) hinge constraint

Constraint in X direction on spring attaching point.

Loaded point on outer panel engine hood (local system with Z perpendicular to outer panel).

- Engine hood is in full opening at (42°) (see Figure 8).

The maximum stress in this case is 93Mpa which means that max. Stresses occur on the engine hood in case of full opened 42º will be in the plastic strain limit, and it is normal for misuse (see Figure 9).

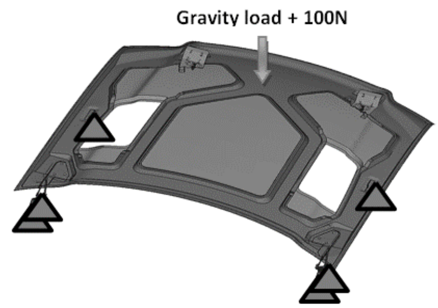

Figure 8 Engine hood Full opening 42°

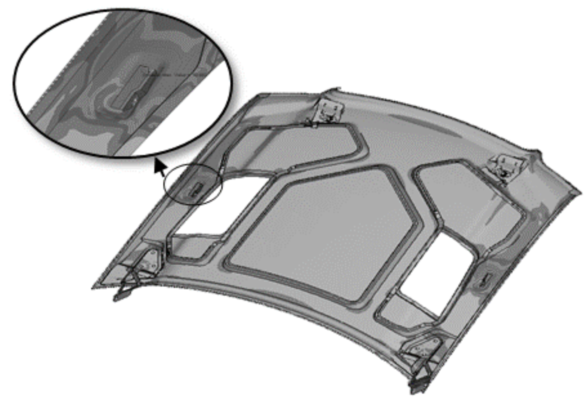

Figure 9 Maximum Stresses 93 Mpa

Stiffness results compared to the targets are shown in Table 5.

Table 5 Global Stiffness results

Analysis	Stiffness	Target
Torsional	K [N/mm]	
Lateral closed	8.47	> 7.0
Lateral opened	40.0	> 50.0
Seal offsets	Mm	
Closed	X=0.72 Y=0.2 Z=1.72	Within gap And flash
Max. open 42°	No plastic	No plastic

Local analysis aimed to improve the functionality of each part of the engine hood during normal use and maintenance, it tests the Latch, Hinges, Bump stopper fixation, Gas spring opened and closed; each according to its function. Global analysis aimed to improve the functionality of engine hood, e.g. torsional test, lateral stiffness (5° opening and full open) and hood offset with seal and spring closed. Both local and global analysis show results that lead to safe engine hood design.

3. Summary and Conclusions

An automobile's engine hood is important. Past research on the engine hood found that it is difficult to master the auto panels shape so FEA is powerful to use. Reducing vehicle weight without sacrificing its safety is a common aim. This paper applies FEA to evaluate global and local stiffness for the first Saudi Arabian designed SUV; where the results indicated that the bump stopper bracket thickness should be increased from 1.2 to 1.5 mm and some parts' geometries should be redesigned in order to improve stiffness. Additional types of FEA analysis such as vibration are being prepared for publication in another manuscript.

The following engine hood's redesign recommendations were determined:

1. Increasing thickness of bump stopper bracket to 1.5mm instead of 1.2mm
2. Improving geometry for some parts
3. Changing material of some parts

4. Acknowledgement

The authors would like to show appreciation to the Advanced Manufacturing Institute at King Saud University for providing the support need to conduct this research.

5. References

Altair Engineering, Inc."Altair HyperWorks User's Guide, HyperMesh 10.0", 2007.

Cerrolaza, M. and J. Osorio (2012). "Relations among stiffness coefficients of hexahedral 8-noded finite elements: A simple and efficient way to reduce the integration time." Finite Elements in Analysis and Design 55: 1-6.

Chao, Y. J. (2003). "Ultimate strength and failure mechanism of resistance spot weld subjected to tensile, shear, or combined tensile/shear loads." [2] Donders, S., M. Brughmans, et al. (2005). "The effect of spot weld failure on dynamic vehicle performance." Sound and Vibration 39(4): 16-25.

Fang, J., C. Hoff, et al. (2000). "Welding modeling in MSC Nastran." Proceedings MSC Worldwide Automotive.

Hughes, T. J. R. (2000). The finite element method: linear static and dynamic finite element analysis, Dover Publications.

Humar, J. L. (2012). Dynamics of structures, CRC Press.

Liu, Q., Y. Xia, et al. (2009). Design Analysis of a Sandwich Hood Structure for Pedestrian Protection. Proceedings of the 21st (ESV) International Technical Conference on the enhanced safety of vehicles, held June 2009, Stuttgart, Germany.

Lanczos, C. (1950). An iteration method for the solution of the eigenvalue problem of linear differential and integral operators, United States Governm. Press Office.

Kajtaz, M., A. Subic, et al. (2010). "A collaborative FEA platform for rapid design of lightweight vehicle structures." International Journal of Vehicle Design 53(1): 110-131.

Kwak, D. Y., J. H. Jeong, et al. (1997). "Optimal design of composite hood with reinforcing ribs through stiffness analysis." Composite structures 38(1): 351-359.

Nastran, M. (2010). "R3 Quick Reference Guide." Santa Ana (CA): MSC Software Corporation.

Palmonella, M., M. I. Friswell, et al. (2004). "Guidelines for the implementation of the CWELD and ACM2 spot weld models in structural dynamics." Finite Elements in Analysis and Design 41(2): 193-210.

Palmonella, M., M. I. Friswell, et al. (2005). "Finite element models of spot welds in structural dynamics: review and updating." Computers & structures 83(8): 648-661.

Qiu, H., Y. Huang, et al. (2007). "The study of engine hood panel forming based on numerical simulation technology." Journal of materials processing technology 187: 140-144.

Ramesh, C., S. Srikari, et al. (2012)"Design of Hood Stiffener of a Sedan Car for Pedestrian Safety." SASTECH Journal, Volume 11, Issue 2, Sep.

Shchepinov, V. P. and V. S. Pisarev (2009). "Strain and stress analysis by holographic and speckle interferometry." Measurement Science and Technology 7(9).

Tao, T. (2006). Nonlinear dispersive equations: local and global analysis, Amer Mathematical Society.
Transactions-American Society Of Mechanical Engineers Journal Of Engineering Materials And Technology 125(2): 125-132.

Yanping, L. and L. Haijiang (2010). Material and Structural Optimization for Engine Hood Inner Panel of Car Body Aimed to Lightweight. Information Engineering (ICIE), 2010 WASE International Conference on, IEEE.

Zhang, J., G. Z. Shen, et al. (2013). "Modal Analysis of a Lightweight Engine Hood Design Considering Stamping Effects." Applied Mechanics and Materials 281: 364-369.

Development of Multi-Floor Facility Layout Technique Considering Evaluation of Layout Plans by DEA

Yutaka SHIRAI [1]
Hiroyuki ONO [1]

[1] *Chiba Institute of Technology, Japan*
yutaka.shirai@it-chiba.ac.jp

Abstract

Data Envelopment Analysis (DEA) is a quantitative efficiency evaluation method intended for improving the management efficiency of a Decision Making Unit (DMU). It is a characteristic that a multi-input/multi-output DMU can be evaluated comprehensively because each DMU is evaluated using the ratio scale of an input (input of resources) and an output (output of profits). However, it is necessary to consider "material handling costs" for operating a production facility, and "construction costs" for building a multilayered structure in a multi-floor facility layout problem, so that it is necessary to evaluate plural layout plans obtained. This study developed a multi-floor facility layout technique that is based on a Genetic Algorithm (GA) considering evaluation of layout plans by DEA. Furthermore, the validity of the developed technique is confirmed using numerical experiments.

1. Introduction

Today, many DMUs exist, such as universities and enterprises. In such a university or an enterprise, how is internal management evaluation conducted, and how is the result analyzed? Alternatively, how is selection of layout plans conducted, such as workplace positioning in an office and machinery arrangement in a department?

Evaluation and analytical methods to deduce a solution for the problems described above included Ordinary Least Squares (OLS) (Hayashi, 2000), Stochastic Frontier Analysis (SFA) (Coelli, Rao, O'Donnell, and Battese, 2005), and Data Envelopment Analysis (DEA) (Cooper, Seiford, and Tone, 2007), (Aristovnik, Seljak, and Mencinger, 2013). These three analytical methods perform evaluation and analysis by seeking maximum efficiency.

A convenient procedure, OLS, can estimate an average resource model of a DMU by regression analysis. It measures inefficiency through averaging or through comparison with other benchmarks. However, the problem is that OLS deems the whole residual inefficient and tends to evaluate non-efficiency excessively.

SFA separates deviation from a production function inefficiently into an error and inefficiency assuming that a production function is indefinite stochastically. It measures the latter: it takes the existence of error into consideration. Its most important shortcoming is that analysis using information about the distribution of specific functions or inefficiency as a premise requires the assumption of related information.

DEA, a quantitative efficiency evaluation method for improvement of management efficiency, has the important characteristic that a multi-input/multi-output DMU can be evaluated comprehensively because each DMU is evaluated using the ratio scale of an input (input of resources) and an output (output of profits). A layout plan has been determined by conventional techniques (Irohara, Fujikawa, and Shirai, 2005), (Kochhar, and Heragu, 1998), (Abdinnour-Helm and Hadley 2000), Lee, Roh, and Jeong, 2005), (Irohara, Fujikawa, and Shirai, 2007), (Abdinnour-Helm, and Hadley, 2000), (Bozer, Meller, and Erlebacher, 1994), (Meller, and Bozer, 1997), (Matsuzaki, Irohara, and Yoshimoto, 1999), (Kaku, Thompson, and Baybars, 1988), (Hahn, MacGregor, and Zhu, 2010), (Chang, Lin, and Lin, 2006), in a multi-floor facility layout problem. However, when the following two objective functions must be considered; "Material Handling Cost" (MHC) for operating a production facility and "Construction Cost" (CC) for building a multilayered structure, which solution (layout plan) to select from a solution set (plural layout plans) obtained completely relies on a designer's intuition and experience. There is not the technique to select the single-best layout as from a solutions set in the conventional techniques. Therefore, the selection of the single-best layout is important.

This study evaluates the use of a DEA solution set obtained using the multi-floor facility layout technique (Irohara, Fujikawa, and Shirai, 2005), (Irohara, Fujikawa, and Shirai, 2007), based on GA (Goldberg, 1989). The authors propose a technique that selects the single-best layout plan. Then the validity of the proposed technique is confirmed by numerical experiment.

2. Data Envelopment Analysis (DEA)

DEA is a quantitative efficiency evaluation method for the improvement of management efficiency (Cooper, Seiford, and Tone, 2007), (Aristovnik, Seljak, and Mencinger, 2013), (Leone, and Lazzari. 1998).

This technique requires input–output data for each DMU. The ratio scale of an output to an input is used as Eq. (1) to measure the efficiency of each DMU.

$$\theta^k = \frac{\sum_{j=1}^{s} r_j^k y_j^k}{\sum_{i=1}^{m} q_i^k x_i^k} \qquad (k = 1, 2, \ldots, n) \tag{1}$$

Here, a restriction that sets the denominator of the objective function θ^k (virtual input) to 1 is applied. Then Linear Programming (LP) for DMU *k* can be formulated as

$$\text{max.} \qquad \theta^k = \sum_{j=1}^{s} r_j^k y_j^k \tag{2}$$

$$\text{s.t.} \qquad \sum_{i=1}^{m} q_i^k x_i^k = 1 \tag{3}$$

$$\sum_{j=1}^{s} r_j^k y_j^k \le 1 \tag{4}$$

$$q_i^k \ge 0 \qquad (i = 1, 2, \ldots, m) \tag{5}$$

$$r_j^k \ge 0 \qquad (j = 1, 2, \ldots, s) \tag{6}$$

The following variables are used:
n is the number of DMUs;
m is the number of inputs;
s is the number of outputs;
q_i^k is the variable weight of input i to DMU k;
r_j^k is the variable weight of output j to DMU k;
x_i^k is the input i to DMU k; and
y_j^k is the output j to DMU k.

Here, q_i^k and r_j^k are variable weights to an input item and an output item, respectively, and their magnitude represents which input item or output item of the DMU is evaluated highly. The fundamental concepts that determine the value of q_i^k and r_j^k are the following.

(1) Input weight and output weight might vary for each subject of evaluation.

(2) Weight should be determined to be the most convenient for the subject.

(3) The same weight (constant weight) is used for the evaluation of other DMUs. Its efficiency is subjected to relative evaluation according to the ratio scale of Eq. (1).

A condition when objective function $\theta^k = 1$ is designated as D-efficient. Figure 1 shows the fundamental concept of DEA to a 1-input/2-output problem. Point P is located on an efficient frontier. The efficiency value of point A can be determined using OA/OP: the ratio of distances from the origin. Points on the efficient frontier are D-efficient.

DEA requires convexity between objective functions, but a non-convex Pareto solution might be found depending on the nature of a problem. Measures against this case include the following two procedures:

[Measure A] The objective functions are transformed to a form that becomes convex easily (For instance, the possibility exists using $f' = \exp(f)$.)

[Measure B] Criteria (threshold) for D-efficiency are adjusted. The concave part of a Pareto solution is detectable by setting the threshold of being D-efficient to $1-\varepsilon(\varepsilon \geq 0)$. However, the number of solutions outside the frontier

increases for a greater ε.

This study adopts [Measure B] because the objective function of problems to be addressed has convexity mostly. Let $\varepsilon = 0.005$, then D-efficiency is assumed when the efficiency value is 0.995 or more.

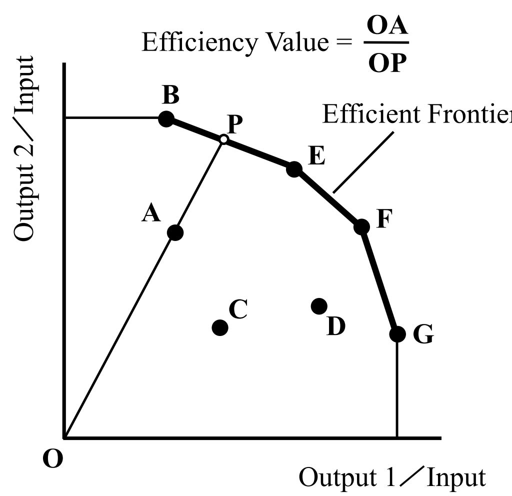

Figure 1. General concept of DEA

3. Multi-floor Facility Layout Problem Addressed in this Study

3.1. Multi-Floor Facility Layout Problem

Today, the trend of diversification of consumer needs has brought subdivision and complication of the type and structure of products and scale-up production facilities. Accordingly, production facilities are transforming from a traditional single-floor structure to a layered story structure considering high efficiency and low cost. When designing a production facility (department) to have a layered story structure, it is common to formulate objective functions and constraints as "a multi-floor facility layout problem" [6–10] and to conduct real design in consideration of the solution. Objective functions of two types are generated in this case: "Material Handling Cost" (MHC) when operating a production facility and "Construction Cost" (CC) when building a layered story structure. The fundamental problems for those in charge of production control are how to reduce these two costs and how to evaluate obtained layout plans.

3.2. Prerequisites

The following are prerequisites for a multi-floor facility layout problem addressed in this study.

(1) All the departments are rectangles. The area of each department is determined to be settled within a range designated in advance for flexibility, in spite of a standard defined area.

(2) The structure is a rectangle. Each floor has the same area.

(3) Aisles of two types exist: the main aisle of a constant width through the floor center, and elevator aisles connecting with the main aisle and located on both sides of the structure.

(4) The distance between departments is measured along the aisle for transfer.

(5) Four elevators have locations fixed at every corner of the structure.

3.3. Objective Functions

As described in Section 3.1, the following two objective functions, material handling cost and construction cost, are minimized in this study.

(1) Material Handling Cost (MHC)

$$MHC = \sum_{k=1}^{N}\sum_{l=1}^{N}\sum_{p=1}^{EV(k,l)}\left(C^H d_{kl}^{H(p)} + C^V d_{kl}^V\right) f_{kl}^{(p)} \quad (7)$$

In that equation,

N is the number of departments,

$f_{kl}^{(p)}$ represents the transfer between departments k and l [Pallets /day],

C^H is the horizontal conveyance cost ratio,

C^V is the vertical conveyance cost ratio,

$d_{kl}^{H(p)}$ is the horizontal distance between departments k and l [m],

d_{kl}^V is the vertical distance between departments k and l [m], and

$EV(k, l)$ is the number of elevators used between departments k and l.

(2) Construction Cost (CC)

Construction Cost (CC) in the case of building a structure is given as Land Cost (LC) + Standard Construction Cost (SCC) + Additional Construction Cost (ACC), as shown in Eq. (8). LC is given as the unit land cost multiplied by the area of a structure, as shown in Eq. (9). SCC is given as the unit standard construction cost multiplied by the area of a structure and the number of floors, with elevator cost added, as shown in Eq. (10). ACC stands for the additional construction cost that arises by department positioning as shown in Eq. (11). Its first term represents an additional cost related to columns and walls. The second term expresses an additional cost attributable to the floor load.

In consideration of the fact that LC and SCC are basically invariant, this study decided to address only ACC as a construction-related objective function, as

$$CC = LC + SCC + ACC \quad (8)$$

$$LC = C^{land} \times W \times R \quad (9)$$

$$SCC = C^{std} \times W \times R \times M + C^{elv} \times E^{elv} \quad (10)$$

$$ACC = \sum_{i=1}^{M}\left\{\max_k\left((H_k - H^{std}) \times V_{ik}\right)\right\} \times \left\{C^{column} + 2(W+R) \times PC^{wall}\right\}$$
$$+ \sum_{i=1}^{M}\sum_{k=1}^{N}\max(L_k - L^{std}, 0) \times A_k \times V_{ik} \times \left(C_i^{skelton} + C_i^{floor}\right)$$

(11)

In those equations,

M is the number of floors,

E^{elv} is the number of elevators,

W is the width of a structure [m],

R is the length of a structure [m],

A_k is the increase or decrease in area compared with the standard area of department k [m^2],

H_k is the floor height of department k [m],

H^{std} is the standard floor height [m],

L_k is the floor load of department k [t/m^2],

L^{std} is the standard floor load [t / m^2],

C^{land} is the unit land cost [\$ / m^2],

C^{std} is the unit standard construction cost [\$/m^2],

C^{column} is the unit column cost [\$/m],

C^{wall} is the unit wall cost [\$/m^2],

$C_i^{skeleton}$ is the unit framework cost at story i [\$ / t・m^2],

C_i^{floor} is the unit floor load cost at story i [\$ / t・m^2],

C^{elv} is the unit elevator construction cost [\$/stand], and

V_{ik} is a binary variable that is 1 when arranging department k on story i, and 0 otherwise.

When MHC is regarded as important, departments of large floor load and great floor height are arranged at upper stories. Therefore, ACC increases. Conversely, when ACC is emphasized, departments with much mutual transfer tend to be located as mutually distant, so that MHC increases. Consequently, a tradeoff relation exists between MHC and ACC.

4. Developed Technique

4.1. Layout Technique Employed in this Study

GA [18] is an approach that imitates the genetic process as a combinational optimization approach. An individual suitable for a given environment can occur by repeated crossover and mutation of individuals (alternation of generations). This study determines a solution set (layout plans) with a GA-based multi-floor facility layout technique (see reference [6][10]).

4.2. Valuation Method of Layout Plans by DEA

This study carries out the technique described in the preceding section, evaluates obtained layout plans using DEA, and selects the single best solution (best layout). Figure 2 depicts a flow chart according to this technique.

In this technique, the multi-floor facility layout was expressed based on the idea of FBS (Flexible Bay Structure) [10]. In addition, the Pareto solution set is requested by repeating uniform crossover, mutation, and parallel selection up to the number of maximum generations. Finally, the single-best layout plan is requested from the obtained solution set by DEA.

As criteria for evaluation when applying DEA, output items used are “MHC” and “ACC”, while the input item is set to 1 for convenience to compute layout plans from the identical state. The efficiency of output items “MHC” and “ACC” is evaluated for the same input, i.e., 1-input/2-output configuration. Because a layout plan is efficient as the values of “MHC” and “ACC” are smaller, DEA is applied using the reciprocals of “MHC” and “ACC.”

The layout plans obtained with the technique of the preceding section is subjected to evaluation by DEA, and input weight q_i^k, output weight r_j^k, and D-efficiency value of layout plan k are determined by Eqs. (2)–(6). To respond to cases with multiple layout plans of a D-efficiency value of 1 in this step, the constant input–output weight (average of each weight) of all the layout plans is computed using Eqs. (12)–(13).

$$g_i = \frac{1}{n}\sum_{k=1}^{n} q_i^k \quad (i = 1, 2, \ldots, m) \tag{12}$$

$$v_j = \frac{1}{n}\sum_{k=1}^{n} r_j^k \quad (j = 1, 2, \ldots, s) \tag{13}$$

Therein,

q_i^k denotes the variable weight of input *i* to layout plan *k*,

r_j^k signifies the variable weight of output *j* to layout plan *k*,

g_i represents the constant weight of input *i*, and

v_j stands for the constant weight of output *j*.

Next, the ratio scale of each layout plan *k* is determined by Eq. (14):

$$z^k = \frac{\sum_{j=1}^{s} y_j^k \times v_j}{\sum_{i=1}^{m} x_i^k \times g_i} \quad (k = 1, 2, \ldots, n) \tag{14}$$

Where z^k is the ratio scale for layout plan *k*.

Then evaluation values are determined using this ratio scale. Evaluation values are ratio scales of the whole normalized so that their maximum is 100, and a layout plan of an evaluation value of 100 is the best layout.

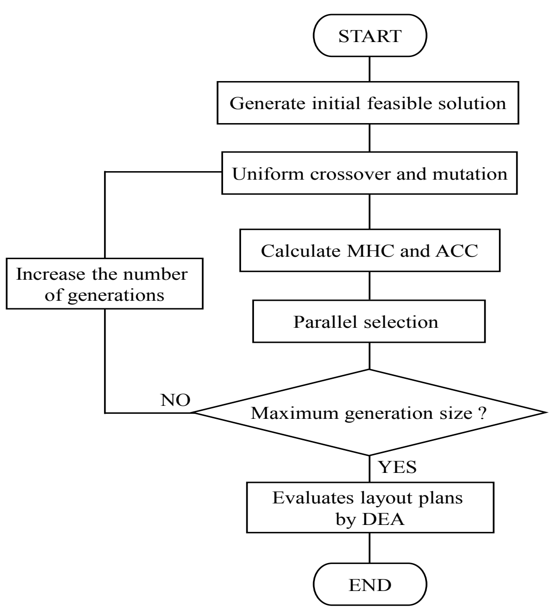

Figure 2. Flow chart of a GA-based multi-floor facility layout technique considering evaluation of layout plans by DEA

5. Numerical Experiment

5.1. Input Information

This study applied the developed technique to a 3-story 20-department building and a 5-story 50-department building as numerical experiments. Input information is shown below.

• Data related to structure
- Aspect ratio of structure: 1.5
- Main aisle width: 4 [m]
- Elevator aisle width: 2 [m]
- Standard floor height H^{std}: 3.5 [m]
- Standard floor load L^{std}: 0.5 [t/m^2]
- Unit land cost C^{land}: 300 [$/m^2]
- Unit standard construction cost C^{std}: 830 [$/m^2]
- Unit column cost C^{column}: 5,800 [$/m]
- Unit wall cost C^{wall}: 100 [$/m^2]
- Unit framework $C_i^{skelton}$, floor reinforcement cost C_i^{floor}:
  - 1F: 122 [$/t-m^2]
  - 2F: 128 [$/t-m^2]
  - 3F: 134 [$/t-m^2]
  - 4F: 144 [$/t-m^2]
  - 5F: 166 [$/t-m^2]
- Unit elevator construction cost C^{elv}: 50,000 [$/stand]

• Data related to department and transfer
- Standard area of each workplace, floor height H_k, floor load L_k, ideal aspect ratio: see Table 1.
- Transfer between departments $f_{kl}^{(p)}$: see Table 2.
- Horizontal transfer cost ratio C^H: 1
- Vertical transfer cost ratio C^V: 5

GA parameters are set as the following: population size, 200; intersection ratio, 0.4;

mutation rate, 0.05; and the number of maximum generations, 3,000.

5.2. Results and Discussion

Figures 3(a) and 3(b), respectively present the results of layout plans obtained for the 3-story, 20-department building and a 5-story 50-department building. Solution sets are obtained from Figure 3. The single best layout should be chosen from these solution sets finally. Point A and B of Figure 3 can be obtained by using the technique described in 4.2 sections. Point A in Figure 3(a) (3-story, 20-department) and point B of Figure 3(b) (5-story, 50-department) represent the best layout obtained using DEA. The best layout can be selected quantitatively and effectively from given solution sets using DEA.

The best layout patterns for the 3-story, 20-department building and 5-story, 50-department building are presented, respectively, in Figures 4(a) and 4(b). Table 4 presents detailed data of these layouts, which shows that departments with large floor load are positioned at lower stories to the greatest extent possible. Regarding floor height, it is desirable that departments with great floor height are located at lower stories to reduce additional construction cost. Departments with great floor height were arranged in this result at the upper story. When carrying out DEA, adjustment is possible by weighing considering additional construction costs.

In Table 3, Pareto solution is extracted from the obtained solution set, and input-output data (MHC and ACC) of those solutions and the experimental result of DEA is shown. As a result, the single-best layout can be determined from the solution set according to "D-efficiency value", "the ratio scale" and "the evaluation value" obtained by technique described in 4.2 sections. A and B of Table 3 correspond to A and B of Figure 3 (In the case of the evaluation value of 100).

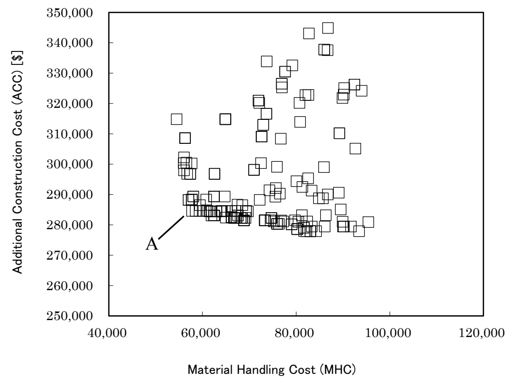

(a) 3-story, 20-department building
Figure 3. Obtained layout plans

In OLS, there is a possibility that the inefficiency is evaluated from the comparisons of averages etc. and the inefficiency is evaluated excessively. In SFA, the setting of a production function is difficult. In DEA, each DMU can be evaluated comprehensively. Therefore, it is thought that the evaluation with DEA used this time is effective.

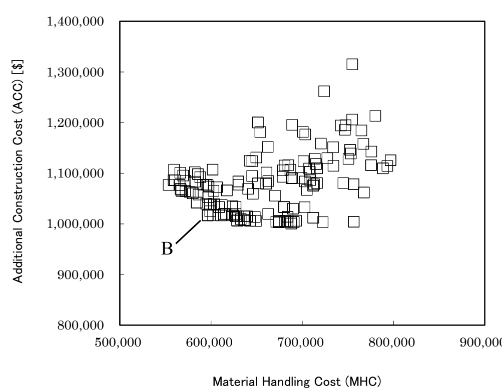

(b) 5-story, 50-department building
Figure 3. Obtained layout plans

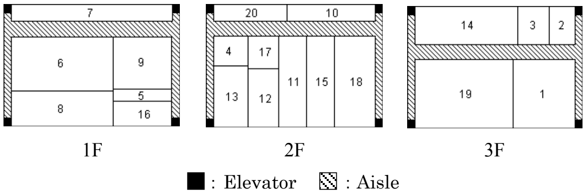

(a) 3-story, 20-department building (Point A of Figure 3(a))

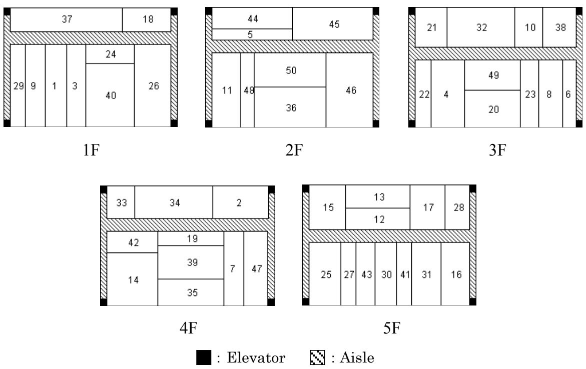

(b) 5-story, 50-department building (Point B of Figure 3(b))

Figure 4. Best layout pattern

Table 3. Input and output data of layout plans and result of DEA

(a) 3-story, 20-department building

	Input	Output MHC	Output ACC	D-efficiency Value	Ratio Scale	Evaluation Values	
1	1.00	54477.50	314866.09	1.0000	0.9305	92.82	
2	1.00	75242.64	281166.19	0.9956	0.9601	95.78	
3	1.00	76312.81	280382.31	0.9974	0.9591	95.68	
4	1.00	89971.66	279452.84	0.9947	0.9242	92.20	
5	1.00	57664.97	300275.13	0.9789	0.9592	95.69	
6	1.00	56039.93	302247.81	0.9956	0.9586	95.63	
7	1.00	61031.28	284611.31	0.9966	0.9923	98.99	
8	1.00	62495.46	283116.72	1.0000	0.9921	98.97	
9	1.00	58008.13	289373.38	0.9893	0.9880	98.56	
10	1.00	64962.06	282417.06	1.0000	0.9867	98.43	
11	1.00	57736.28	284611.34	1.0000	1.0024	100.00	A
12	1.00	66236.27	282557.16	0.9985	0.9825	98.01	
13	1.00	84248.47	277970.94	1.0000	0.9433	94.10	
14	1.00	75934.79	280358.84	0.9978	0.9603	95.80	
15	1.00	83012.58	277970.97	1.0000	0.9467	94.44	
16	1.00	68428.70	282308.25	0.9975	0.9767	97.43	
17	1.00	66857.59	282308.28	0.9988	0.9813	97.90	
18	1.00	56984.27	288244.22	1.0000	0.9943	99.19	
19	1.00	69159.91	282308.28	0.9969	0.9745	97.22	
20	1.00	74685.54	282308.28	0.9923	0.9586	95.63	
21	1.00	80221.56	278623.78	1.0000	0.9528	95.05	
22	1.00	56262.02	308617.38	0.9860	0.9414	93.92	
23	1.00	93423.59	277970.97	1.0000	0.9188	91.66	
24	1.00	79035.05	280221.81	0.9957	0.9519	94.96	
25	1.00	61909.64	284502.56	0.9960	0.9900	98.76	

(b) 5-story, 50-department building

	Input	Output MHC	Output ACC	D-efficiency Value	Ratio Scale	Evaluation Values	
1	1.00	576402.56	1063439.88	0.9899	0.9756	97.34	
2	1.00	596077.19	1017089.63	1.0000	1.0023	100.00	B
3	1.00	610894.75	1017089.56	0.9962	0.9966	99.43	
4	1.00	553287.75	1076844.38	1.0000	0.9745	97.23	
5	1.00	579766.00	1060511.75	0.9890	0.9765	97.42	
6	1.00	566237.69	1069041.38	0.9945	0.9754	97.31	
7	1.00	614049.88	1019756.31	0.9932	0.9934	99.11	
8	1.00	558686.06	1086446.13	0.9908	0.9658	96.35	
9	1.00	627244.56	1015191.00	0.9936	0.9918	98.94	
10	1.00	671384.13	1004479.06	0.9983	0.9830	98.07	
11	1.00	598236.06	1038190.19	0.9871	0.9858	98.35	
12	1.00	594612.25	1039862.38	0.9889	0.9859	98.36	
13	1.00	602085.63	1016835.50	0.9987	1.0002	99.79	
14	1.00	687817.94	1000952.38	1.0000	0.9794	97.71	
15	1.00	559210.69	1107175.88	0.9894	0.9512	94.90	
16	1.00	584260.44	1042334.25	0.9953	0.9880	98.57	
17	1.00	690466.19	1004105.19	0.9969	0.9761	97.39	
18	1.00	683816.13	1004105.31	0.9974	0.9786	97.63	
19	1.00	649028.13	1005781.13	0.9992	0.9904	98.81	
20	1.00	674555.56	1005781.06	0.9968	0.9808	97.85	
21	1.00	628451.25	1007033.13	1.0000	0.9974	99.50	
22	1.00	722276.44	1003756.56	0.9972	0.9648	96.25	
23	1.00	636618.06	1007032.94	0.9992	0.9942	99.19	
24	1.00	687484.38	1004105.25	0.9971	0.9772	97.50	
25	1.00	711913.56	1012377.81	0.9887	0.9625	96.02	

Table 4. Detailed data of the best layout in Figure 4

Floor	3-story, 20-department building (Figure 4(a))		5-story, 50-department building (Figure 4(b))	
	Height [m]	Weight* [t / m^2]	Height [m]	Weight* [t / m^2]
1F	4.50	1.28	4.10	1.56
2F	3.30	0.61	3.10	1.53
3F	5.50	0.75	5.70	1.11
4F			4.80	1.08
5F			3.70	0.60
Total	13.30		21.40	
Building Area [m^2]	1,575.86		2,073.53	
Material Handling Cost (MHC)	57,736.28		596,077.19	
Construction Cost (CC) [$]	4,881,263.50		10,444,282.00	
Additional Construction Cost (ACC) [$]	284,611.34		1,017,089.63	

* shows the average floor load bearing capacity of each story.

6. Conclusion

This study has developed a GA-based multi-floor facility layout technique considering evaluation of layout plans by DEA. Furthermore, the best layout can be chosen from the obtained solution sets (layout plans) by DEA evaluation, by the numerical experiments of “3-story, 20-department” and “5-story, 50-department building”. Consequently, the validity of the developed technique has been confirmed.

The best layout obtained using the developed technique is an efficient layout plan of MHC and ACC, so that it is regarded as leading to reduction of time and expense in layout design.

The best layout was selected quantitatively by the DEA this time. The valuation method of DEA incorporating the intention of a designer to weigh the importance of MHC and ACC should be investigated as a subject of future research.

References

[1] Hayashi, F.: Econometrics, Princeton University Press (2000).

[2] Coelli, T.J., Rao, D.S.P., O'Donnell, C.J. and Battese, G.E.: An Introduction to Efficiency and Productivity Analysis, Second Edition, Springer (2005).

[3] Cooper, W. W., Seiford, L. M. and Tone, K.: Data Envelopment Analysis, Springer (2007).

[4] Aristovnik, A., Seljak, J. and Mencinger, J.: Relative Efficiency of Police Directorates in Slovenia: A Non-parametric Analysis, Expert Systems with Applications, Vol.40, Issue 2, pp.820–827 (2013).

[5] Leone, R. D. and Lazzari, C.: Measuring Efficiency using Data Envelopment Analysis, University of Camerino Technical Report No.OR-CAM-1998-03, pp.1-12, (1998).

[6] Irohara, T., Fujikawa, H. and Shirai, Y.: Multi-storied Facility Layout Problem Considering Initial Cost and Running Cost Simultaneously, Proceedings of the 35th International Conference on Computers & Industrial Engineering, Vol.1, pp.979-984, (2005).

[7] Kochhar, J. S. and Heragu, S. S.: MUTI-HOPE: A Tool for Multiple Floor Layout Problems, International Journal of Production Research, Vol.36, No.12, 3421-3435, (1998).

[8] Abdinnour-Helm S. and Hadley S. W.: Tabu Search based Heuristic for Multi-floor Facility Layout, International Journal of Production Research, Vol.38, No.2, 365-383, (2000).

[9] Lee, K. Y., Roh, M. I. and Jeong, H. S.: An Improved Genetic Algorithm for Multi-floor Facility Layout Problems Having Inner Structure Walls and Passages, Computers & Operations Research, Vol.32, No.4, pp.879-899, (2005).

[10] Irohara, T., Fujikawa, H. and Shirai, Y.: Multi-floor Facility Layout Problem Considering Initial and Running Cost Simultaneously, Journal of the Logistics System Japan, Vol.7, No.1, pp.67-78, (2007).

[11] Abdinnour-Helm, S. and Hadley, S. W.: Tabu Search based Heuristics for Multi-floor Layout, International Journal of Production Research, Vol.38, No.2, pp.365-383, (2000).

[12] Bozer, Y. A., Meller, R. D. and Erlebacher, S. J.: An Improvement-type Layout Algorithm for Single and Multiple-floor Facilities, Management Science, Vol.40, No.7, pp.918–932, (1994).

[13] Meller, R. D. and Bozer, Y. A.: Alternative Approaches to Solve the Multi-floor Facility Layout Problem, Journal of Manufacturing Systems, Vol.16, No.3, pp.192–203, (1997).

[14] Matsuzaki, K., Irohara, T. and Yoshimoto, K.: Heuristic Algorithm to Solve the Multi-floor Layout Problem with the Consideration of Elevator Utilization, Computers & Industrial Engineering, Vol.36, No.2, 487–502, (1999).

[15] Kaku, B. K., Thompson, G. L. and Baybars, I.: A Heuristic Method for the Multi-story Layout Problem, European Journal of

Operational Research, Vol.37, No.3, pp.384–397, (1988).

[16] Hahn, P., MacGregor, S. J. and Zhu, Y. R.: The Multi-story Space Assignment Problem, Annals of Operations Research, Vol.179, No.1, pp.77–103, (2010).

[17] Chang, C. H., Lin, J. L. and Lin, H. J.: Multiple-floor Facility Layout Design with Aisle Construction, Industrial Engineering & Management Systems, Vol.5, No.1, pp.1–10, (2006).

[18] Goldberg, D. E.: Genetic Algorithms in Search, Optimization and Machine Learning, Addison-Wesley Publishing Company, (1989).

Table 1. Detailed data of department

(a) 3-story, 20-department building

Departments	Area [m^2]	Height [m]	Floor Load [t / m^2]	Ideal Aspect Ratio
1	350	5.0	1.0	3.0
2	40	2.8	0.3	1.5
3	60	2.8	0.5	1.5
4	40	2.8	0.3	1.5
5	20	3.5	0.8	1.5
6	450	4.5	2.0	3.0
7	230	3.8	1.5	3.0
8	300	4.3	1.5	3.0
9	250	2.7	0.8	3.0
10	120	3.3	0.5	2.0
11	200	3.3	0.5	3.0
12	150	3.0	0.8	3.0
13	170	3.0	0.8	3.0
14	320	2.8	0.5	3.0
15	200	3.0	1.2	3.0
16	120	3.5	1.0	2.0
17	80	2.5	0.3	1.7
18	300	3.2	0.5	3.0
19	550	5.5	1.0	3.0
20	100	2.6	0.3	2.0

(b) 5-story, 50-department building

Departments	Area [m^2]	Height [m]	Floor Load [t / m^2]	Ideal Aspect Ratio	Departments	Area [m^2]	Height [m]	Floor Load [t / m^2]	Ideal Aspect Ratio
1	200	3.7	1.4	1.5	26	340	4.1	2.6	1.5
2	200	4.6	1.6	2.0	27	100	3.3	0.2	2.0
3	170	2.7	2.0	2.0	28	120	2.8	0.4	1.5
4	250	4.5	1.8	2.0	29	140	2.5	0.8	1.0
5	100	2.6	1.5	1.0	30	150	2.7	0.5	1.5
6	100	3.4	0.3	1.0	31	200	3.4	0.7	2.0
7	160	4.2	0.8	1.5	32	300	5.7	1.4	1.5
8	180	3.6	1.2	1.5	33	100	2.5	0.2	1.5
9	180	2.8	1.7	2.0	34	280	4.8	0.9	1.5
10	120	2.6	0.6	1.0	35	200	4.1	0.6	2.0
11	240	2.6	1.3	1.5	36	320	3.1	3.0	1.5
12	150	2.7	0.3	2.0	37	300	3.6	2.1	1.5
13	160	3.7	1.2	2.0	38	150	5.0	0.4	1.5
14	300	4.5	2.3	1.5	39	240	4.1	0.8	1.5
15	180	3.2	0.5	1.5	40	340	2.5	1.7	1.5
16	200	2.5	0.3	2.0	41	100	2.5	0.3	2.0
17	170	2.5	0.4	2.0	42	120	2.6	0.7	1.0
18	130	3.6	0.8	1.0	43	130	3.1	1.1	1.0
19	100	2.5	1.2	2.0	44	190	3.0	1.5	1.5
20	230	4.9	1.9	2.0	45	290	2.7	1.1	1.5
21	140	4.5	1.4	2.0	46	390	2.5	2.1	1.5
22	120	3.1	0.9	1.5	47	200	2.5	1.8	1.0
23	140	4.0	1.3	2.0	48	110	3.0	0.3	2.0
24	100	2.9	1.4	1.5	49	180	2.7	1.1	1.5
25	220	3.5	1.2	1.5	50	270	2.5	1.7	1.5

Table 2. Transfer between departments

(a) 3-story, 20-department building

	1	2	3	4	5	6	7	8	9	10	11	12	13	14	15	16	17	18	19	20
1		60	4	4	4				20			2		27		2	2	4		
2	60													15			4	8		
3	4													7			1	2		
4	4					10	7	5		11	13			2		5	3	6		17
5						4														
6				10						20	10	2	21	6	3		4	8		
7				7									17	1	1		3	6	38	4
8				5			12						7				2	4	10	2
9						30	10													
10				11			20													8
11				13				10												11
12						2														
13						21	17	7						3	17		2	4		
14	27	15	7	2		6	1						3		7		5	10	19	
15						2	3	1					17	7						
16				5				2												
17	2	4	1	3		4	3	2					2	5						1
18	4	8	2	6		8	6	4					4	10						2
19	52													19						
20				17							8	11					1	2	6	

(b) 5-story, 50-department building

	1	2	3	4	5	6	7	8	9	10	11	12	13	14	15	16	17	18	19	20	21	22	23	24	25	26	27	28	29	30	31	32	33	34	35	36	37	38	39	40	41	42	43	44	45	46	47	48	49	50
1			24	6			17	4		6											78	10				51	3												6		17									
2									7						26								10			45		10			20	5																		
3	24								12		30					4											11					5				6														
4	15							10		7		52																	3			5				7														
5		24	8			16		3														6										5				2														
6		20			16			1														5						4				5																		
7	10	7	2																			12																34												
8	48			10	3	1						9										8									56	5																		
9		7	12					5		50			7																																			14		
10		4		27		24			50		6																																							
11			30						21	6												6																			2									
12		12	5			20			4		5		15					8			12										12					1						7								
13		15					10		5			15										21																												
14																		3				23																	6									27		
15		26			24		5	5														17																												
16			4															27	13												8					7														
17		20		32						16	32	34																													43									
18			29			11						31		81		47						15				87									8															
19								91								89												32				5	65					45												
20																																																		
21	78																												5		3													23						
22	10	8	2	5	6	3	14	2	5	9	12	9	13	12	12	21	6	15			12		33																					23				12	34	50
23		10							34	38							6					33																		17										
24																																																		
25																																12																		
26	51											48						87														5				3					12									
27	3	45	11								3				65											90																								
28																													11																					
29	7					4			2												8									2							9					3		8						
30	4			3		9	5			5	6							13										11	2																					
31																																																		
32	32		54	34		11	73	56									80																				4													
33		5	5	5	5	5				5	5	5	5																								5													
34																																																		
35		12														11										24											4			11		16								
36																																					7			37										
37			6	7	2							1				7		8				2				3																								
38																																												90			41			
39		98	93									86														71																					6			
40	6										7												20																						11	37				
41																																																		
42	40	19	45	20	18																61	78				12		5	3						16						27			45			10			
43													65	40											70			68																						
44	68									4																					39							90				45								
45																																															3			
46																																															4			
47		36			19					38						21					38							55										41	6			10			3	4				23
48																																																		
49		71																																				78				5						56		
50	45	3									1		1	1	1	1							7					1	1		49	1	1		91		60				5	9	61	70	63	85		78		

Improving Localization Accuracy of Autonomous Guided Vehicles for Material Handling Applications

Ayman S. Abbas[1]
[1] *Associate Professor, Mechanical Engineering Department, Faculty of Engineering, The British University in Egypt*

Tamer A. Mohamed[2]
[2]*Associate Professor, Mechanical Engineering Department, Faculty of Engineering, The British University in Egypt*

Mohamed G. Hafez[3]
[3]*Mechanical Engineering Department, Faculty of Engineering, The British University in Egypt*

aabbas@bue.edu.eg; tamer.mohamed@bue.edu.eg

Abstract

The aim of this study is to enable guided vehicles to navigate efficiently through knowledge of the vehicle position throughout its path. A major factor that has been identified as being significant for this application is the accuracy of detecting the vehicle's position throughout its path. Hence the vehicle could perform path planning tasks to navigate around the manufacturing environment. This process demands the application of efficient localization techniques to keep track of the vehicle whereabouts during operation, loading and unloading. A system has been developed which employs the visual detection algorithms to detect landmarks placed in the manufacturing facility. Unique landmarks correspond to the coordinates of an exact location that are mapped onto the AGV memory, hence the AGV position is detected once a landmark is detected.

Several controllable factors have been identified to affect the accuracy of positioning the vehicle namely; distance between the AGV and the landmark, environment brightness, and speed of the AGV. One response factor controls the positioning of the AGV, which is the accuracy of landmark detection, quantified as the numerical error of the number of spokes detected and a landmark with a preset spokes number. A numerical regression model was developed to quantify the error in detection as a function of the controllable factors. This mathematical model was subsequently used as a correction factor to average out any inaccuracy in detection.

1. Introduction to localization techniques

The primary aim of any material handling process is to reduce the cost of production per unit. This can be achieved through the introduction of Autonomous Guided Vehicles (AGV) as a form of an automation technique in the material handling applications. A fundamental aspect of AGV operations is the need to accurately position the vehicle within the manufacturing facility while avoiding static and dynamic obstacles encountered along the path which present a serious problem for the vehicle that might hinder the task completion or cause accidents. These obstacles may be static such as production workstations or storage depots, or dynamic such as moving human operators or other AGVS or misplaced pallets. Of particular concern are the dynamic obstacles. Once the AGV detects the existence of an obstacle through its sensors, it maneuvers to avoid it. This will lead the AGV to deviate from its planned path. This necessitates the adoption of localization techniques which allow the AGV to determine its current location and how to return to its planned path (Antonio Sgorbissa, 2012) (S Campbell, 2012).

Localization techniques have developed largely in the last two decades (Desouza, 2002). This contributed in creating a rather rich taxonomy outlined by (J. Borenstein, 1996), (R.Murphy, 2000) and (Muñoz, 2010) for navigational problems. Two broad categories are outlined for localization techniques; the first of these are positioning systems employing proprioceptive sensors for tracking the robot's position such as odometry and inertial navigation. The second category, are absolute position measurements that employs exteroceptive sensors for identifying the surrounding environment such as (magnetic compasses, active beacons, GPS, landmark navigation, and map based positioning) (J. Borenstein, 1996; Thrun, 1998). Proprioceptive are sensors which measure the state of the AGV itself while exteroceptive sensors measure the state of the AGV with respect to the environment. The typical cluttered environment of an indoor manufacturing facility eliminates the applicability of a GPS and magnetic compasses, while inertial navigation and active beacons are undesirable due to cost issues (Kurian, 2008).

The odometry localization is advantageous over other alternatives due to the simplicity of the concept employed and its inexpensive cost (Grimes, 2009). Nonetheless, it is an inaccurate method for positioning since the location is heavily dependent on wheel turns which are prone to slippage. Furthermore, odometry data are subject to accumulating errors that eventually grow out of bound and result in misleading estimates about the position (Jensfelt, 2001).

The most commonly used landmark navigational technique is vision based techniques due to their highest resemblance with human behavioral approaches. Humans are capable of reaching their target location by looking at a fixed landmark and move to the target accordingly without keeping track of their absolute position with respect to the environment (DeSouza, 2002). Furthermore, vision based navigation is more robust compared to other landmark positioning techniques in addition to their low cost (Park, 2008) (Paulraj, 2010). On the other hand, navigation based on vision requires high computational cost, an issue which needs to be carefully considered.

Hassan and Diab (2010) introduced an online 100% visual inspection approach which is based on digital imaging of products and analyzing their data using advanced mathematical approaches to extract the product features. In their study statistical tools are applied to compare the extracted features with a master feature of the product. The developed model results in enhancing the inspection of multi-dimension products.

Another study by Hassan and Diab (2011) utilizes image processing tools to deal with the product image and extract features of its geometrical characteristics. The study focuses on the visual inspection of dimensions and positions of geometrical quality characteristics. Based on the tolerance bands of each characteristic, an index is experimentally developed to reflect the deviation of a quality characteristic dimension from its nominal value. This index is proved to have a linear association with the deviation from nominal sizes.

Indoor vision systems can be categorized to map-based approaches and non-map based vision systems (Paulraj, 2010). Map based approaches include systems which rely on prior geometric models of the environment and system where the map is created through vision sensors and used later for localization. While non-map based vision systems rely on recognition of objects placed in the environment to infer the AGV location. This is identified in our research as "Landmark"

Landmarks used can either be natural landmarks in the manufacturing environment such as doors and windows, or artificial landmarks placed in the facility for the sake of localization. Commonly used artificial landmarks used for the purpose of localization include circles with unique bar codes for each landmark, and concentric circles with unique numbers of circles for each landmark (DeSouza, 2002). Using barcodes as landmarks are not a preferred alternative in manufacturing facilities as they are affected by illumination (Gallo, 2011). On the other hand, the use of concentric contrasting circles may cause further inaccuracies due to scaling as the distance increases and smaller circles become undetectable. Consequently, the landmark might be mistaken for another position.

The aim of this paper is to improve the localization accuracy of an AGV for the purpose of navigation in a manufacturing facility to perform material handling tasks. There are many challenges to such an application both present in the operating environment and related to the tasks performed. All of these challenges, affect the accuracy with which the AGV can position itself. Those present in the operating environment, include brightness of the environment. While challenges related to the tasks performed, include robot speed and distance between the vehicle and the landmark.

2. The localization technique

The development of an algorithm for detection of an artificial landmark in manufacturing facilities for the purpose of AGV navigation is a vital step for the localization system implementation. This can be achieved through:

1. Reviewing localization algorithms applicable for indoor applications;
2. Development of a landmark recognition and feature extraction algorithm for positioning the AGV;
3. Experimental validation of the algorithm to infer the optimum values for the controllable factors under study;
4. Inferring a regression model for generating a correction factor to minimize the errors in detection according to various scenarios.

A novel approach is presented in this study through the use of a circle with different numbers of spokes to correspond to different positions. Therefore, spokes scale equally as the distance increases which is expected to reduce its effect on the accuracy of detection. A pattern available in the MATLAB vision toolbox can be utilized as an artificial landmark as illustrated in Figure 1.

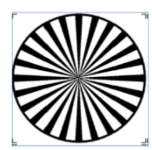

Figure 1. Proposed Artificial Landmark (The MathWorks, 2012)

3. Preliminary control architecture

A control architecture has been developed which addresses the issues discussed above. This architecture is implemented in MATLAB Simulink platform as exhibited in Figure 2. The control architecture consists of an image acquisition and a pre-processing algorithm, followed by the blob analysis and feature extraction algorithm. The outcome of the control architecture is the counted number of spokes. The error in detection is calculated as the actual difference between the measured number of spokes and the actual number of spokes in the utilized artificial landmark used in the experiment. This difference can assume positive or negative values.

The first stage of the architecture, shown in Figure 3, is the extraction of the red color in the environment to search for the landmark within a red sign. According to observations, the selection of the red color was motivated by the fact that it is the least found color in a typical facility at the level of manufacturing equipment. This is envisaged to improve the detection by focusing feature extraction to a single region of interest in the frame rather than attempting to locate the feature in the entire frame.

The more popular RGB color space have indicated its limited functionality in variable

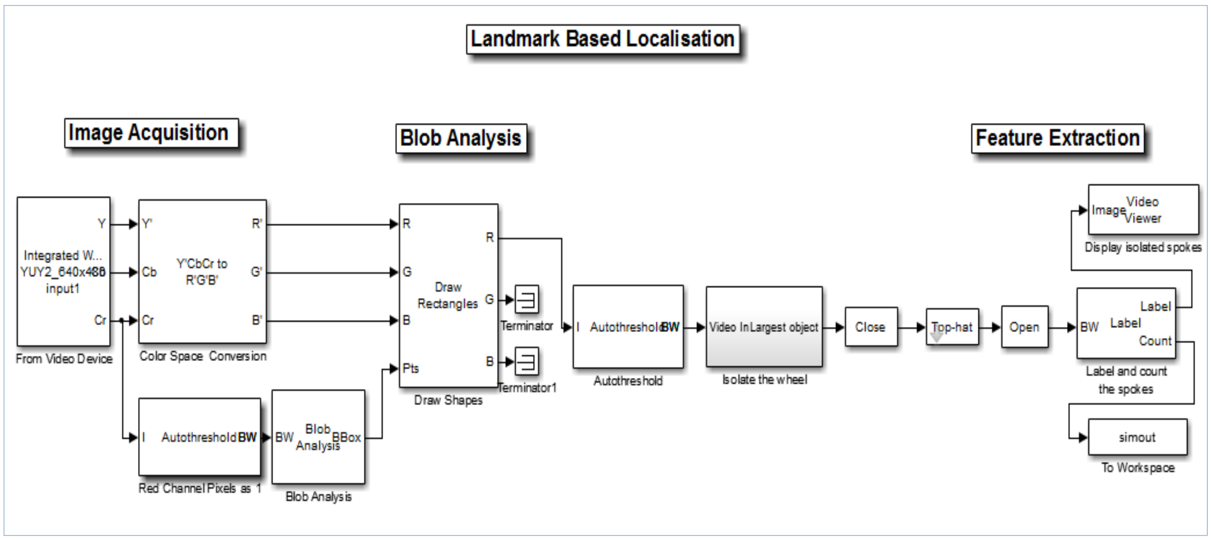

Figure 2. MATLAB Simulink Implementation

lighting conditions (Kaufmann, 2012). Thus Y|Cb|Cr space has been used for the image acquisition process. Later color space is converted back to RGB for the purpose of further processing techniques until the final display of the landmark.

Subsequently, the image is converted to a binary image through automatic thresholding to convert all pixels corresponding to the red color to “1” and the rest of the image converted to “0” black pixels. Hence the pixels within which the landmark is located, can be extracted from the frame. A geometric feature (a black bounding box) is drawn over the area whose pixels’ binary values are 1. This technique is called Blob analysis to define the region of interest.

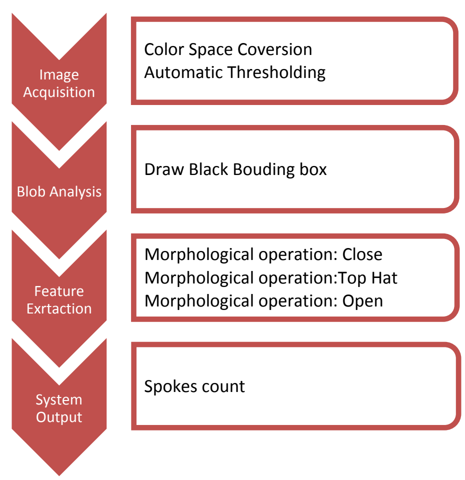

Figure 3. Control Architecture Stages

The circle shown in Figure 1 above, in the feature is separated from the background, based on the fact that it is the largest connected object in the region of interest. Hence, spokes are isolated through a series of morphological operations, namely:

- close to join the spokes at the wheel centre
- top hat to remove the centre of the wheel
- open to remove the rim of the wheel

The spokes are labeled where pixels equal to 0 represent the background, pixels equal to 1 represent the first object, and pixels equal to 2 represent the second object, and so on. Finally the number of labeled objects are counted to reach the number of spokes. The aforementioned feature extraction is implemented using the MATLAB Simulink example (The MathWorks, 2012).

4. Experimental setup

The algorithm was validated through an experimental setup comprised of a commercial mobile robot, shown in Figure 4, "Robotino from Festo, Germany" which moves alongside a landmark. The robot is fitted with a camera to detect the landmark and velocity sensors to measure the speed of the robot. Moreover, the robot is also fitted with 9 infrared distance sensors that surrounds the body of the robot (Festo, 2014).

The algorithm is tested at 3 levels for each controllable factor which are brightness, speed and distance between the robot and the landmark. Varying each factor at three levels was done in order to reach a close estimate of the most optimum settings. More levels could be investigated for more accurate assessments, however the experiment was varied over 3 levels to reduce experimental cost while still achieving good accuracy. Two levels of each factor are used only during screening experiments, however, the objective of this research is far more than screening of the controllable factors. For these reasons, three levels of each factor was tested in this experiment. Firstly, the brightness is varied at 80, 300 and 400 Lux which were selected to represent low, medium and high levels of illumination in a typical indoor manufacturing environment. Moreover, the robot was tested at speeds of 0.3 m/s, 1 m/s and 1.5 m/s. The selection of the maximum speed was based on safe stopping distance of 3.2 m which corresponds to 1.7 m/s for forklifts in indoor manufacturing environments (SafeWork, 2010). The maximum level was set at 1.5 m/s during experimental validation as AGVs operate at lower speeds to accommodate for autonomous processing. Finally the distance between the landmark and the robot path was set at 0.3 m, 0.7 m and 1 m to model various distances the AGV may encounter throughout its journey.

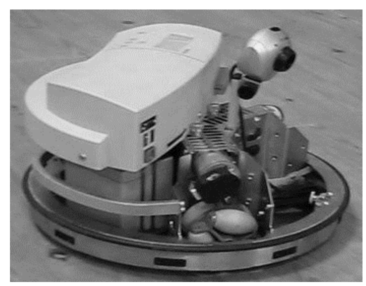

Figure 4. Robotino Robotic Platform (Festo, 2014)

4.1. Experimental design

In order to reduce the error in the accuracy of the localization of the AGV and the landmark, three controllable factors (distance between the AGV and the landmark, landmark brightness, and speed of AGV) were tested each at three levels. One response factor controls the positioning of the AGV which is the accuracy of the landmark detection quantified as the numerical error between the number of spokes detected and a landmark with a preset number of spokes. The above experiment uses the general factorial design with three controllable factors replicated three times and one response factors (81 factorial-experiment). The output of the above experiment is shown below in Table 1. The last column of this Table is called the correction factor and will be explained in Section 4.2.

Table 1. Design Matrix and Observed Response

Serial	Brightness (Lux)	Speed (m/s)	Distance (m)	Error in Spoke Detection			Correction Factor
				1st	2nd	3rd	
1	80	0.3	0.3	0	0	-1	-0.333
2	300	0.3	0.3	-1	-3	-4	-2.667
3	400	0.3	0.3	-24	-22	-21	-22.34
4	80	1.0	0.3	5	7	8	6.667
5	300	1.0	0.3	-4	-2	-2	-2.667
6	400	1.0	0.3	-22	-24	-19	-21.667
7	80	1.5	0.3	14	12	12	12.667
8	300	1.5	0.3	-3	-4	-2	-3.00
9	400	1.5	0.3	-10	-8	-12	-10.00
10	80	0.3	0.7	23	23	23	23
11	300	0.3	0.7	0	0	0	6.55831E-12
12	400	0.3	0.7	4	3	3	3.33
13	80	1.0	0.7	23	23	23	23
14	300	1.0	0.7	-1	1	0	-3.75167E-11
15	400	1.0	0.7	20	19	17	18.66
16	80	1.5	0.7	23	23	23	23
17	300	1.5	0.7	13	13	11	12.33
18	400	1.5	0.7	21	21	22	21.33
19	80	0.3	1.0	24	24	24	24
20	300	0.3	1.0	-2	-1	0	-1
21	400	0.3	1.0	23	23	24	23.33
22	80	1.0	1.0	24	24	24	24
23	300	1.0	1.0	0	-2	-3	-1.667
24	400	1.0	1.0	24	24	24	24
25	80	1.5	1.0	24	24	23	23.667
26	300	1.5	1.0	10	15	14	13
27	400	1.5	1.0	23	22	23	22.667

Analysis of Variance (ANOVA) is used to study the effect of the controllable factor (brightness, speed and the distance) on the response variable (error in spoke detection).
The results of the ANOVA are shown in Table 2.

Table 2. Analysis of Variance for the Error in Detection

Source	Sum of Squares	df	Mean Square	F Value	p-value Prob > F
Model	16053.50	25	642.14	435.37	< 0.0001
A-Brightness	75.83	1	75.83	51.41	< 0.0001
B-Speed	176.04	1	176.04	119.36	< 0.0001
C-Distance	139.44	1	139.44	94.54	< 0.0001
AB	235.22	1	235.22	159.48	< 0.0001
AC	567.49	1	567.49	384.76	< 0.0001
BC	177.04	1	177.04	120.04	< 0.0001
A^2	549.11	1	549.11	372.30	< 0.0001
B^2	108.30	1	108.30	73.43	< 0.0001
C^2	2.30	1	2.30	1.56	0.2166
ABC	0.059	1	0.059	0.040	0.8418
A^2B	0.028	1	0.028	0.019	0.8917
A^2C	1318.90	1	1318.90	894.22	< 0.0001
AB^2	19.31	1	19.31	13.09	0.0006
AC^2	39.43	1	39.43	26.73	< 0.0001
B^2C	108.49	1	108.49	73.56	< 0.0001
BC^2	25.38	1	25.38	17.21	0.0001
A^2B^2	115.69	1	115.69	78.44	< 0.0001
A^2BC	354.93	1	354.93	240.65	< 0.0001
A^2C^2	117.44	1	117.44	79.62	< 0.0001
AB^2C	22.91	1	22.91	15.53	0.0002
ABC^2	164.66	1	164.66	111.64	< 0.0001
B^2C^2	21.56	1	21.56	14.62	0.0003
A^2B^2C	131.97	1	131.97	89.48	< 0.0001
AB^2C^2	31.66	1	31.66	21.47	< 0.0001
A^2B^2C^2	45.46	1	45.46	30.82	< 0.0001
Residual	81.12	55	1.47		
Lack of Fit	5.12	1	5.12	3.64	0.0618
Pure Error	76.00	54	1.41		
Cor Total	16134.62	80			

In order to achieve a statistically significant model, a higher order polynomial model was fitted in a forward pattern starting from linear, quadratic, cubic, quartic, fifth and sixth order prediction equations. Moving from one order to another is done based on an improvement in the regression coefficients which reveals better prediction accuracy. The achieved significant statistical model was found to be of the sixth order. As can be seen, the model used is significant at a significance level of 0.0001 (p-value <0.0001) and the lack of fit is not significant (p-value = 0.0618). This indicates that no significant factors are excluded from the model and the model contains all the significant factors or their interactions, i.e. the model captures all the influential factors and their interactions that will affect the response factor (Montgomery, 2012).

To be able to trust the above ANOVA results, model graphics are visually tested and revealed no violation for the ANOVA assumptions.

4.2. Correction model

As a secondary output of the analysis, An R-squared statistic is calculated and found to be equal to 0.9950 which means that there is a very strong relationship between the dependent variable (error in spoke detection) and the independent variables (distance between the AGV and the landmark, landmark brightness, and speed of AGV). This relationship is illustrated by Equation (1) below which is developed using multiple nonlinear regression modeling (Abraham and Ledolter, 2006).

$$\begin{aligned}\text{Error in Detection} = {} & -103.51586 + 0.81879 * \text{Brightness} + 39.30388 * \text{Speed} + 340.15504 * \text{Distance} + 0.12605 * \text{Brightness} * \text{Speed} \\ & - 2.27839 * \text{Brightness} * \text{Distance} - 144.31584 * \text{Speed} * \text{Distance} - 1.50728\text{E-003} * \text{Brightness}^2 + 11.88887 * \text{Speed}^2 \\ & - 197.01357 * \text{Distance}^2 - 0.15639 * \text{Brightness} * \text{Speed} * \text{Distance} - 1.22497\text{E-003} * \text{Brightness}^2 * \text{Speed} \\ & + 3.42771\text{E-003} * \text{Brightness}^2 * \text{Distance} - 0.33608 * \text{Brightness} * \text{Speed}^2 + 1.21019 * \text{Brightness} * \text{Distance}^2 \\ & + 9.29283 * \text{Speed}^2 * \text{Distance} + 182.47289 * \text{Speed} * \text{Distance}^2 + 1.09470\text{E-003} * \text{Brightness}^2 * \text{Speed}^2 \\ & + 3.59139\text{E-003} * \text{Brightness}^2 * \text{Speed} * \text{Distance} - 1.41928\text{E-003} * \text{Brightness}^2 * \text{Distance}^2 \\ & + 0.54391 * \text{Brightness} * \text{Speed}^2 * \text{Distance} - 1.08159 * \text{Brightness} * \text{Speed} * \text{Distance}^2 - 73.91783 * \text{Speed}^2 * \text{Distance}^2 \\ & - 2.34870\text{E-003} * \text{Brightness}^2 * \text{Speed}^2 * \text{Distance} + 0.55361 * \text{Brightness} * \text{Speed}^2 * \text{Distance}^2 \\ & - 3.60858\text{E-004} * \text{Brightness}^2 * \text{Speed}^2 * \text{Distance}^2\end{aligned}$$

Equation (1)

Using Equation (1), the error is detection is computed for each combination of the controllable factors. This is shown above in the last column of Table 1. This error in detection will then be used as a correction factor to average out any inaccuracy due to the controllable factors. The adoption of the correction factor into the control architecture is shown in Section 5.

5. Modified control architecture

The control architecture was updated based on the findings of the experimental results as shown in Figure 5. The regression model generated from the experimental validation model is used to calculate a correction factor for the error in detection as a function of the 3 controllable factors, brightness, speed and distance. Hence, a continuous measurement is essential for the controllable factors. This is accomplished through the infrared distance sensors and speed sensors available in the Robotino robotic platform in addition to a light sensor to measure the brightness of the environment. Thereby, the control architecture executes the same stages of image acquisition, pre-processing and feature extraction as the initial version. However, the spokes account is corrected through the regression model based on the settings of the controllable factors. Finally the correction factor is added to the initial counted number of spokes to display the

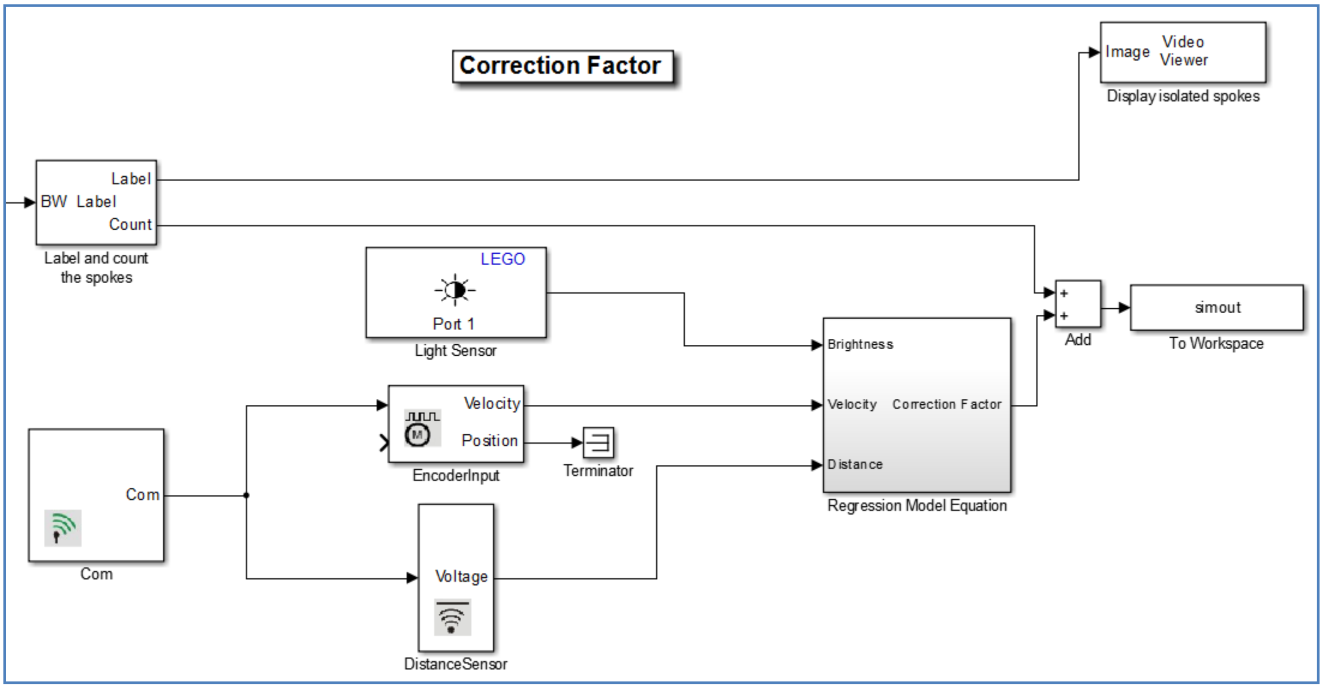

Figure 5. Correction Factor Simulink Implementation

actual number of spokes excluding the effects of the controllable factors by taking into account the correction factor.

More data has been collected for the AGV after embedding the error function into the control architecture and the experiment is repeated at the same levels of combination of the controllable factors. Once data is collected, the output data is analyzed using the ANOVA analysis and reveals that no significant factors/model can be derived, which means that the effect of the controllable factors diminishes and that the errors in detection is no longer significantly different than the zero. This indicates the AGV is currently accurate in determining its location.

Conclusions

Several controllable factors have been identified to affect the accuracy of positioning the AGV namely; distance between the AGV and the landmark, environment brightness, and speed of AGV. One response factor controls the positioning of the AGV which is the accuracy of landmark detection quantified as the numerical error of the number of spokes detected and a landmark with a preset spokes number. A mathematical regression model of sixth order was found to describe the relationship between the controllable factors and the error in detection of the landmark. This mathematical model was then used as a correction factor to average out the effect of the controllable factors on the AGV localization accuracy. Doing so, the accuracy of the AGV improved tremendously and the error in detection was found to be statistically equal to zero despite the levels of the controllable factors used.

References

Abraham, B. and Ledolter, (2006). Introduction to Regression Modeling. Thomson

Antonio Sgorbissa, R. Z. (2012). Planning and Obstacle Avoidance in Mobile Robotics. *Robotics and Autonomous Systems, 60*(4), 628–638.

DeSouza. (2002, February). Vision for Mobile Robot Navigation: A Survey. *IEEE Transaction on Pattern Analysis and Machine Intelligence, 24*(2). Retrieved 2013

Festo. (2014). *Robotino®*. Retrieved from http://www.festo.com/cms/en_corp/9766.htm

Gallo, R. M. (2011). Reading 1-D Barcodes with Mobile Phones Using Deformable Templates. IEEE Transactions on Pattern Analysis and Machine Intelligence, *33*(9).

Grimes, M. (2009). Efficient Off-Road Localization Using Visually Corrected Odometry. International Conference on Robotics and Automation ICRA09. Kobe, Japan.

Hassan, M. H. and Diab, S. L. (2010) *New Approaches for online visual inspection of products with Multiple-characterstics and known tolerance: Int. J. Rapid Manufacturing, 1(3), pp. 363-375.*

Hassan, M. H. and Diab, S. L. (2011). V*isual inspection of dimensions and positions of geometrical quality characteristics: Int. J. Rapid Manufacturing, 1(3), pp. 363-375.*

J. Borenstein, H. R. (1996). *Where am I ?* Michigan, United States : United States Department of Energy. Retrieved 2 15, 2013

Jensfelt, P. (2001). *Approaches to Mobile Robot Localisation in Indoor Environments.* School of Electrical Engineering. Stockholm: PhD Thesis. Royal Institute of Technology. Sweden.

Kaufmann, M. (2012). Machine Vision, Theory, Algorithms and Practicalities. Academic Press. ISBN: 978-0123869081

Kurian, J. (2008). *A Beacon based Localization System for Autonomous Mobile Robots and its Applications in Traffic and Transport Control.* Cochin. PhD Thesis. Department of Electronics, Faculty of Technology, Cochin University of Science and Technology. India.

Muñoz, M. (2010). *Global Localization based on a Rejection Differential Evolution Filter.* In: Robot Localization and Map Building, Hanafiah Yussof (Ed.), ISBN: 978-953-7619-83-1. InTech.

Park, S. Y. (2008). *Mobile robot localization in indoor environment using scale-invariant visual landmarks.* 18th IAPR International Conference on Pattern Recognition, pp. 159–163, 2008..

Paulraj, M. (2010). Vision based Systems for Localization in Service Robots. In: Robot Localization and Map Building, Hanafiah Yussof (Ed.), ISBN: 978-953-7619-83-1, InTech.

Montgomery, D. C. (2012). Design and Analysis of Experiments: John Wiley & Sons. ISBN: 978-1118146927.

Murphy, R. (2000). *Introduction to AI Robotics.* Cambrdige, MA, USA: MIT Press. ISBN: 978-0262133838.

S Campbell, W. N. (2012). A Review on Improving the Autonomy of Unmanned Surface Vehicles Through Intelligent Collision Avoidance Manoeuvres. *Annual Reviews in Control, 36*(2), 267–283.

SafeWork. (2010). *Forklift Safety, Reducing the Risk.* Government of South Australia.

The MathWorks, I. (2012). Simulink Demos, Feature Extraction Model.

Thrun, S. (1998). Bayesian Landmark Learning for Mobile Robot Localization. Machine Learning 33, pp. 41-76.

Adoption Process and Complexity of Innovation in Social Networking

Karol I. Pelc
School of Business and Economics
Michigan Technological University
kipelc@mtu.edu

Abstract

The purpose of this paper is to introduce a new approach to analysis of innovation adoption that is applicable to innovation in social networking. This approach combines measures of innovation adoption with dimensions of technology complexity. Innovation adoption is viewed in the context of innovation diffusion, usually measured by the rate of adoption expressed by the number of adopters or by penetration rate within given population. Those measures are based on statistics of acquisition. However each individual adopter needs to complete the adoption process to fully benefit from innovation. It implies that adoption of innovation should not be viewed just as an event but rather as a learning process. Six basic phases of adoption of innovation in social networking are proposed. On the basis of a literature review and available empirical data, a new dimension called "interactivity level" is proposed and defined. It is specific to innovations in social networking. The interactivity level reflects amount of active knowledge and effective use of social media and technologies. Surveys of social media users and comparative study of average interactivity levels in different countries demonstrate application of that dimension. Complexity of innovation being the subject of adoption may be a factor influencing the adoption. It is suggested that three dimensions of technology complexity introduced by M. Jacobs (2013) could be applied in the analysis of the adoption process of innovation in social networking. Two hypotheses are proposed for further research.

1. Introduction

Traditionally, the rate of innovation diffusion has been measured by the number of adopters. That number is based on statistics of purchase and acquisition decisions. For example, the more new products that have been acquired in a given year the higher the rate of diffusion. Such an approach appears to be inadequate to several new areas of innovation. The adoption process starts after acquisition. Benefits of innovation in communication are mostly dependent on the range and depth of the adoption process after the acquisition of respective tools, systems and procedures. The whole domain of social media and social networking may be viewed as a large scale innovation in communication. All elements of this broad innovation constitute an implementation of the Web 2.0 platform for bidirectional and multidirectional exchange of information and opinions as well as for active collaboration among multiple actors participating in a network. According to Kaplan and Haenlein (2010) "the *social media* is a group of Internet-based applications that build on the ideological and technological foundations of Web 2.0, and that allow the creation and exchange of User Generated Content." Web 2.0 sites allow users to interact and collaborate with each other in a dialogue as creators of user-generated content in a virtual community, in contrast to websites of Web 1.0 where users were limited to the passive viewing of content that was created for them. The same authors proposed a classification of social media in which they distinguished six types of media. Three of them provide a high level of self- presentation. These are: *blogs, social networking sites*, and *virtual social worlds*. Other three: *collaborative projects*, *content communities*, and *virtual game worlds* assume a relatively low level of self-presentation. The main subject of this paper is innovation in social networking as a contemporary phenomenon of growing importance in business and all spheres of social life. The purpose of the paper is to introduce a new approach to analysis of innovation adoption that could provide an insight into the learning process taking place during the early phases of innovation implementation. An additional dimension of innovation diffusion in social networking is proposed. That dimension is called “interactivity level.” It is intended to characterize the innovation diffusion process not only by the number of adopters (as a function of time) but also by assessment of mode/depth of adoption, demonstrated by the range and frequency of usage of individual elements or features of the adopted social media/technologies. Empirical data and illustrations concerning the practice of innovation adoption in different countries have been derived or compiled for purposes of this paper from survey results published by Forrester Research, McKinsey Global Institute, and Socialbakers. Importance of social networking for business has been explored and discussed in several publications. Brown and Sikes (2012) indicated that social networking is one of the most effective means of digital business. Their survey data suggest that 28% of executives emphasized benefits for their companies due to this new approach. More particular measurable benefits from using the Web 2.0 media/technologies for increasing the speed of access to knowledge and for reducing communication costs have been confirmed by more than 60% of respondents in the McKinsey survey of companies (Bughin and Chui, 2010). According to another McKinsey study the most effective social media in support of business processes are blogs, social networking sites and video-sharing when used for scanning of external environment, finding new ideas, and for managing projects (Bughin, 2012), (Bughin and Chui, 2013). Those data and opinions suggest that an insight into detailed mechanisms of adoption of those innovative tools for social networking is needed. In the following section, a review is presented of conventional models of innovation diffusion. Then a definition of interactivity level, as a new dimension of innovation adoption, is proposed together with a suggested way of its application for assessment of advances in social networking. The next section of the paper presents international comparative data on innovation adoption and interactivity. These comparisons suggest that cultural and social factors may be playing an important role in adoption viewed as a complex learning process. The last section of the paper presents basic dimensions of complexity of the social networking innovation. Those dimensions have been adopted from the work of Jacobs (2013). Two working hypotheses are proposed concerning the relationship between complexity of innovation and the dynamics of its adoption. In the final remarks we propose some new directions of further research.

2. Rate of innovation diffusion

The diffusion rate, expressed by number of adopters as a function of time, is an indicator of adoption of innovation by a population of users. Based on the literature review, at least three groups of models can be distinguished: *Coleman model*, *Dodd model*, and *Mahajan-Schoeman model*. In the case of diffusion of innovation in social networking it is important to consider the possibility of different “depth of adoption” by individual adopters. That “depth” is gradually changing during the learning process. As the main functional purpose of social media/technologies is to enable interactive communication involving the user created content (according to Web 2.0 philosophy) the extent of interactivity among adopters is changing with time. Adoption is not just an event, it is a learning process. Individual users, i.e. participants in social networking, operate in different modes depending on their phase of learning. It suggests there is a need to introduce an additional dimension for analysis of this kind of innovation.

3. Interactivity level: A new dimension of innovation adoption

According to Kiousis (2002) *interactivity* can be defined as "the degree to which a communication technology can create a mediated environment in which participants can communicate (one-to-one, one-to-many, and many-to-many), both synchronously and asynchronously, and participate in reciprocal message exchanges (third-order dependency)."

In the case of social networking, a measure of interactivity level has to reflect operational capability and effective application of either individual or combined social media for communication in the modes of *one-to-many* and *many-to-many*. We propose the following definition: *interactivity level* (in social networking) is a number, e.g. on a scale of one to six, reflecting complexity and intensity of interactive operation mode of actors involved in social networking. The higher the number, the more complex the operation mode and/or more frequent use of respective social media. Li and Bernoff (2008) distinguished interactivity levels of different actors involved in social networking by grouping them into clusters called: creators, critics, collectors, joiners, spectators and inactives. Those groups are identified by surveys of on-line consumers in different communities and constitute a "social technographics profile" for each of those communities. The authors presented a very useful empirical material, based on Forrester Research surveys, which can be used for illustration of practical application of the concept of interactivity level.

The correspondence between interactivity levels and operational modes in subsequent innovation adoption phases on one part, and tasks analyzed in the studies presented by Li and Bernoff (2008) on the other, is shown in Table 1. The following innovation adoption phases (levels of interactivity) are included: initial learning, field exploration, focused observation, selection and classification, evaluation, design and implementation. They are reflecting the learning process of interactive communication in social networking. All adopters practice interactivity by gradually moving from Level 1 of initial learning about existence of social media to Level 6 of design and full implementation of interactivity through contribution and exchange of user created contents.

Table 1. Interactivity levels, interactivity modes/phases, and corresponding interactivity tasks by actor groups in surveys conducted by the Forrester Research (Li and Bernoff, 2008)

INTER ACTIVITY LEVEL	INTERACTIVITY MODE AND INNOVATION ADOPTION PHASE	INTERACTIVITY TASKS ACCORDING TO FORRESTER RESEARCH SURVEYS
1	**Initial learning** Learning about existence of social media	No tasks
2	**Field exploration** Random observations of different user created contents Acquaintance with some features and communication potential of social media	Passive tasks Reading social media presentations e.g. blogs, online forums, customer reviews and ratings Listening to podcasts Watching videos (YouTube)
3	**Focused observation** Observation of social networking sites; testing own capability to use them Learning how to use social networking effectively	Visiting social networking sites (e.g. Facebook, Twitter, LinkedIn) Maintaining profile on a social networking site
4	**Selection and classification** Limited use of social media for communication Classifying different forms of social media	Applying tags for classification of webpages, photos etc Online voting for websites Using RSS feeds
5	**Evaluation** Experimenting with interactive communication through selected media Contributing to contents created by other users	Comments on logs of other authors Rating products/services Editing wiki texts
6	**Design and implementation** Interactive broad range networking and communication with other users of social media Creating own contents and publishing in a broad range of social media	Webpage design and publication Blog design and publication Photo/video creation and publication Music creation and publication Texts creation and posting

4. Global adoption of innovation in social networking

Diffusion of innovation is dependent on many factors: economic, social, technological, cultural etc. In the case of social networking that process has been relatively fast in both the adoption rate by the general population and the adoption rate by businesses, customers, suppliers etc. In this section we focus on adoption of innovation in social networking in different countries as characterized by the overall rate of adoption of social media in a population, and by changes in the level of interactivity in social networking among the on-line consumers. The adoption of social networking sites by the general population is illustrated by statistics on the use of Facebook. We apply “penetration of population” as equivalent to the adoption rate of innovation i.e. percentage of the population using the social networking site at a given point of time.

In Tables 2, 3, and 4 the penetration by Facebook in 2014 is shown for three groups of countries. Table 2 presents the top seven countries in terms of the level of Facebook penetration above 60% of the population. It is interesting to note that the leader of this “elite group” is the UAE United Arab Emirates with penetration rate over 80%. Only three, relatively small European nations qualified in the group of global top: Monaco and Gibraltar with over 75% and Iceland with almost 70% penetration of population. There is no country in North America among them. Majority in this group is constituted by countries of small total population and high level of GNP per capita such as United Arab Emirates (population 5.4 million, GDP/capita $43,000), Monaco (population 36.3 thousand, GDP/capita $153,000), Gibraltar (population 30 thousand, GDP/capita $43,000). Table 3 presents Facebook penetration rates of selected developed countries. It may be seen that the highest Facebook penetration in this group of countries is almost 60% in the U.S. and Norway. There are four countries listed with penetration below 50%: France, Germany, S. Korea and Japan. In terms of total number of Facebook users, the U. S. is still at the global top with over 180 million users (2014). Table 4 presents the bottom ten countries ordered by the lowest percentage of Facebook penetration (less or equal 3%). All countries on the list of lowest penetration are located in Africa or Asia with penetration levels ranging from around 0.9% to 3.0%.

As mentioned in the previous section of the paper, we suggest applying *interactivity level* as an important dimension of innovation diffusion in social networking. In Table 5 data have been compared for interactivity levels in selected five countries between 2007 and 2013. They indicate changes in levels of interactivity among on-line consumers in each country reflecting the dynamics of the adoption process according to surveys conducted by Forrester Research reported by Li, C. and Bernoff, J. (2008) and in the Forrester Research Report (2014). Those changes illustrate the phases of the innovation adoption process according to the concept presented in the earlier part of this paper.

Table 2. Highest Facebook penetration in population of countries above 60% level (2014)

Ranked from the lowest	COUNTRY	FACEBOOK PENETRATION RATE % OF POPULATION (2014)
1.	Tajikistan	0.89
2.	Niger	0.91
3.	Uzbekistan	0.97
4.	Burkina Faso	1.46
5.	Somalia	1.95
6.	Madagascar	2.03
7.	Malawi	2.14
8.	Afghanistan	2.51
9.	Guinea	2.86
10.	Mali	3.00

Table 3. Facebook penetration in population of selected developed countries (2014)

RANK ORDER	COUNTRY	FACEBOOK PENETRATION RATE % OF POPULATION (2014)
1.	United Arab Emirates	80.4
2.	Monaco	78.7
3.	Gibraltar	75.6
4.	Iceland	69.7
5.	Brunei	62.5
6.	Singapore	62.3
7.	Falkland Islands	61.3

Table 4. Lowest Facebook penetration in population of countries: Less than 3% (2014)

COUNTRY	FACEBOOK PENETRATION RATE % OF POPULATION (2014)
U. S.	59.96
Norway	59.05
Denmark	57.55
U. K.	56.78
Canada	55.55
France	42.49
Germany	34.52
S. Korea	26.55
Japan	17.30

It is possible to recognize, from the data in Table 5, that the most dynamic changes of interactivity levels (adoption phases of innovation) took place in South Korea, where the percentage of on-line consumers actively involved in social networking increased most visibly at each level of interactivity higher than Level 1. For instance the percentage of users communicating interactively at Level 6 changed from 38% to 49% between 2007 and 2013. It means that 49% of on-line consumers performed fully interactive communication using a broad range of social media in 2013 (see Table 1 for description). It is the highest percentage of interaction at that level achieved in all five countries under consideration. At the same time, the percentage of Level 1 interactivity (initial on-line consumers involved in social networking still remained at the lowest level of interactivity learning) decreased in that country from 36% in 2007 to 9% in 2013. It means that only 9% of consumers did not advance to a higher level of interactivity in 2013. For comparison, data of the same Table 5 indicate that the least dynamic changes of interactivity level took place in Germany, where the percentage of on-line consumers actively involved in social networking at several levels of interactivity has changed very little. For instance the percentage of users communicating interactively at Level 6 remain almost the same 8% and 9% between 2007 and 2013. At the same time, the percentage of on-line consumers operating at the lowest Level 1 (initial learning) remained also almost unchanged (from 49% to 52%). Both of these data indicate a very low dynamics of adoption of interactivity in social networking by on-line consumers in that country. Accuracy, representativeness and verifiability of all those data are limited due to the very nature of surveys.

Table 5. Changes of interactivity levels of social media users in selected countries in 2007 and 2013.
Average % of on-line consumers involved in interactive social networking at different interactivity levels.
Data compiled from: Forrester Research surveys presented by Li and Bernoff (2008) and in http://empowered.forrester.com/tool_consumer.html (2014).

	U. S.		U. K.		Germany		Japan		S. Korea	
INTERACTIVITY LEVEL	**2007 %**	**2013 %**	**2007 %**	**2013 %**	**2007 %**	**2013 %**	**2007 %**	**2013 %**	**2007 %**	**2013 %**
1. Initial learning	44	18	54	37	49	52	26	23	36	9
2. Field exploration	48	73	37	50	44	38	70	69	39	76
3. Focused observation	25	51	21	38	12	21	22	26	41	48
4. Selection & classification	12	21	5	6	12	4	6	11	14	19
5. Evaluation	25	37	16	21	22	12	36	30	27	46
6. Design & implementation	18	24	9	15	8	9	22	34	38	49

5. Dimensions of complexity and innovation adoption

Complexity is a common challenge faced by innovation adopters. As in any learning process the adopters have to engage more time and effort if the innovation is more complex. Adopters of innovation in social networking have to continuously watch for novelties and updates available across the whole spectrum of social media. If we consider Web 2.0 as the object of study, i.e. complex innovation that has been gradually adopted during the last decade in various formats of social networking, then analysis of this object should take into account different dimensions of complexity. One possible approach could be based on the set of three dimensions proposed by Jacobs (2013) for a generalized and quantitative complexity measurement of products, supply chains and service organizations. It consists of the following items:

(1) Multiplicity (V)

V = number of variants/versions in all elements (components, modules, features, products, suppliers etc)

(2) Diversity (D) ; (degree of dissimilarity)

D = 1 – (unique elements/total elements) = 1 – U/T, where U = number of unique elements, T = total number of elements

(3)Interconnectedness (I); (degree of connectivity) I = connections/max connections = A/M, where A = number of connections existing between elements, M = maximum number of connections theoretically possible. First of those dimensions, *multiplicity*, represents number of individual options, features and configurations of the complex object. In the case of social media (or Web 2.0), multiplicity corresponds to the number of versions of respective media and their features, which have to be analyzed by a potential adopter. The second dimension, *diversity*, characterizes dissimilarity of elements of innovation being the subject of adoption i.e. the higher the proportion of unique elements in the total number of elements the more complex innovation becomes for a potential adopter because that adopter has to learn each property of the given social media separately. The third dimension, *interconnectedness*, reflects the complexity of relations between elements of an object i.e. between different social media applications as illustrated in Figure 1. Once those three dimensions have been defined it is possible to combine them into one generalized complexity index. Jacobs (2013) proposed that such an index could be calculated as a product of all three dimensions.

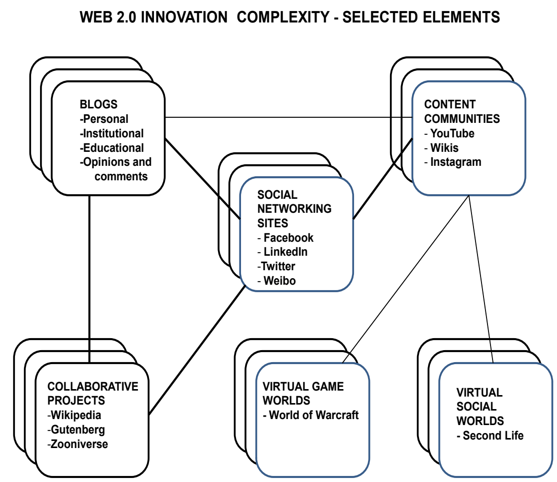

Figure 1. Complexity of innovation in social networking: example of multiplicity of elements and interconnectedness.

At the same time, it appears appropriate to propose two hypotheses for further research relevant to understanding of adoption of innovation in social networking:

H.1. *Innovation adoption process depends on the level of complexity measured by complexity dimensions e.g those derived from the paper of Jacobs (2013).*

H.2. *Advances in interactivity are not accelerated if users don't share their learning experience (e.g. in a forum mode); exploration of the "learning community effect." Then if the proper testing is done the null be could rejected with the end result that "Advances in interactivity may well be accelerated if users share their learning experience."*

Hypothesis H1, if verified empirically, could constitute basis of a theory of innovation adoption applicable beyond the area of social networking. Hypothesis H2 may be viewed in the context of observations and empirical data given in Table 5. They suggest that cultural tradition and models of social behavior have an impact on modes of innovation adoption (e.g. *the learning community effect* known to be characteristic in some Asian countries, case of S. Korea).

6. Conclusions

Results of the study reported in this paper support the initial concept of adoption process as a learning process. In the initial section of the paper we reviewed the possibility of applying conventional models of innovation diffusion to analysis of social networking. We found that an additional new dimension is needed to improve and expand that analysis. Hence the *interactivity level* has been proposed as a new dimension of innovation adoption in social networking. It is as an indicator of the "depth" of innovation adoption that shows how far an adopter mastered new tools and technology and how many features he or she is capable to use. It is based on an observation that in social networking the innovation adoption is not just a single event. It is a process, during which an adopter is learning experientially how to communicate interactively through social media. We suggest that six phases of this process can be distinguished. Those phases have been illustrated with data derived from surveys conducted by other authors (see Table 5). However our own study has been focused on three essential conceptual elements: (1) representing the innovation adoption as a learning process, (2) introducing the *level of interactivity* as a new dimension of innovation diffusion in social networking, and (3) proposing six phases of adoption characterized by corresponding levels of interactivity.

The proposed dimension of interactivity level should be explored further by collecting data and time series in a longer period of observations. Distinction of just six levels of interactivity (Table 1) within the adoption process of social networking may also require verification. The global aspect of social networking adoption (Tables 2, 3 and 4) could be the subject of further research encompassing an enlarged set of countries and their cultural, economic, social and technological conditions. It should be added that data illustrating the learning process and its phases are based on surveys. Hence their verifiability is quite limited.

7. References

Bughin, J., Chui, M. (2010). "The rise of the networked enterprise: Web 2.0 finds its payday," *McKinsey Quarterly*, December 2010. Retrieved from https://www.mckinseyquarterly.com/article=2716,

Bughin, J., Chui, M., (2013) "Evolution of the networked enterprise: McKinsey Global Survey results," *McKinsey Insights & Publications*, March Issue.

Forrester Research (2014), "What's The Social Technographics Profile Of Your Customers?," Retrieved from http://empowered.forrester.com/tool_consumer.html .

Jacobs, M. A. (2013). "Complexity: Toward an empirical measure," *Technovation*, 33, 111-118.

Kaplan, A. M., Haenlein, M. (2010). "Users of the world, unite! The challenges and opportunities of Social Media," *Business Horizons,* 53, 59-68.

Kiousis, S. (2002). "Interactivity: a concept explication," *New Media & Society***,** September , 4, 3, 355-383

Li, C., Bernoff, J. (2008). *Groundswell: Winning in a World Transformed by Social Technologies*, Boston: Harvard Business Press.